CHAPTER 4

RESULTS AND DISCUSSION

This chapter begins with the presentation of results pertaining to the characterization of raw powders and deposited coatings which is followed by the results on friction and wear behavior of these coatings under different normal loads, sliding speeds and temperatures. The results and discussion on tribological behavior are presented in three parts: (a) the room temperature (RT) behavior of the coatings under normal loads of 5, 10, 15 and 20 N and sliding speeds of 0.5 m/s and (b) tribological behavior at a constant load of 5 N and speed of 0.3 m/s but at different temperatures ranging from RT to 800 ℃ and (c) elevated temperature (RT to 800 °C) wear under different speeds of 0.3, 0.5, 0.7 and 0.9 m/s and at a fixed load of 5 N.

4.1 RESULTS

4.1.1 CHARACTERIZATION OF POWDERS

Figure 4.1 shows the SEM morphologies of Ni, Al, Ag, MoS_2 and hBN powders used in the present study. Both Ni and Al (99 % pure) powder particles are observed to be spherical in shape with particle size ranging from 80-120 μm and 20-50 μm, respectively. The particles of MoS_2 powder (purity- 99 %) are angular in shape with particle size ranging from 30-70 μm whereas the Ag powder particles (purity- 99 %) have

irregular shape with particle sizes in the range from 45-75 µm. The particle size of hBN (purity- 99 %) is around 70 nm.

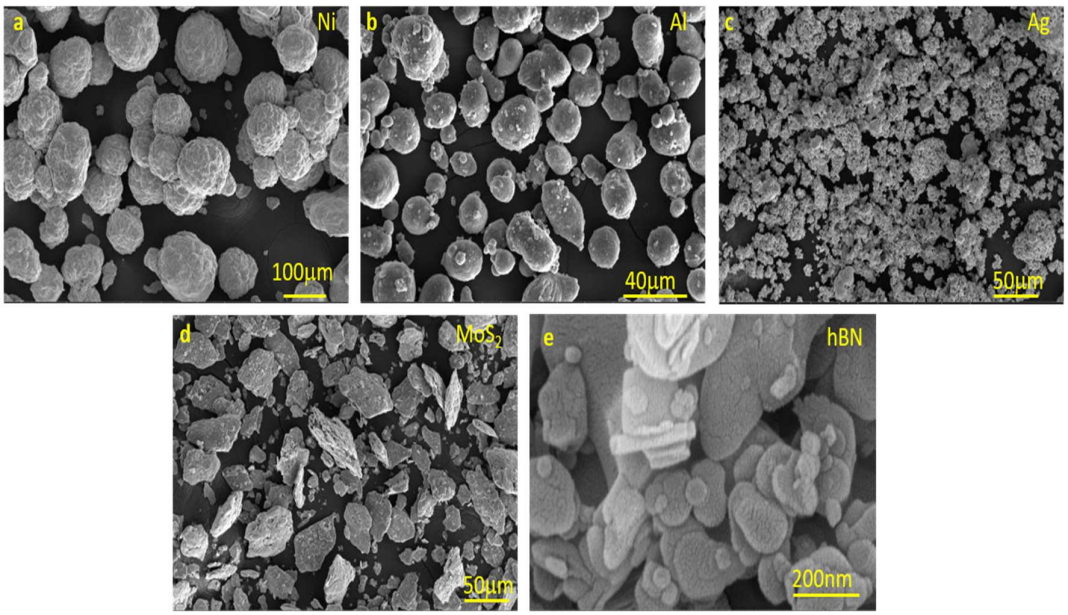

Fig. 4.1 SEM micrographs of feedstock powders of (a) Ni, (b) Al, (c) Ag, (d) MoS_2 and (e) hBN.

4.1.2 CHARACTERIZATION OF COATINGS

Figure 4.2 shows the XRD patterns of composite coatings, namely, Ni-Al-Ag-MoS_2 (NAMB0), Ni-Al-Ag-MoS_2- 5 wt. % hBN (NAMB5) and Ni-Al-Ag-MoS_2- 10 wt. % hBN (NAMB10). It can be seen from the XRD patterns that all the coatings primarily comprise of Ni based solid solution (γ phase), Ni_3Al phase (γ′ phase) and NiAl phase. It could further be seen that all the solid lubricants are available in their original form in coatings as evident from corresponding peaks. Owing to the low wt. % of hBN in NAMB5, the peak of hBN is not visible in the XRD patterns. However, the presence of hBN could be observed in NAMB10 coating as shown by the peak of BN in Fig. 4.2 (c). Therefore, it may be concluded that powders are deposited without any oxidation or disintegration under the investigational spraying conditions.

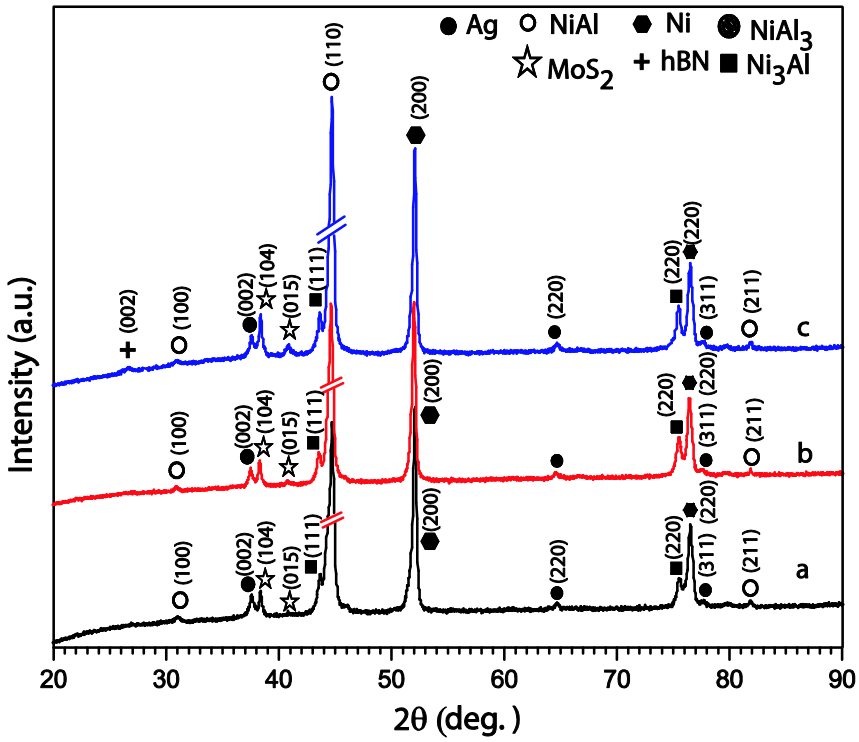

Fig. 4.2 XRD pattern of as deposited coatings (a) NAMB0 (b) NAMB5 and (c) NAMB10.

The polished cross-section morphologies of as-sprayed NAMB0, NAMB5 and NAMB10 composite coatings are presented in Fig.4.3. The NAMB0 coating is observed to be dense in comparison to NAMB5 and NAMB10. The NAMB5 coating presents a fairly compact but a relatively dense (in comparison to NAMB0) structure comprising of the droplets impacted on the substrate. The NAMB10 composite coating exhibits a typical lamellar structure but appears to have more porosity in comparison to other coatings. The measured thickness is about 250 μm for all the composite coatings.

Table 4.1 presents the area percentage porosity, the micro hardness as measured by Vickers micro hardness test. The porosity has been observed to increase with increasing addition of hBN in the coating. Furthermore, the hardness of the coatings has been found to decrease with addition of hBN as indicated in Table 4.1.

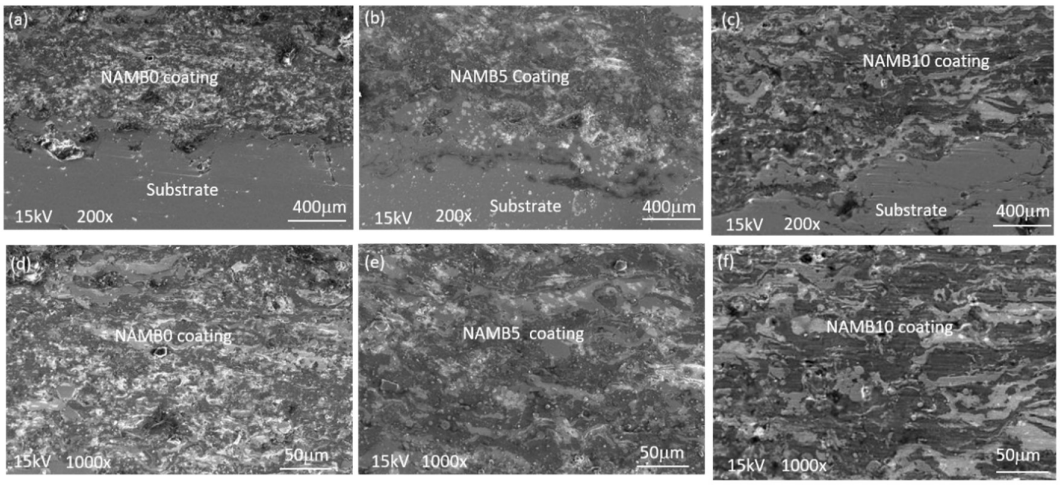

Fig. 4.3 Cross-section morphologies of (a) NAMB0 (b) NAMB5 (c) NAMB10 composite coating, and (d) high magnification image of (a), (e) high magnification image of (b), (f) high magnification image of (c).

Table 4.1 Designation, Hardness, and Porosity of coatings.

Designation	**Porosity**	**Hardness ($HV_{0.2}$)**
Ni-Al-Ag-MoS_2 **(NAMB0)**	4.8 ± 0.7%	182.4
Ni-Al-Ag-MoS_2-5wt. % hBN **(NAMB5)**	8.0 ± 1.0%	164.6
Ni-Al-Ag-MoS_2-10wt. % hBN **(NAMB10)**	24 ± 1.4%	155.3

In plasma spray process the deposition of coating takes place by the successive layers of molten droplets which build up as the process moves and flatten with solidification resulting in typical lamellar microstructure as seen in Fig. 4.3. Spreading instability depends on the incomplete melting or rapid localized solidification of the powder droplets which strike on the surface of the substrate. Due to larger interfacial areas of fine Ni and Al powders the exothermic reaction generates a large amount of heat during thermal spray (Chen et al., 1996) which leads to complete melting of the composite powders and delays the localized solidification. A delayed solidification helps in proper

spreading of impacted droplets and results in a compact coating as reported by (Du et al., 2010 and Chen et al., 2013). The porosity of NAMB0 composite coating has been found to be about 4.8 ± 0.7%. However, the porosity increased with the addition of hBN and attained values of 8.0 ± 1.0% and 24 ±1.4%, respectively, for NAMB5 and NAMB10 coatings, containing 5 and 10 wt. % hBN, respectively. The increase in porosity may be attributed to the poor wettability and sinterability of hBN which hampers the close contact between other constituent materials of coating and hence, the densification process as suggested by (Kimura et al., 1999). However, a little higher porosity in coating containing 10 wt. % may be due to the pulling out of some loosely bound particles of hBN during metallographic polishing which has also been indicated earlier by Du et al. (2011). A decrease in hardness of coatings with addition of hBN may also be explained on the basis of poor sintering characteristics of hBN. The hardness decreases as the wt. % of hBN increases up to 10 wt. % hBN in the coating (NAMB10) due to poor sinterability of hBN with the matrix.

4.1.3 FRICTION AND WEAR BEHAVIOR OF COATINGS

The following sections present the results and discussion on friction and wear characteristics of deposited coatings. The results have been presented and discussed in three parts: (a) the room temperature (RT) behavior of coatings under normal loads of 5, 10, 15 and 20 N and at a sliding speed of 0.5 m/s and (b) tribological behavior at a constant load of 5 N and speed of 0.3 m/s but at different temperatures ranging from RT to 800 °C and (c) elevated temperature (RT to 800 °C) wear under different speeds of 0.3, 0.5, 0.7 and 0.9 m/s and at a fixed load of 5 N.

4.1.3.1 Room Temperature Tribological Behavior of Coatings

The present section presents the results on the effect of load on room temperature (RT) tribological behavior of deposited coatings examined by conducting friction and wear tests under different loads of 5, 10, 15 and 20 N at a fixed sliding speed of 0.5 m/s.

(i) Variation of coefficient of friction with time

The real time variations of coefficient of friction (COF) with respect to time for all the coatings are illustrated in Fig. 4.4 (a through d) at the loads of 5, 10, 15 and 20 N, respectively. All the coatings have been observed to show a fluctuating trend of variation at all the loads but with a varying amplitude of fluctuation. However, the amplitude appears to be more at the lowest load of 5 N in comparison to other loads used in the present investigation for all the coatings as evident from a comparison of Figs. 4.4 (a, b, c and d). Also, one may observe that the fluctuations are a little higher for NAMB0 coating in comparison to NAMB5 and NAMB10, particularly at relatively higher loads of 10, 15 and 20 N. The coefficient of friction, for a particular coating, has been observed to decrease with increasing load from 5 to 15 N beyond which an increase is found to occur till 20 N. However, among the coatings, the coating containing 5 wt. % hBN i.e., NAMB5 has shown the lowest COF at all the loads.

(ii) Variation of average coefficient of friction with normal load

Figure 4.5 shows the variation of average COF with load for all the coatings. It is apparent that average COF decreases with increasing load from 5 to 15 N and increases thereafter till 20 N for all the coatings. However, the coatings containing hBN

i.e., NAMB5 and NAMB10 have consistently lower COF in comparison to NAMB0 coating at all the loads as evident from Fig.4.5. The NAMB5 has the lowest COF at all the loads used in the present investigation and a minimum COF value of 0.29 achieved at a load of 15 N.

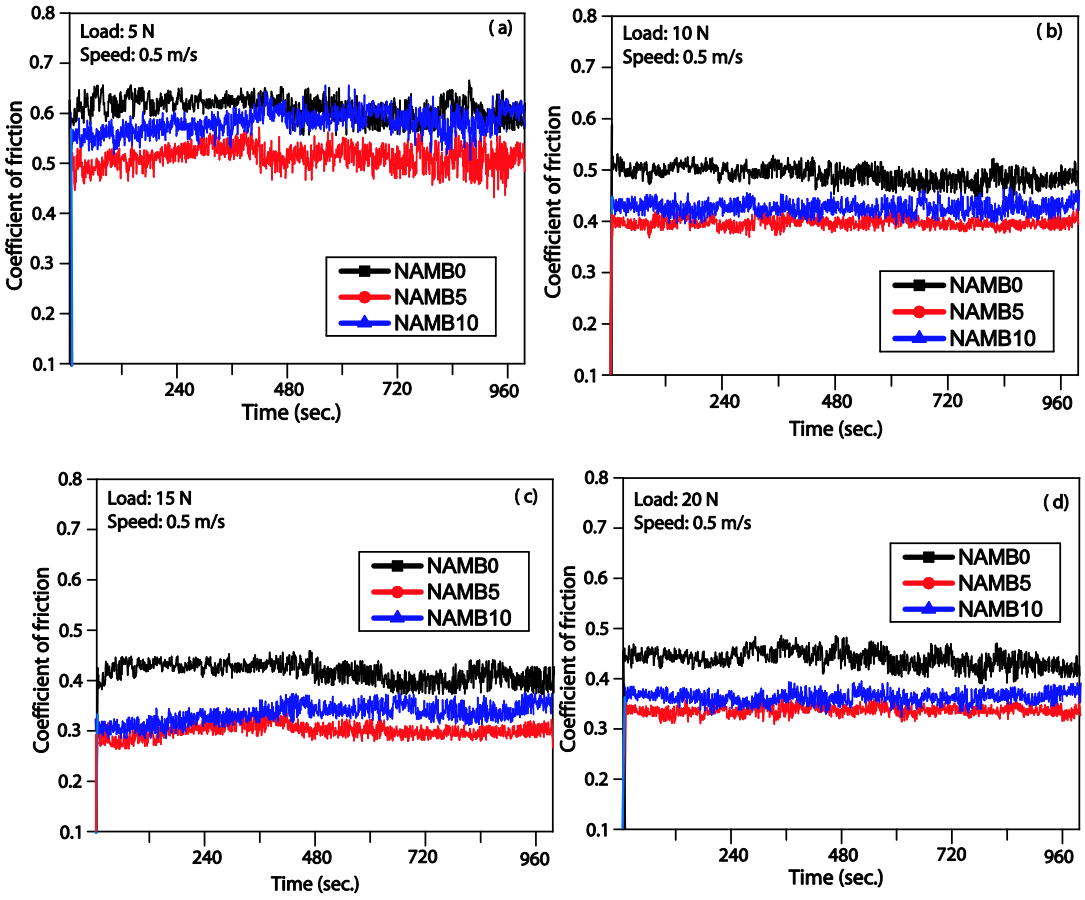

Fig. 4.4 Variation of coefficient of friction with time for NAMB0, NAMB5 and NAMB10 coatings at different loads (a) 5 N, (b) 10 N, (c)15 N and (d) 20 N.

(iii) Variation of wear rate with normal load

The variation of wear rate of coatings with respect to applied normal load is illustrated in Fig.4.6. The wear rate for all the coatings is observed to decrease with increasing load from 5 to 15 N followed by an increase beyond 15 N. NAMB0 coating

has shown a consistently higher wear rate than NAMB5 and NAMB10 at all loads as evident from Fig.4.6. It could further be observed that the wear rate of the coatings gets significantly reduced with the addition of hBN as seen from Fig.4.6. The coating NAMB5 has shown the lowest wear rate at all the loads.

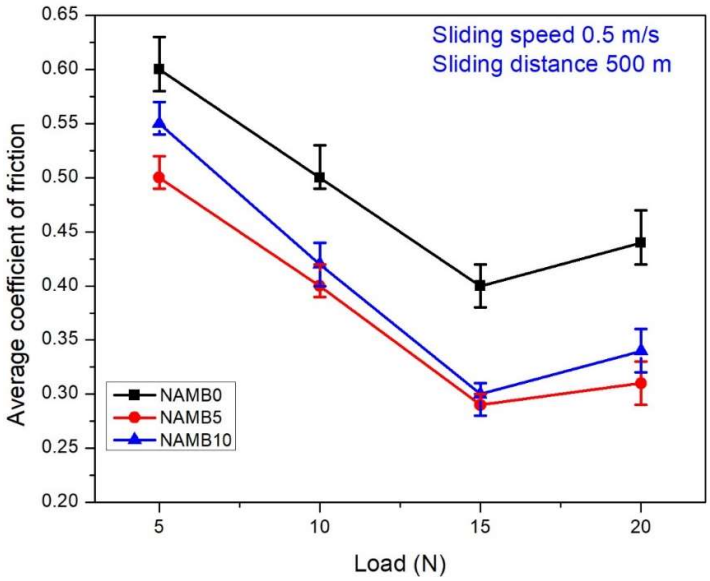

Fig. 4.5 Variation of average coefficient of friction with load for composite coatings.

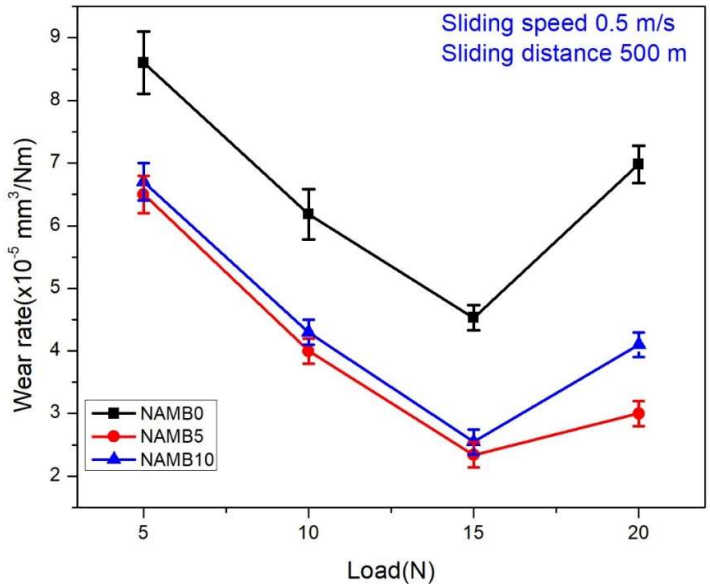

Fig. 4.6 Variation of wear rate of the coatings with load.

4.1.3.2 Examination of Worn Surface of Coatings

SEM micrographs of the worn surfaces of NAMB0, NAMB5, and NAMB10 at loads of 5, 10, 15 and 20 N are presented in Figs. 4.7, 4.8, 4.9 and 4.10, respectively. Fig. 4.7 (a) presents some pits, small wear debris particles spread over the wear track and some scoring marks along the direction of sliding on the surface of NAMB0 after sliding under a load of 5 N. The worn surface of NAMB5, shown in Fig. 4.7 (b) appears to have a discontinuous transfer layer of wear debris at several locations, whereas a patchy transfer layer of wear debris with some loose wear particles could be seen on the worn surface of NAMB10 given in Fig. 4.7 (c) after sliding under a load of 5 N.

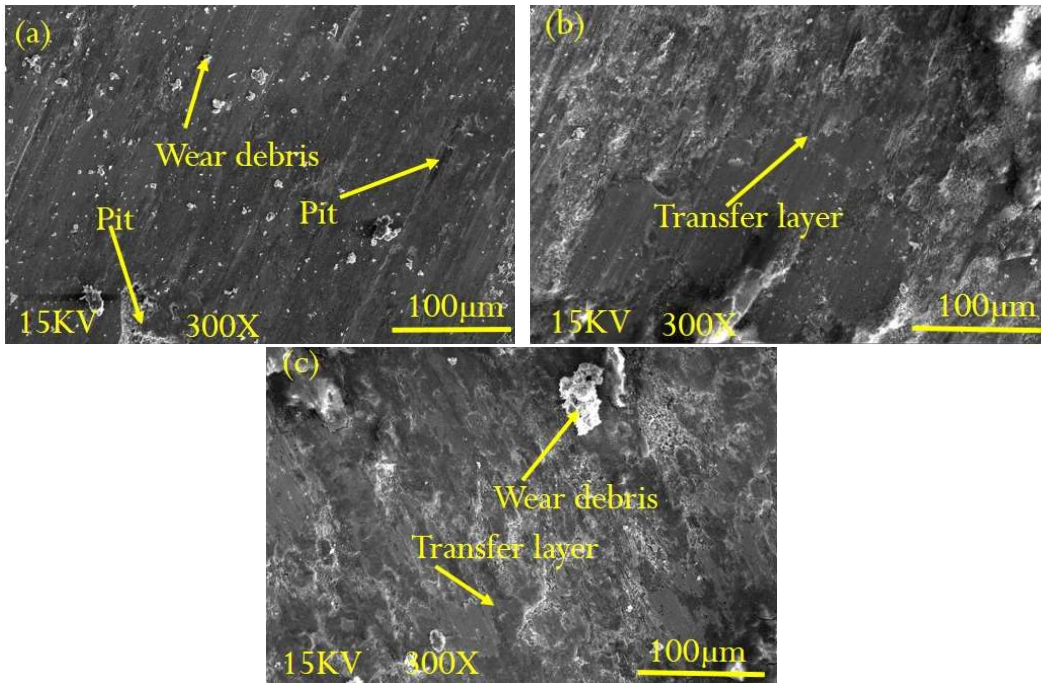

Fig. 4.7 SEM images of worn surfaces of coating at a load of 5 N (a) NAMB0 (b) NAMB5 (c) NAMB10.

The morphology of the surface of NAMB0 coating worn at a load of 10 N, presented in Fig. 4.8 (a) reveals the presence of very few wear debris particles and a transfer layer along with some scoring marks. The worn surface of NAMB5 (Fig. 4.8 b) also shows the

presence of transfer layer but the extent of coverage is more in comparison to NAMB0. Figure 4.8 (c) shows the presence of very smooth and compacted tribo-layer on the worn surface of NAMB10 coating. However, the layer appears to have been detached at few places.

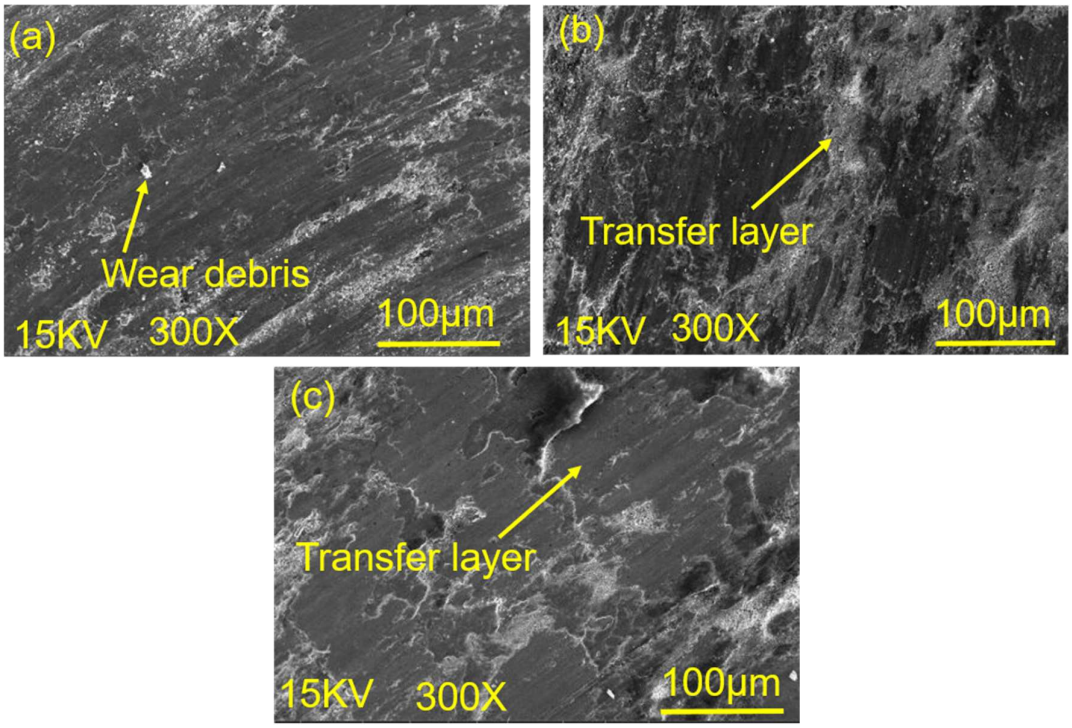

Fig. 4.8 SEM images of worn surfaces of coating at a load of 10 N (a) NAMB0 (b) NAMB5 (c) NAMB10.

The morphologies of the surfaces and corresponding EDS spectra of NAMB0, NAMB5 and NAMB10 worn at 15 N load are presented in Figs.4.9 (a through c). Fig. 4.9 (a), wear track of NAMB0 coating at a load of 15N appears to have fine wear debris particles containing elements of coating materials, whereas, in Fig. 4.9 (b) corresponding to NAMB5**,** the wear tracks are covered with a compacted and smooth tribo-layer with very few visible scoring marks at several locations. However, one could observe the existence of very smooth and compacted tribo-layer (Fig. 4.9 c) of wear debris

on the wear track of NAMB10 coating along with a few locations from where the layer appeared to have cracked.

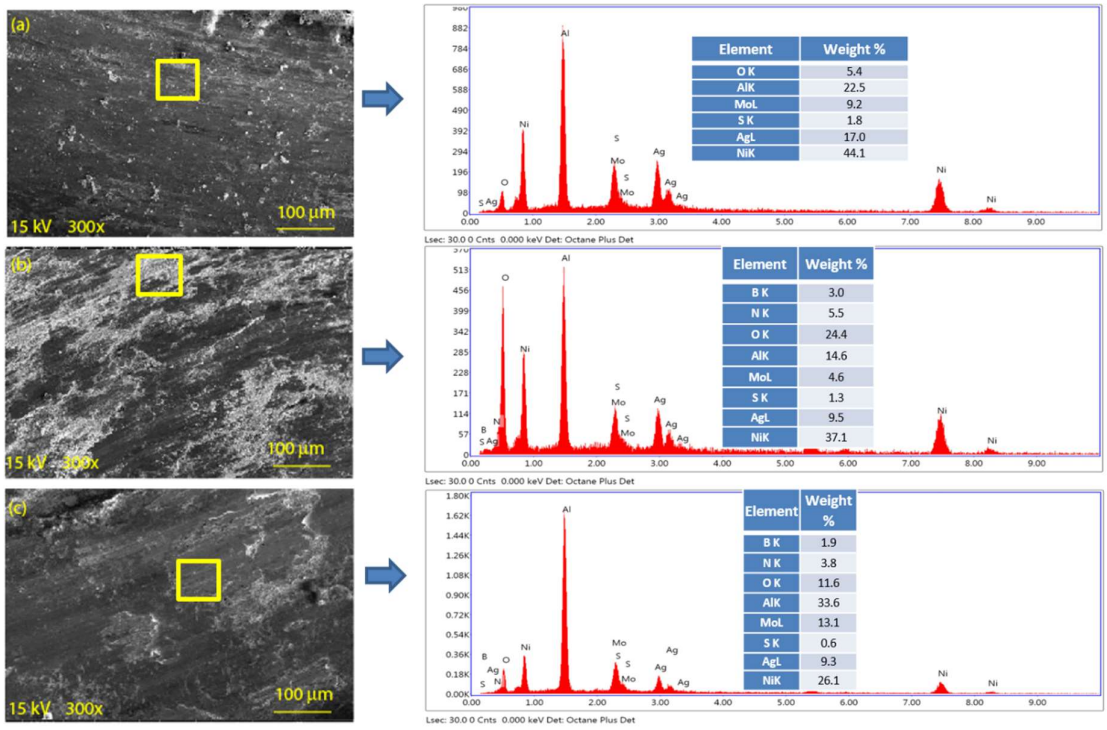

Fig. 4.9 SEM images of worn surfaces of coating at a load of 15 N of (a) NAMB0 (b) NAMB5 (c) NAMB10 coatings with corresponding EDS spectrums.

Figure 4.10 (a through c) demonstrates the morphology of worn surfaces of NAMB0, NAMB5, and NAMB10 coatings after sliding at a load of 20 N. The worn surface of NAMB0 illustrated in Fig. 4.10 (a) presents some deeper grooves and locations from where the transfer layer might have flaked off along with some signs of delamination. The worn surface of NAMB5 coating given in Fig. 4.10 b shows the existence of a transfer layer at several locations along with abrasive marks. The worn surface of NAMB10 coating given in Fig. 4.10 (c) shows the presence of relatively deeper grooves and lump of loose wear debris. However, no transfer layer could be observed on the worn surface of NAMB10 coating.

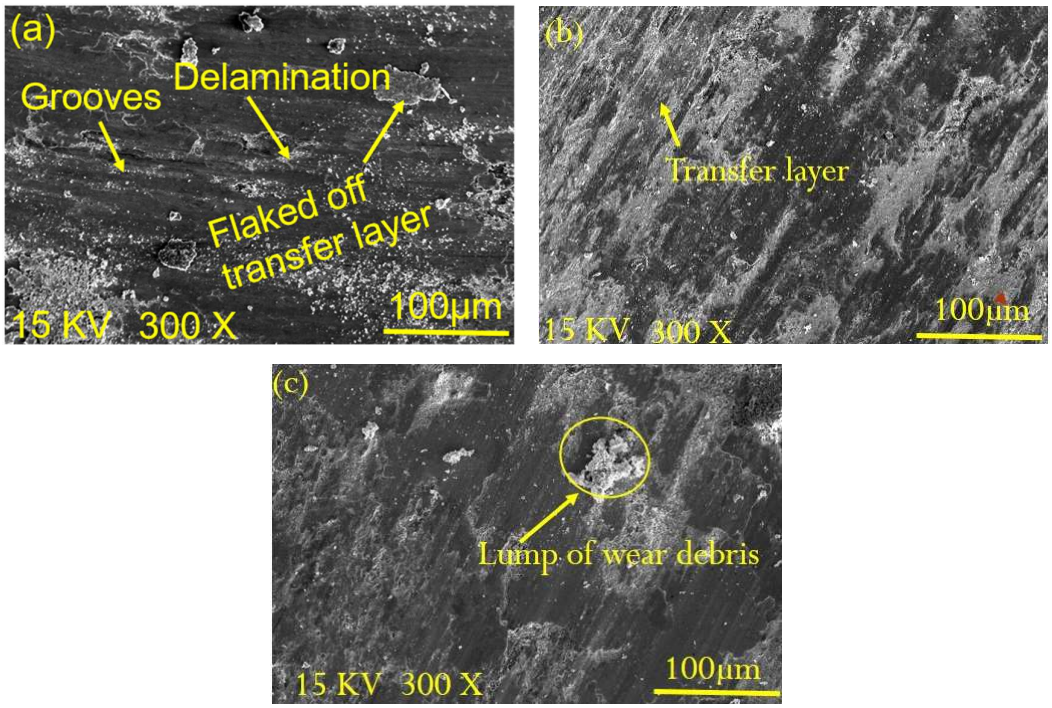

Fig. 4.10 SEM images of worn surfaces of coating at a load of 20 N (a) NAMB0 (b) NAMB5 (c) NAMB10.

4.1.3.3 Worn Surface Morphology of Counterface

The morphologies of the worn surface of alumina ball slid against NAMB0, NAMB5, and NAMB10 composite coatings at loads of 5, 10, 15 and 20 N are presented in Figs. 4.11, 4.12, 4.13 and 4.14, respectively**.** The morphology of alumina ball slid against NAMB0 at a load of 5 N and depicted in Fig. 4.11 (a) reveals the layer of transferred material from the coating at the bottom left corner along with a rough region from where the transferred material appears to have been detached during the sliding motion. The transfer of material has been confirmed by EDS analysis of the worn surface of counterface. The worn surface of ball slid against NAMB5 illustrated in Fig. 4.11 (b) shows a smooth surface with a layer of compacted material transferred from the coating along the direction of sliding. The worn surface of alumina ball slid against NAMB10 coating given in Fig. 4.11 (c) also reflects the presence of a tribo- layer of transferred

material from coated samples to the alumina ball but the layer does not appear to be well compacted at several locations. The transfer of material from coated surface to counterface alumina ball has been confirmed by EDS analysis.

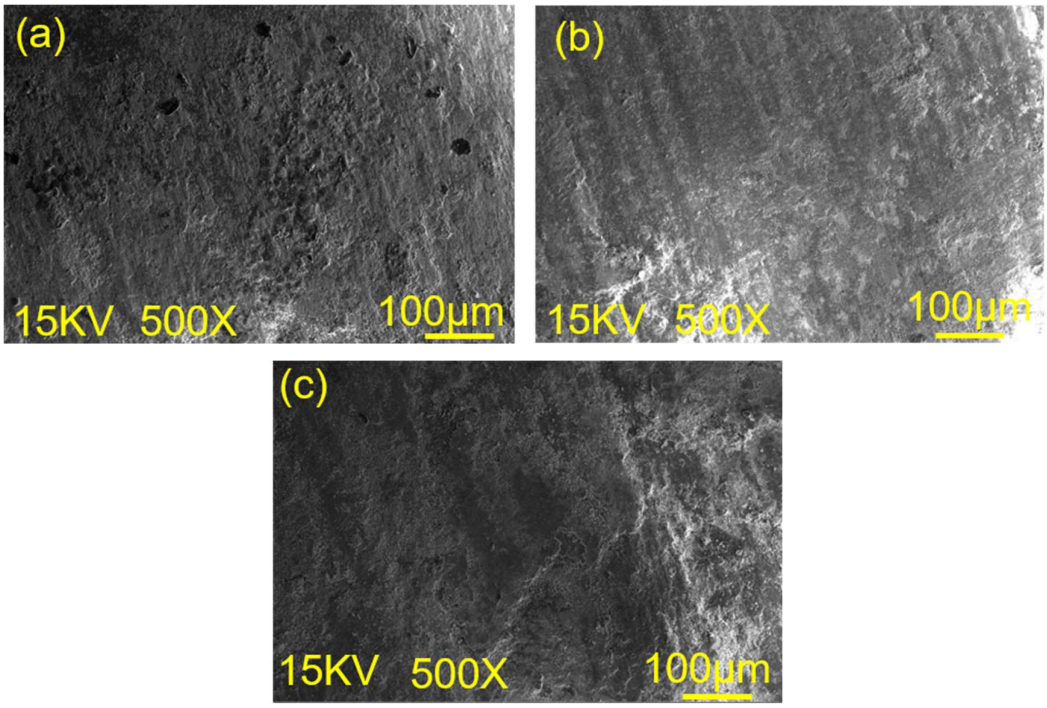

Fig. 4.11 Worn surfaces of alumina ball slid against (a) NAMB0 (b) NAMB5 (c) NAMB10 composite coating at a load of 5N.

The worn surface of alumina ball slid against NAMB0 coating at a load of 10 N also shows a compacted and relatively smooth layer at some places along with some transferred materials from coated specimen as seen from Fig. 4.12 (a). However, the detachment of layer is also observed on the surface. Fig. 4.12 (b) shows the presence of a relatively well compacted and continuous transfer layer of transferred material from the coating. The worn surface of alumina ball slid against NAMB10 coating given in Fig. 4.12 (c) also reflects the presence of a compacted tribo- layer of transferred material from coated samples to the alumina ball.

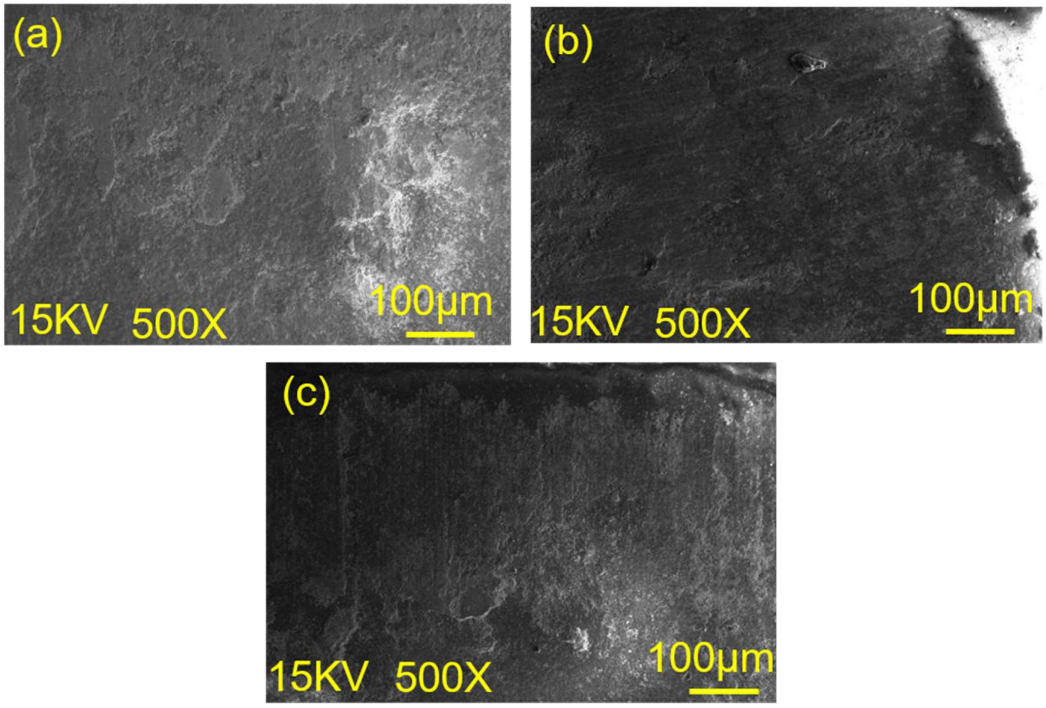

Fig. 4.12 Worn surfaces of alumina ball slid against (a) NAMB0 (b) NAMB5 (c) NAMB10 composite coating at a load of 10 N.

Figure 4.13 illustrates the SEM micrographs of worn surface of alumina ball slid against (a) NAMB0 (b) NAMB5 (c) NAMB10 coatings at a load of 15 N along with corresponding EDS spectra. The alumina ball morphology depicted in Fig. 4.13 (a) presents a rough surface. One may observe the presence of transferred material from the coated samples on the surface of alumina ball during the sliding motion which is confirmed by EDS analysis. Fig. 4.13 (b) shows the presence of a well compacted and continuous transfer layer of transferred material from samples as evident from the corresponding EDS spectrum. The worn surface of alumina ball slid against NAMB10 coating given in Fig. 4.13 (c) also reflects the presence of a tribo- layer of transferred material from coated samples to the alumina ball but the layer does not appear to be continuous.

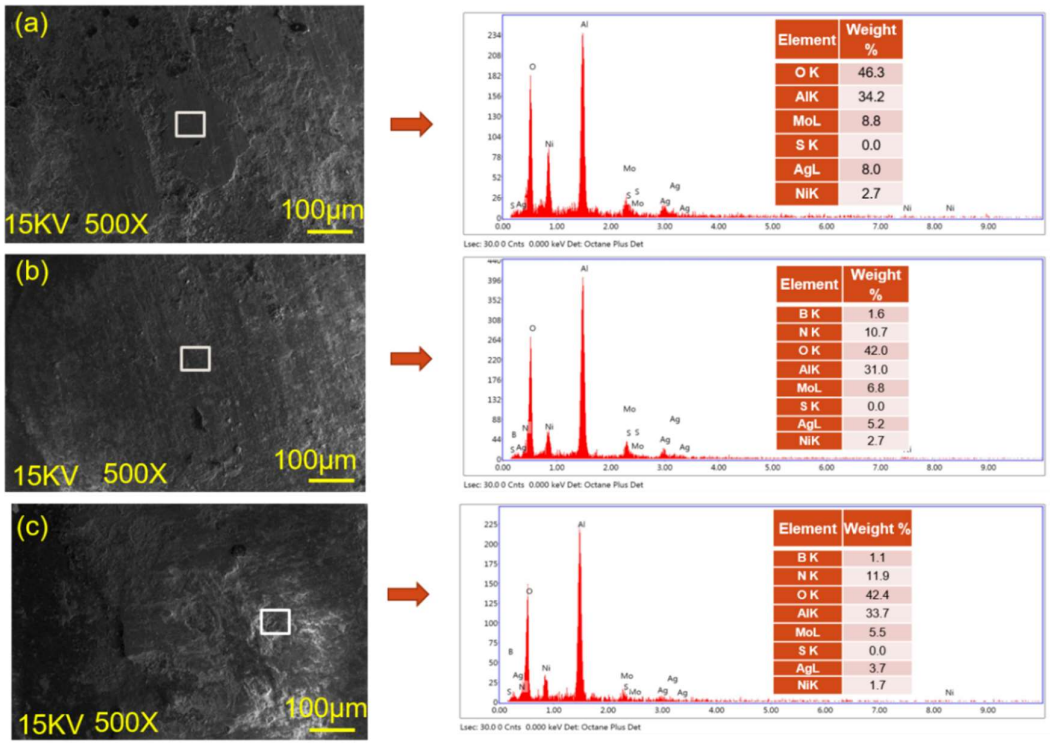

Fig. 4.13 Worn surface of alumina ball slid against (a) NAMB0 (b) NAMB5 (c) NAMB10 composite coating with EDS analysis at a load of 15N.

Fig. 4.14 (a) shows the worn surface of alumina ball slid against NAMB0 at the highest load of 20 N used in the present study. The surface reveals the presence of a well compacted transfer layer, but the layer is found to have detached at some locations. The worn surface of counterface ball slid against NAMB5 at a load of 20 N shows the presence of a well compacted and continuous transfer layer of transferred material from samples as seen from Fig. 4.14 (b). The worn surface of alumina ball slid against NAMB10 coating given in Fig. 4.14 (c) also reflects the presence of a discontinuous tribo-layer of transferred material from coated samples to the alumina ball and appears to have broken or detached at few locations.

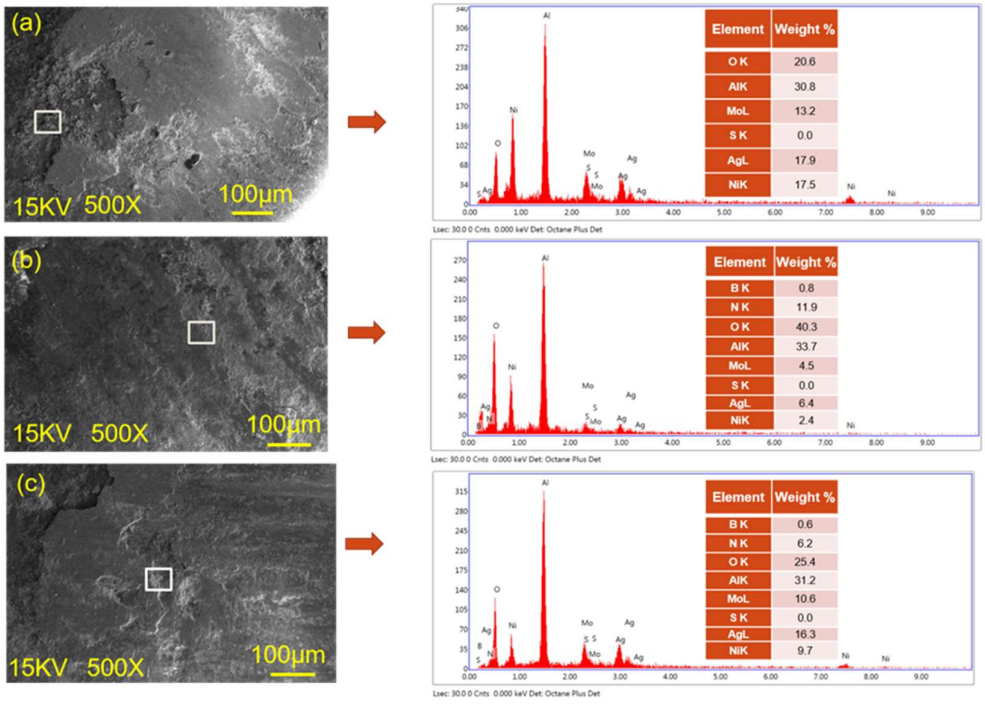

Fig. 4.14 Worn surface of alumina ball slid against (a) NAMB0 (b) NAMB5 (c) NAMB10 composite coating at a load of 20 N and corresponding EDS spectrums.

The worn surfaces of coated specimens have been subjected to x-ray diffraction analysis to examine the formations of new phases that might have resulted from the tribo-chemical reactions at the interface during sliding. Fig. 4.15 (a) gives the XRD patterns of worn surfaces of the NAMB0 composite coating slid under 5, 10, 15 and 20 N at a speed of 0.5 m/s. One may observe the presence of peaks corresponding to coating materials only and no extra peak could be seen on the worn surface as evident from Fig. 4.15 (a). XRD patterns of the worn surfaces of NAMB5 and NAMB10 after sliding under different loads depicted in Figs 4.15 (b) and (c), respectively, also reveal the presence of peaks corresponding to coating materials only may be due to a relatively less amount of new phases (if, at all they might have formed during sliding) which might have been below the detection limit of x-ray. Hence, to check the possibility of formation of new phases, the worn surfaces have further been examined under Raman spectroscopy.

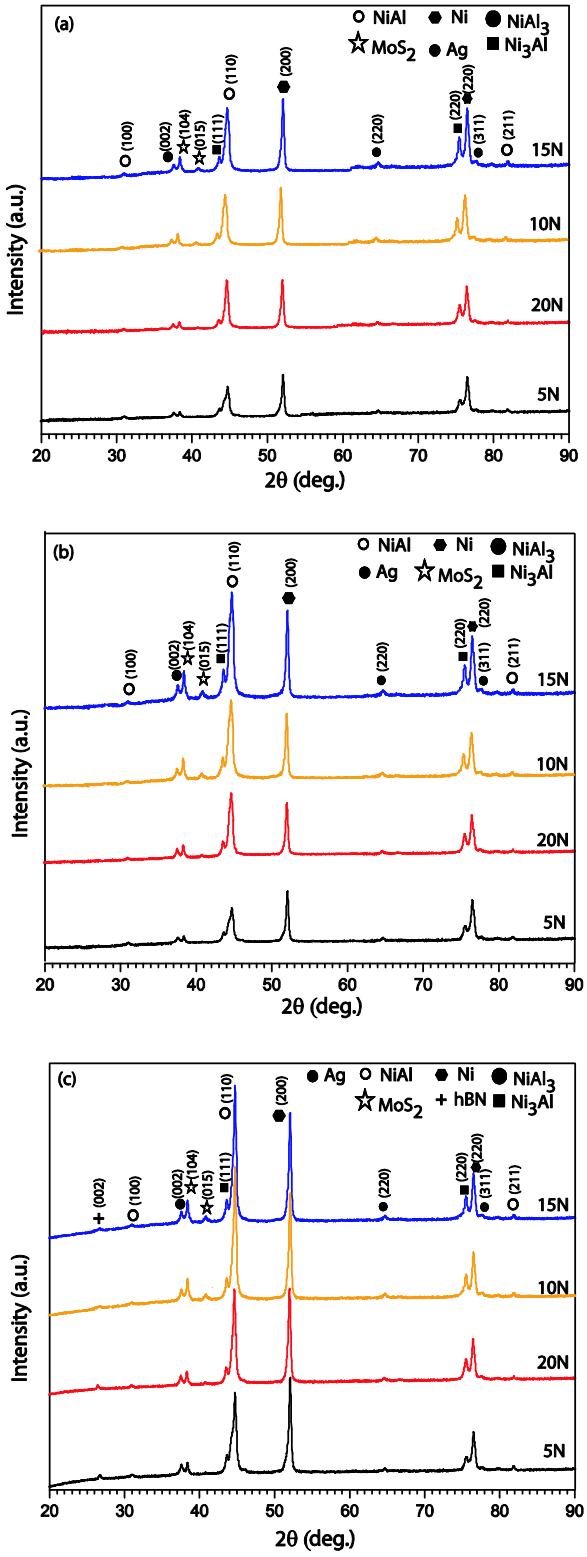

Fig. 4.15 XRD patterns of the worn surfaces of (a) NAMB0 (b) NAMB5 (c) NAMB10 coating at 5, 10, 15 and 20 N load.

The Raman spectra of coatings given in Fig.4.16 reveal the evolution of the compositions on the wear track due to the tribo-chemical reactions. Raman spectrum corresponding to 5 N load shows absence of any new phase for all the coatings. However, presence of new phases for all the coatings is observed as the load is raised to 10 and 15 N. This may be attributed to the rise in temperature caused by increased frictional heating which might have triggered the tribo-chemical reactions leading to formation of new lubricious phases. Due to friction process, silver and molybdenum are expected to get oxidized and form several new phases like Ag_2MoO_4, $NiMoO_4$ apart from AgO and MoO_3.

Raman spectrum corresponding to NAMB0 coating (Fig. 4.16 (a)) shows the presence of Ag_2MoO_4 only at a load of 10 and 15 N whereas one could see peaks of Ag_2MoO_4 along with MoO_3, AgO and $NiMoO_4$ phases on other coatings (Fig. 4.16 b and c) along with presence of hBN. As the load is increased to 20 N, the traces of new phases formed are observed in a low quantity which could be judged by the presence of a relatively broad peak at this load in comparison to 15 N despite the expected increase in frictional heat due to relatively higher load.

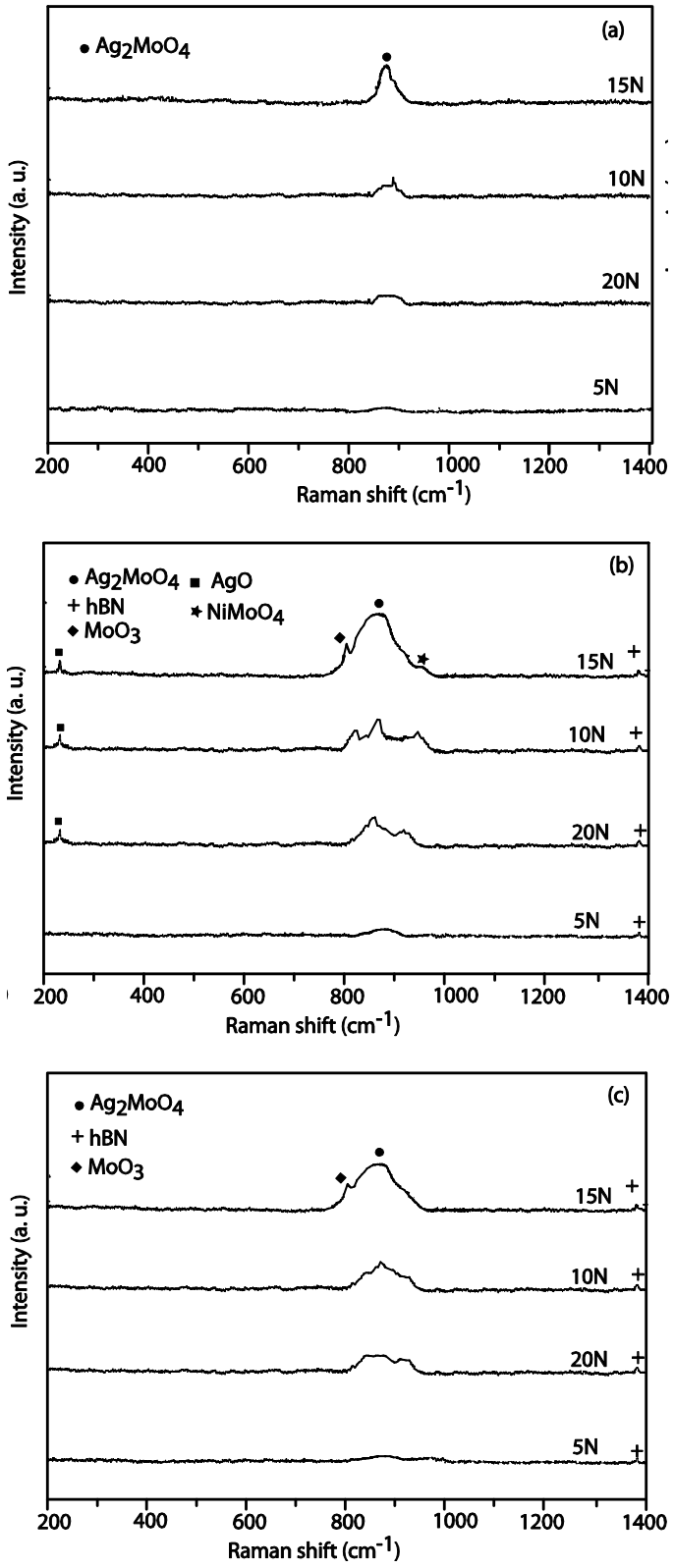

Fig. 4.16 Raman spectra of the worn surfaces of (a) NAMB0 (b) NAMB5 (c) NAMB10 coating at 5, 10, 15 and 20N load.

4.2 DISCUSSION

A decrease in hardness with addition of hBN may be attributed to the poor integration of hBN in the matrix leading to reduction in strength of the coating. Relatively smaller amplitude of fluctuation in variation of friction coefficient at a load of 15 N in comparison to 5 N (Fig. 4.4) may be attributed to the better compaction of the wear debris due to relatively higher frictional heating which led to the formation of a smoother layer at the surface as indicated by morphology of respective worn surfaces given in Figs. 4.7, 4.8 and 4.9. Both the average coefficient of friction and wear rate have been observed to decrease with increasing load from 5 to 15 N for all the coatings whereas the friction coefficient has been found to increase beyond 15 N as shown in Figs. 4.5 and 4.6. The NAMB5 coating has shown the lowest COF and wear rate under all the loads. The observed behavior may be explained on the basis of (i) the formation and extent of compaction of the transfer layer containing solid lubricant on the sliding surface, (ii) the transfer of solid lubricant/s from coating to counterface alumina ball and (iii) the generation and presence of new lubricating phases due to tribo-chemical reactions at the interface caused by the temperature rise. The reduction in friction coefficient with increasing load from 5 to 15 N may be attributed to the formation and degree of compaction of the transfer layer of wear debris containing solid lubricants. The NAMB0 coating does not show a presence of transfer layer at the lowest load of 5 N as seen from Fig. 4.7 whereas the transfer layer is seen to be present at higher loads of 10, 15 and 20 N as indicated in Figs. 4.8 (a), 4.9 (a) and 4.10 (a). A relatively higher coefficient of friction at all the loads shown by NAMB0 could be due either the absence of transfer layer as in Figs. 4.7 (a) or relatively smaller coverage provided by the transfer layer and the flaking off of the transfer layer (Fig. 4.10 a) which might have led to increased contact between ball and coating. However, a decrease in friction coefficient with increasing load

in NAMB0 may be due to the presence of solid lubricants on MoS_2, Ag as indicated by XRD patterns shown Fig. 4.15 (a through c) and the presence of lubricious Ag_2MoO_4 as revealed by Raman spectrum (Fig. 4.16 a) at 15 N. The increase in friction beyond 15 N i.e., at 20 N may be attributed to the delamination and flaking off of the transfer layer (Fig. 4.10 a) resulting in direct contact between coating and counterface ball. One could observe the presence of a transfer layer on the worn surface of coatings containing hBN at each load but the extent of coverage by this layer appears to be more at 15 N in comparison to 5, 10 N and 20 N as seen from a comparison of Figs. 4.7 (b, c) to 4.10 (b, c) which might have been a reason for lowest coefficient of friction at 15 N. The lower friction coefficient and wear rate shown by coatings containing hBN may be due to the presence of lubricious phases like Ag_2MoO_4, MoO_3, $NiMoO_4$ and hBN on the worn surface as shown by the Raman spectra given in Figs. 4.16 (b and c) which are not observed in Raman spectrum of NAMB0 coating except Ag_2MoO_4. The other factor may be the transfer of hBN to the counterface alumina as evident from Fig. 4.11 (b, c) to 4.14 (b, c) which might have resulted in contact between hBN transferred to counterpart and hBN present in coated sample and provided easy to shearing capability at the interface due to the lamellar structure. A relatively higher coefficient of friction (Fig. 4.5) and wear rate (Fig. 4.6) in NAMB10 in comparison to NAMB5 may be due to the increased amount of hBN which has poor integration properties in the matrix leading to more porosity and reduced hardness of coating. It has been reported (Du et al., 2010) that hBN has a poor wettability with many metals which causes bond strength weakening effect and reduces the effectiveness of hBN in reducing friction when added beyond a certain limit. A reduced friction and wear in coatings having hBN reflects the synergistic action of hBN to work in conjunction with MoS_2 and Ag at room temperature.

Under the conditions used in the present investigation, the mechanism of wear in NAMB0 coating is a mixture of ploughing and delamination. The mechanism of wear in NAMB5 coatings are adhesion and transfer layer formation under all the loads, whereas for NAMB10 coating is a mix of adhesion and delamination.

4.3. HIGH TEMPERATURE TRIBOLOGICAL BEHAVIOR

The following section presents the results and discussion on the friction and wear behavior of NAMB0, NAMB5 and NAMB10 coatings at temperatures ranging from room temperature (RT) to 800 °C at a constant load of 5 N, and a fixed sliding speed of 0.3 m/s.

4.3.1 DRY SLIDING FRICTION AND WEAR

4.3.1.1 Dry Sliding Friction

(i) Variation of coefficient of friction with time

Figures 4.17 (a through e) illustrate the variation of coefficient of friction with time for NAMB0, NAMB5 and NAMB10 coatings at RT, 200, 400, 600 °C and 800 °C. All the coatings show a fluctuating trend of variation of coefficient of friction but with different amplitude of fluctuations depending on the type of the coating and test temperature. The amplitude of fluctuations is observed to be relatively high for all the coatings at RT and 400 °C than that observed for 200 °C as evident from a comparison of Figs. 4.17 (a, b and c). However, the amplitude of fluctuations is found to decrease at relatively higher temperatures of 600 and 800 °C for all the coatings in comparison to RT, 200 and 400 °C as evident from a comparison of Figs. 4.17 (a through e). At 800 °C

the variation of friction coefficient is relatively smooth for coatings containing hBN in comparison to the one without hBN. The friction coefficient shown by NAMB5 coating is the lowest during the complete duration of sliding at all the temperatures. Also, the NAMB5 coating is able to maintain a lower coefficient of friction around a value of 0.2 during the entire test.

(ii) Variation of average coefficient of friction with temperature

The variation of average coefficient of friction with temperature for all the composite coatings is demonstrated in Fig. 4.18. The average friction coefficient for NAMB0 coating decreases from RT to 200 °C and increases thereafter till 400 °C before decreasing again to a low value of 0.28 at 800 °C. The coefficient of friction of coatings containing hBN i.e., NAMB5 and NAMB10 is found to decrease continuously with increasing temperature from RT to 800 °C. However, NAMB5 composite coating has shown the lowest coefficient of friction at all the temperatures used in the study and the value of friction coefficient is observed to reach a value of 0.23.

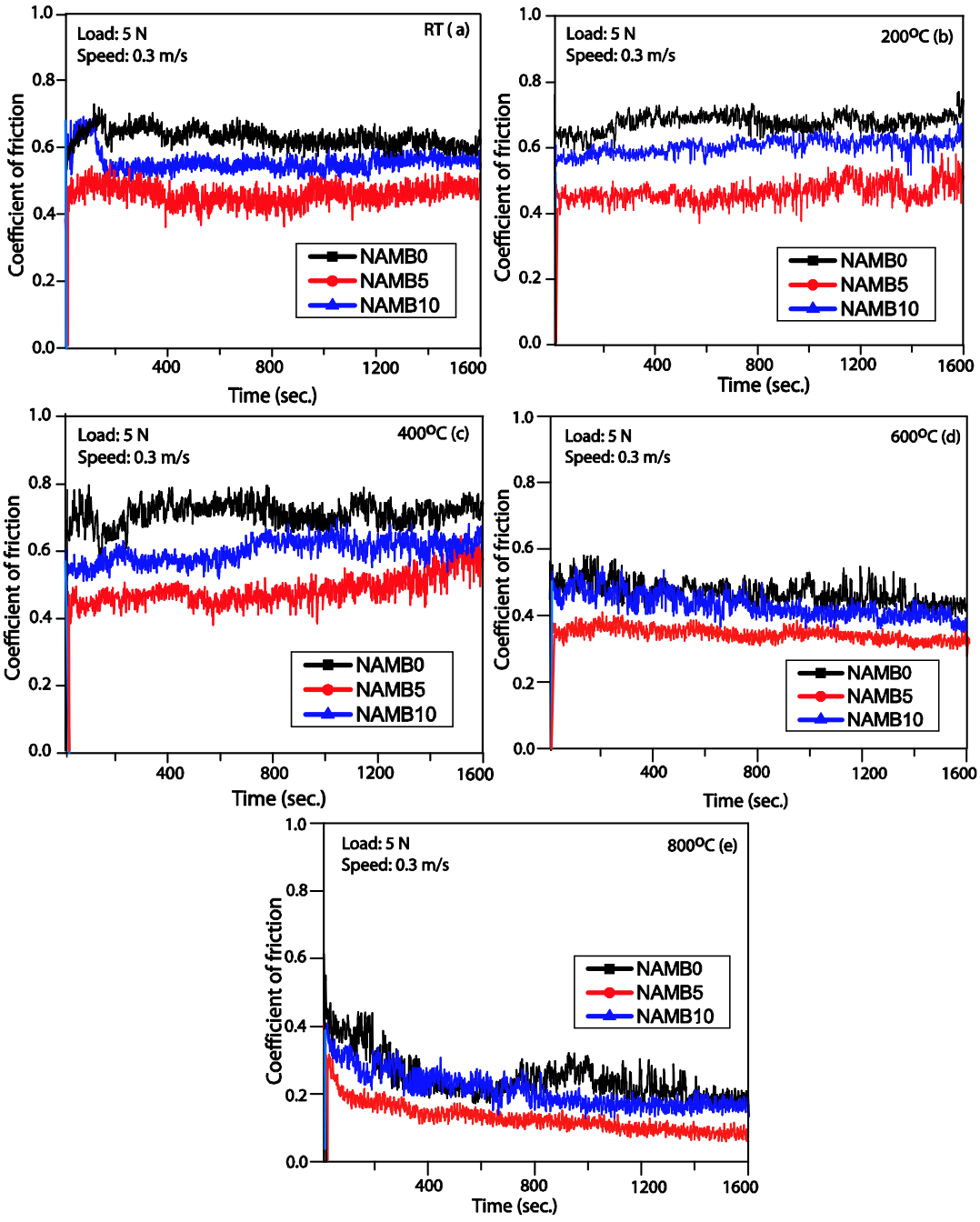

Fig. 4.17 Variation of coefficient of friction with time at (a) Room temperature (RT), (b) 200 °C, (c) 400 °C (d) 600 °C and (e) 800 °C for coatings.

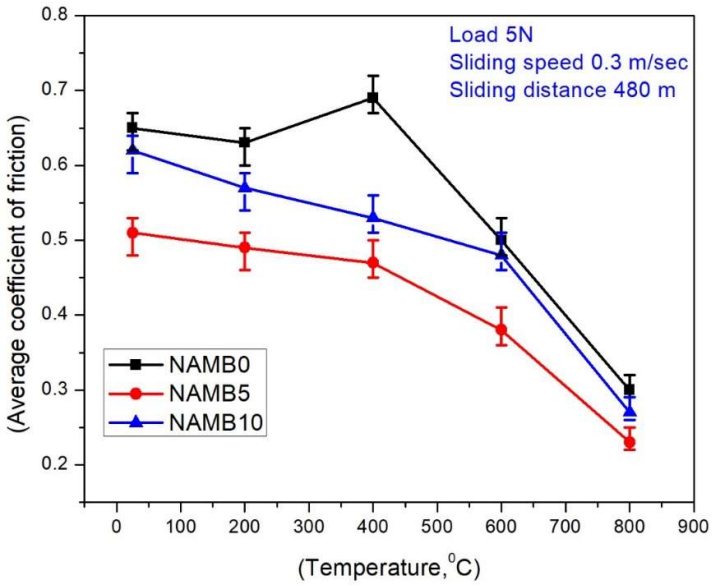

Fig. 4.18 Variation of average coefficient of friction with temperature for composite coatings.

4.3.1.2 Dry Sliding Wear

(i) Variation of wear rate with temperature

Figure 4.19 displays the variation of wear rate with respect to temperature for composite coatings slid against Al_2O_3 ball from RT to 800 °C. It could be seen that the wear rates are all of the order of 10^{-5} mm^3/Nm. The wear rate of NAMB0 composite coating decreases with the increase in temperature from RT to 200 °C, then it increases as the temperature is raised to 400 °C beyond which the wear rate decreases till 800 °C. However, the wear rate is observed to decrease continuously with increasing temperature from RT to 800 °C for the NAMB5 and NAMB10. Between these two coatings it is found that the composite coating NAMB5 possesses a better wear resistance indicating that 5wt. % hBN is good enough for reducing both friction and wear under the conditions used in the present investigation.

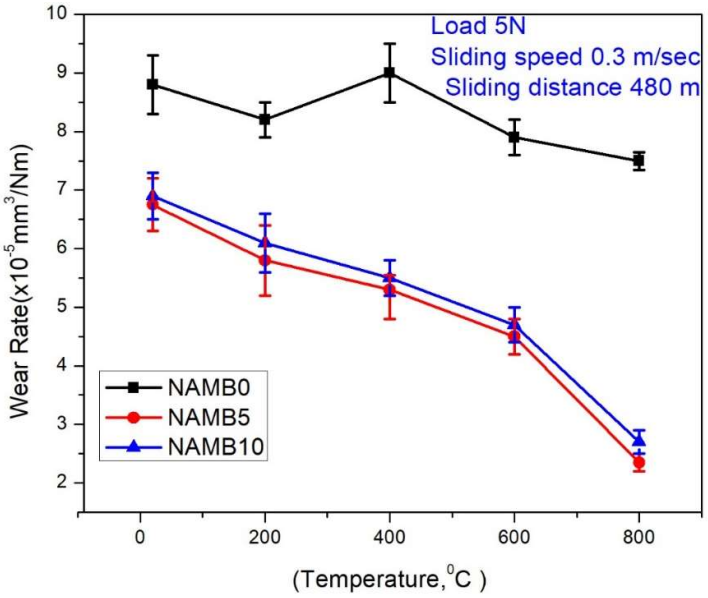

Fig. 4.19 Variation of wear rate with temperature for all the coatings.

4.3.2 EXAMINATION OF SLIDING SURFACES

Figures 4.20, 4.21 and 4.22 present SEM micrographs of worn surfaces of NAMB0, NAMB5 and NAMB10 coatings at RT, 200, 400, 600 °C and 800 °C, respectively. At room temperature, the worn surface of the NAMB0 composite coating shown in Fig. 4.20 (a) appears to be covered with patchy transfer layer on which some loose debris particles could be clearly seen. The surface worn at 200 °C (Fig. 4.20 b) has some wear marks in the direction of sliding along with some grooves and some loose wear particles at several locations. The surface worn at 400 °C (Fig. 4.20 c) shows some deeper wear grooves along with the presence of a transfer layer probably of oxides, whereas at 600 °C (Fig. 4.20 d) the surface is covered with a glazed layer at a few places. The surface worn at 800 °C (Fig. 4.20 e) is covered with a glaze layer at several locations which might have inhibited the direct contact between the alumina ball and the coating.

Figures 4.21 (a through e) show the morphologies of the worn surface of NAMB5 coating after testing at RT, 200, 400, 600 °C and 800 °C, respectively. At room temperature the worn surface is covered by a compacted transfer layer at several locations with no visible sign of wear tracks on the surface. At 200 °C, the worn surface shows the presence of very small wear particles with a compact transfer layer, whereas at 400 °C, the worn surface shows the presence of wear tracks covered with a well compacted tribo-layer at several locations along with some oxide layer (Fig. 4.21 c). However, one can observe the presence of a very smooth and compacted tribo-layer on the surface of NAMB5 coating worn at temperatures of 600 and 800 °C as seen in Figs. 4.21 (d) and (e). Also, the extent of compaction of tribo-layer appears to be more in case of the surface worn at 800 °C in comparison to the one worn at 600 °C.

Figures 4.22 (a through e) elucidate the worn surface morphologies of NAMB10 coating slid at RT, 200, 400, 600 °C and 800 °C. The worn surface at RT presents some relatively fine wear marks along with the presence of transfer layer of wear debris as seen in Fig. 4.22 (a). At 200 °C, the worn surface (Fig. 4.22 b) has fine wear debris particles distributed over the surface along with the presence of a loose transfer layer in the direction of sliding whereas the surface worn at 400 °C (Fig. 4.22 c) reveals the presence of a well compacted transfer layer covering the wear tracks. The surfaces worn at 600 and 800 °C, (Fig. 4.22 d and e) show the presence of well compacted and glazed tribo-layer but with different area of coverage. The extent of cover provided by the glazed layer appears to more at 800 °C (Fig. 4.22 e) than 600 °C (Fig. 4.22 d).

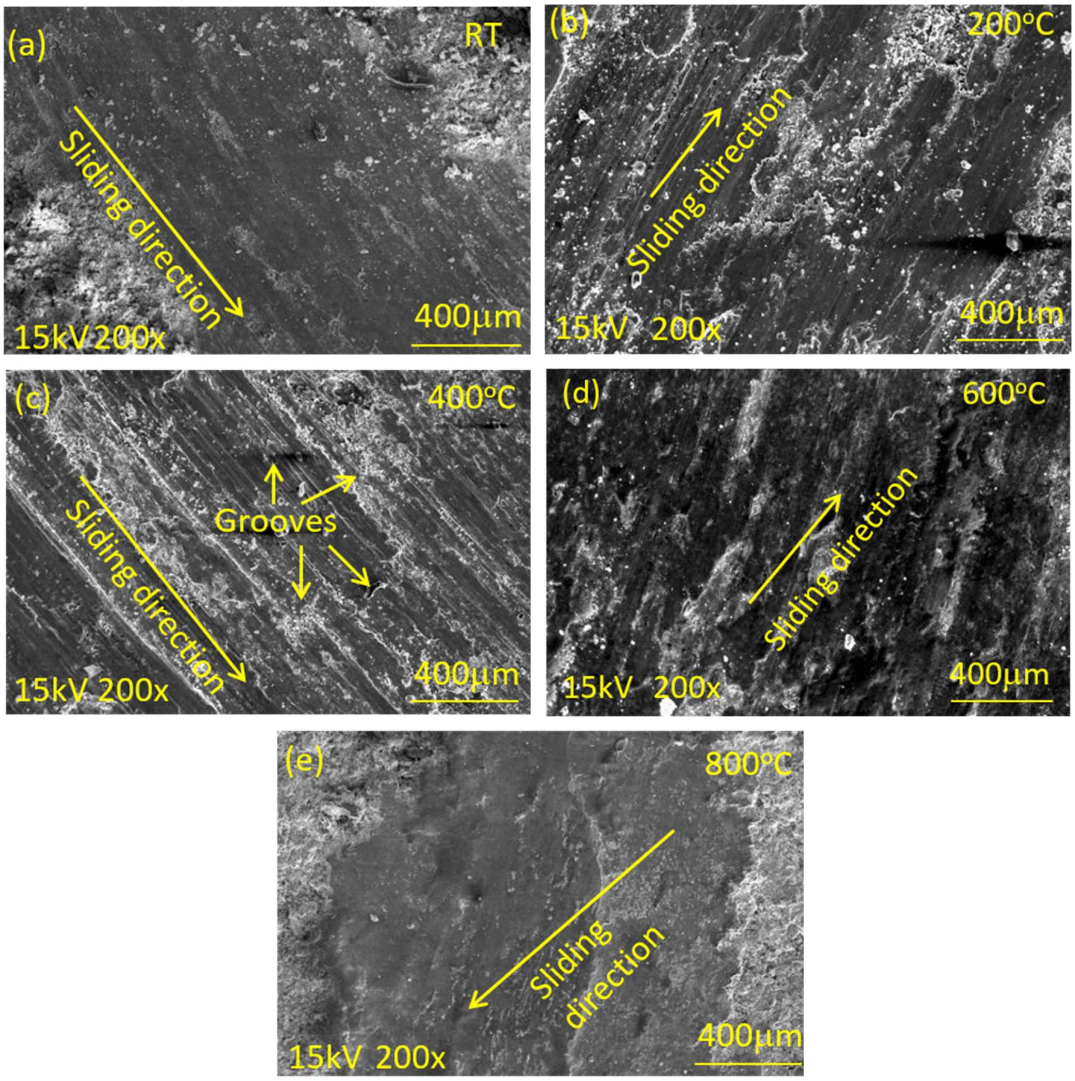

Fig. 4.20 SEM images of worn surfaces of NAMB0 coating at: (a) RT; (b) 200 °C; (c) 400 °C; (d) 600 °C and (e) 800 °C.

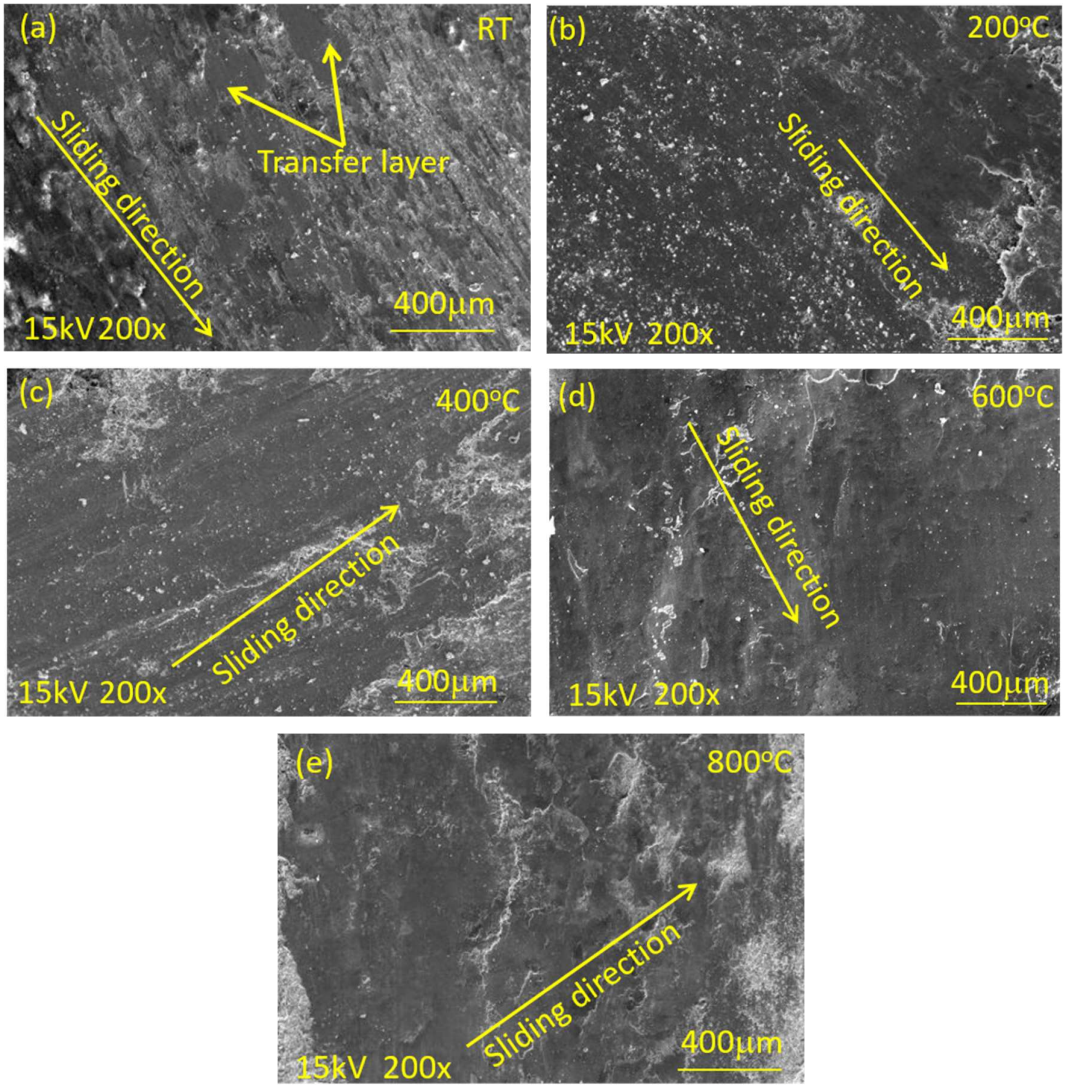

Fig. 4.21 SEM images of worn surfaces of NAMB5 composite coating at (a) RT; (b) 200 °C (c) 400 °C; (d) 600 °C and (e) 800 °C.

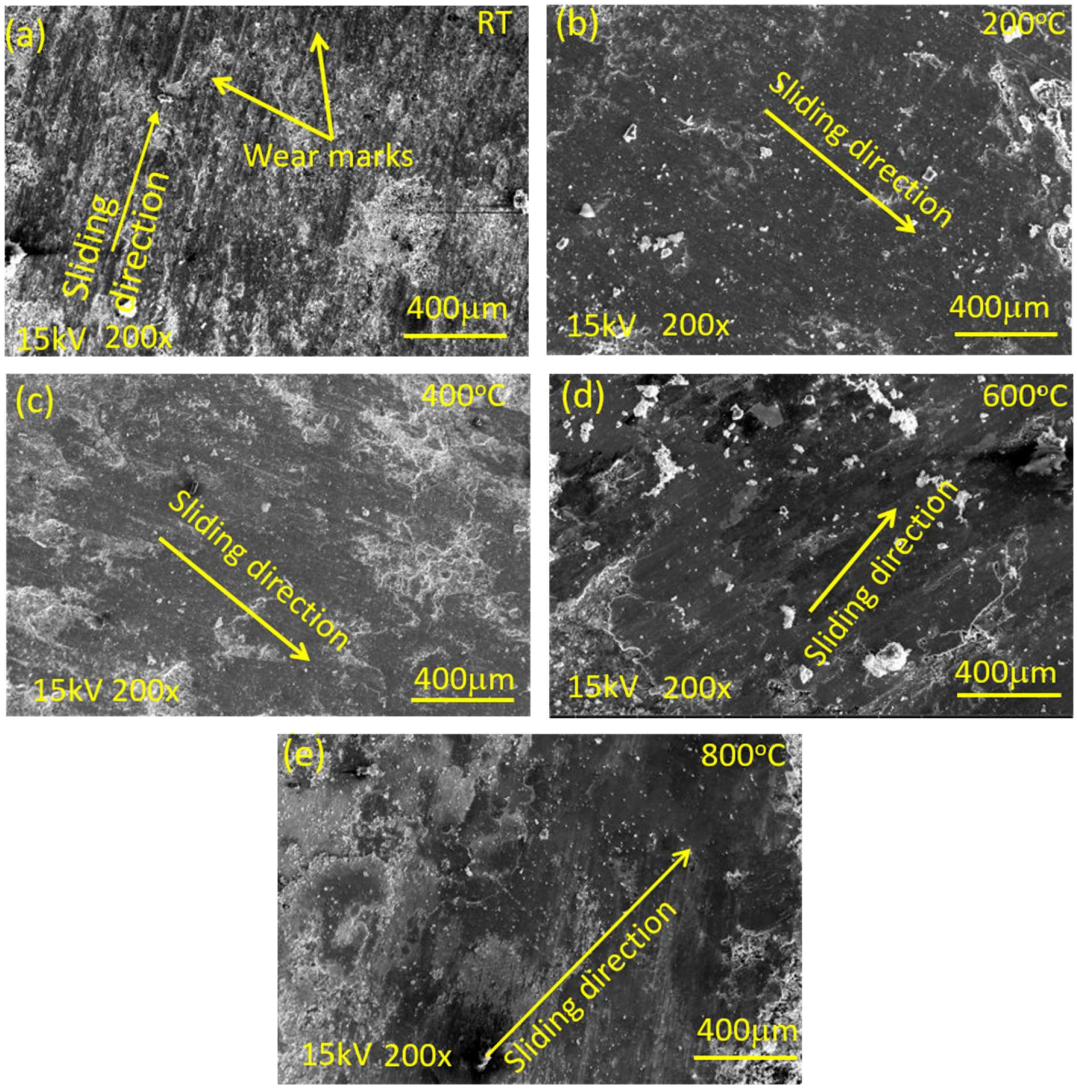

Fig. 4.22 SEM images of worn surfaces of NAMB10 composite coating at: (a) RT; (b) 200 °C; (C) 400 °C; (d) 600 °C and (e) 800 °C.

The morphologies of worn surfaces of alumina ball slid against NAMB0 composite coating under RT, 200, 400, 600 °C and 800 °C are illustrated in Fig. 4.23 (a through e). The transfer of material from coated specimen can be observed on the counterface alumina ball which has been confirmed by EDS analysis. However, the EDS spectrums are not included here. Fig. 4.23 (a) corresponding to room temperature shows some abrasive marks in the direction of sliding. At 200 °C, Fig. 4.23 (b) shows the presence of a compacted layer with some abrasive marks in the direction of sliding,

whereas Fig. 4.23 (c) at 400 °C presents a rough and broken surface with detachment of transferred coating material. The worn surface of alumina ball at 600 °C given in Fig. 4.23 (d) reveals the presence of a compacted transfer layer. The worn surface of alumina ball slid against NAMB0 coating at 800 °C is covered with a relatively smooth and well compacted layer of transferred coating material as seen from Fig. 4.23 (e).

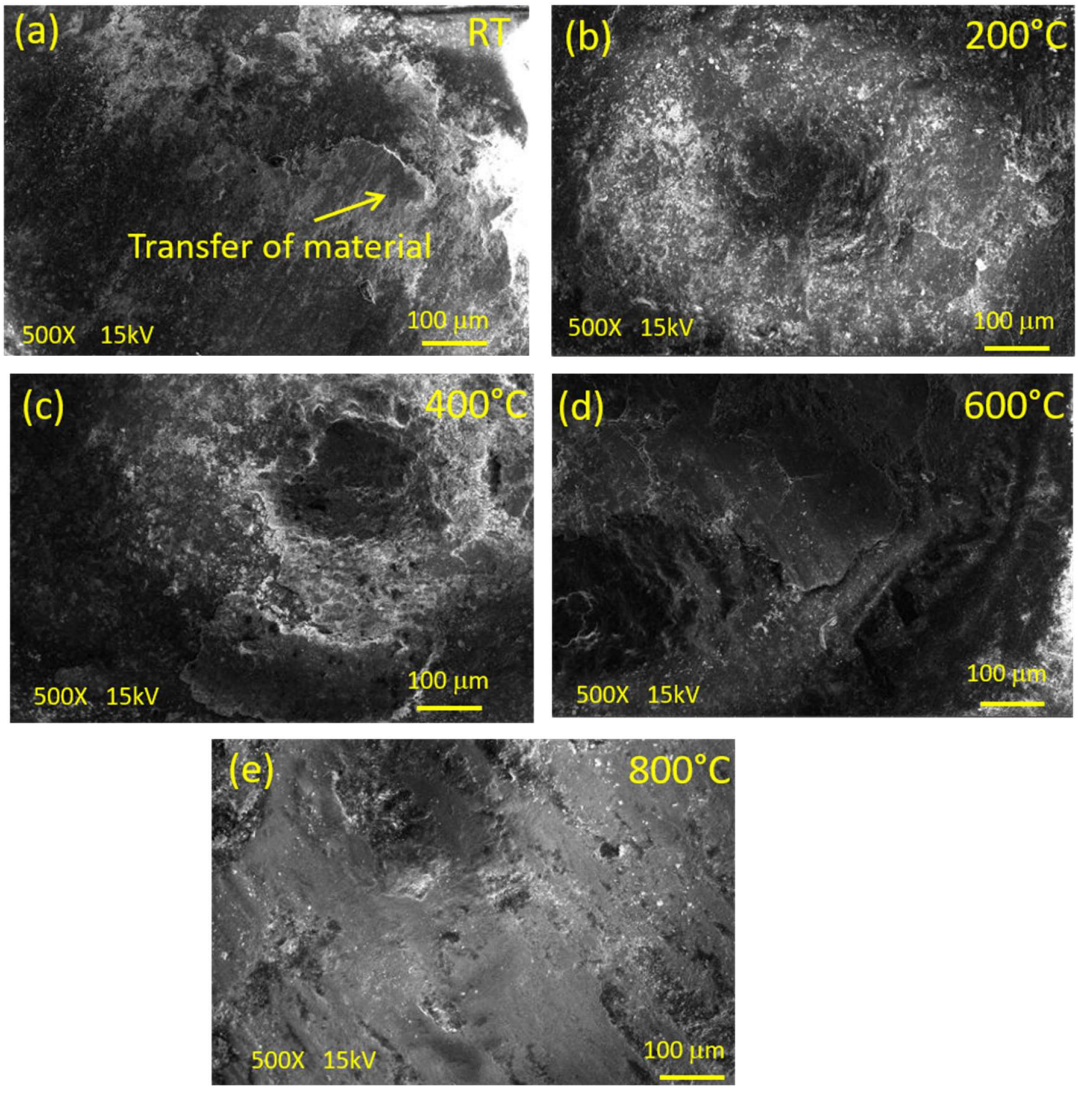

Fig. 4.23 SEM images of worn surface alumina ball slid against NAMB0 composite coating :(a) RT; (b) 200 °C; (C) 400 °C; (d) 600 °C and (e) 800 °C.

The worn surface morphologies of alumina ball slid against NAMB5 composite coating at RT, 200, 400, 600 °C and 800 °C, respectively, are presented in Fig. 4.24 (a to e). Fig. 4.24 (a) presents some loosely adhered and patchy transfer layer along with signs of detachment of the material which got transferred from the coated surface to ball at a few places. At 200 °C, Fig. 4.24 (b), the worn surface of the alumina ball is covered with a compacted layer at few places with some abrasive marks in the direction of sliding. However, Figs. 4.24 (c), (d) and (e) reveal some well compacted and smooth plateaus of transfer layer containing materials transferred from coating. The degree of compaction of the transfer layer and the extent of coverage provided by this layer to the underlying surface depend on the temperature, being more at relatively higher temperatures. The transfer of material (including hBN) from coated specimen to the counterface alumina has been confirmed by the EDS analysis of the surfaces of ball worn under different temperatures.

SEM images of worn surfaces of alumina ball slid against NAMB10 composite coating are shown in Figs. 4.25 (a to e). The worn surface of alumina ball shown in Fig. 4.25 (a) corresponding to RT reveals the presence of a smooth layer which appears to have cracked at few locations along with some abrasive marks. Fig. 4.25 (b), at 200 °C shows some fine abrasive marks along with the transferred coating materials in the direction of sliding whereas, Figs. 4.25 (c) at 400 °C show a relatively rough morphology containing loosely bound transferred material without any evidence of compaction. The surfaces worn at 600 and 800 °C also appear to be covered with a relatively loosely bound material transferred from the coated surface as seen from Figs. 4.25 (d and e) but coverage is more in Fig. 4.25 (e) in comparison to that in Fig. 4.25 (d). Again, the transfer of coating material to the counterface has been confirmed by EDS analysis.

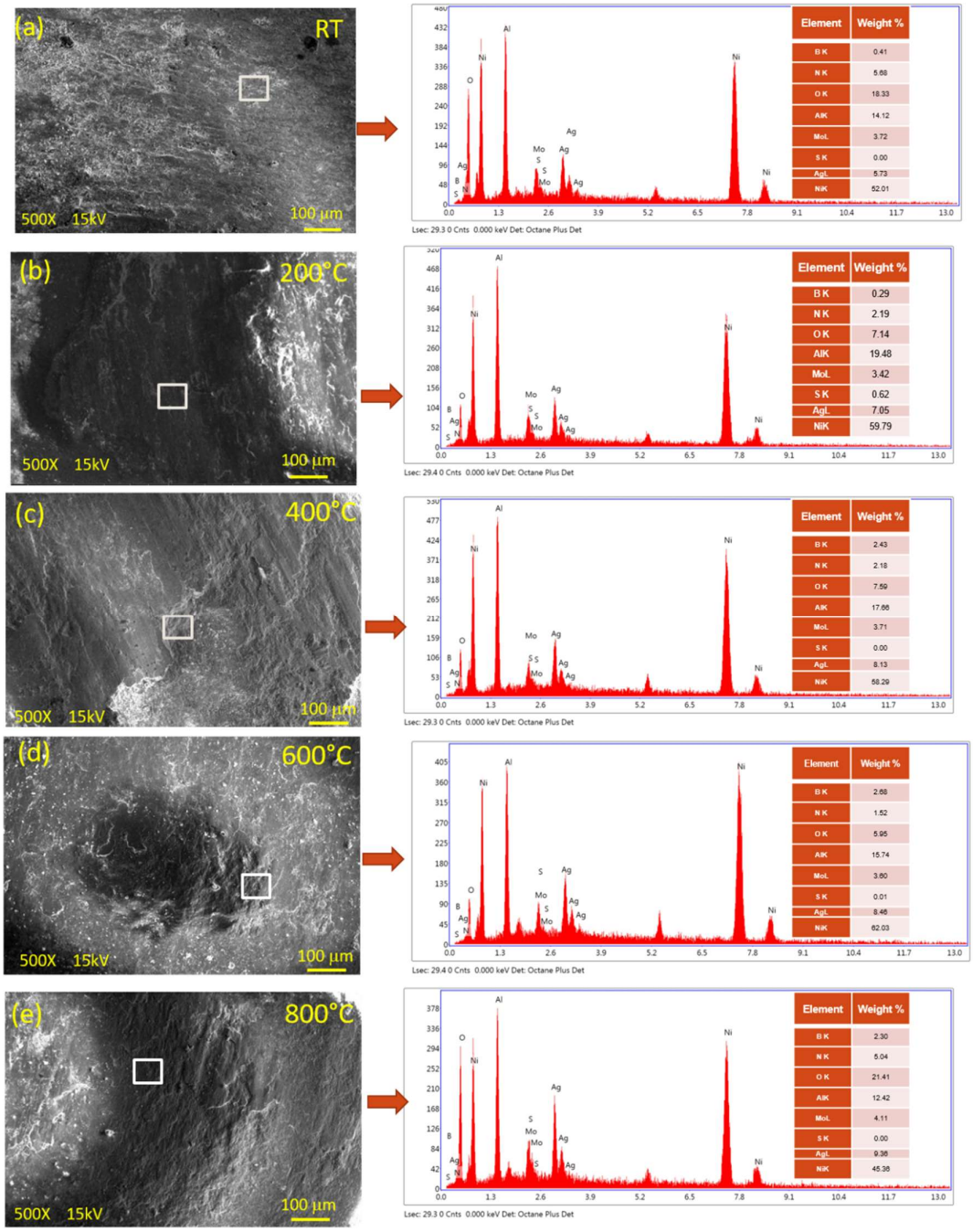

Fig. 4.24 SEM images of worn surface alumina ball slid against NAMB5 composite coating :(a) RT; (b) 200 °C;(c) 400 °C; (d) 600 °C and (e) 800 °C and corresponding EDS spectrums.

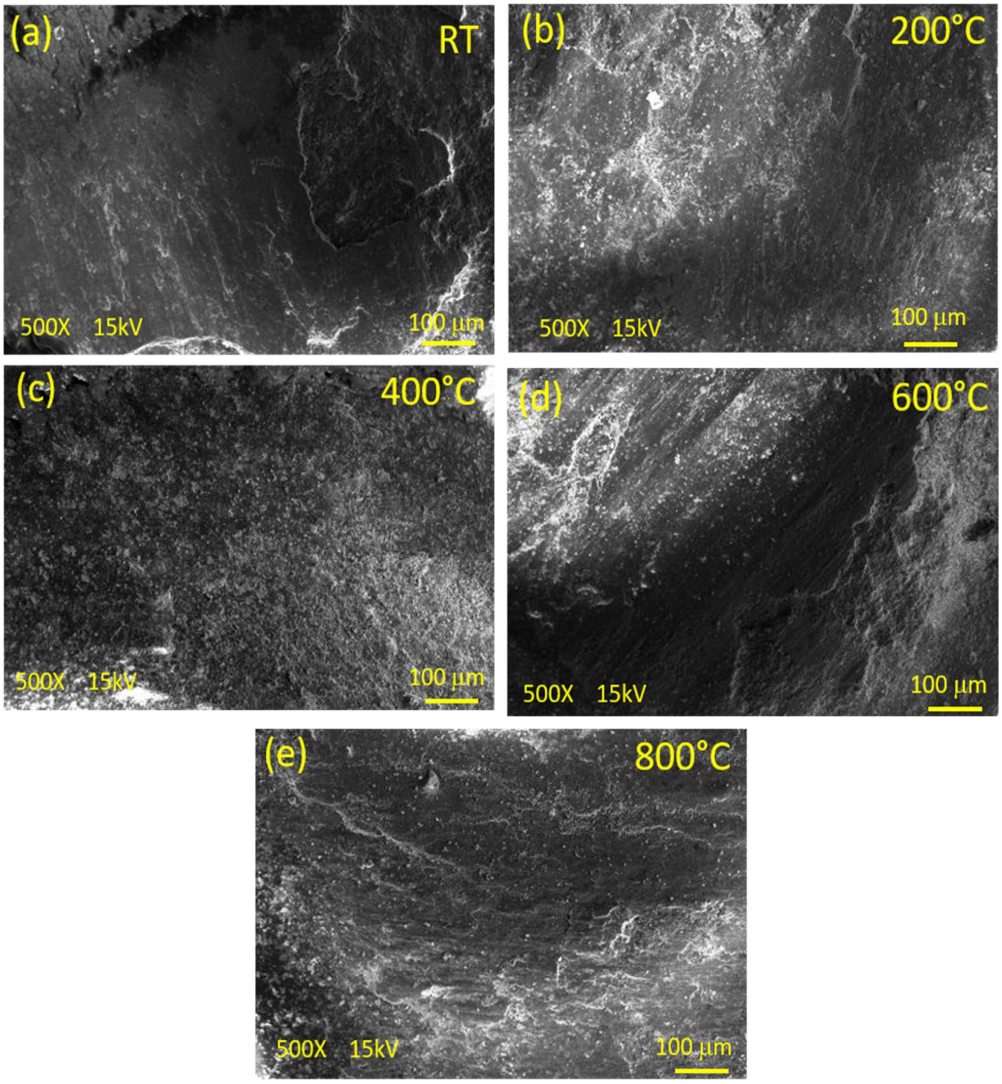

Fig. 4.25 SEM images of worn surface alumina ball slid against NAMB10 composite coating :(a) RT; (b) 200 °C; (C) 400 °C; (d) 600 °C and (e) 800 °C.

Figs. 4.26 (a to c) show the X-ray diffraction patterns of NAMB0, NAMB5 and NAMB10 worn at different temperatures used in present study. The diffraction patterns for all the coatings after friction tests at RT, 200 and 400 °C show the presence of peaks which are similar to as-sprayed coatings given in Fig. 4.2.The worn surface mainly contains Ni_3Al (JCPDF file no.65-3245), Ag (JCPDF file no.89-3722), NiAl (JCPDF file no.65-0431), $NiMoO_4$ (JCPDF file no.86-0362), Ni (JCPDF file no.03-1051), hBN (JCPDF file no. 85-1068). Furthermore, the new diffraction peaks of MoO_3

and $Ag_2Mo_4O_{13}$ are found at 600 °C. After the 800 °C tribological testing, the diffraction peaks corresponding to the presence of $Ag_2Mo_2O_7$ (JCPDS file no. 75-1505), Ag_2MoO_4 (JCPDS file no. 76-1747) and NiO (JCPDS file no. 89-7390) which form through the tribo-reactions during the friction process at this temperature could also be seen in the patterns. The molybdates of silver and NiO have been shown to provide effective lubrication at elevated temperatures (Liu et al., 2012, 2013).

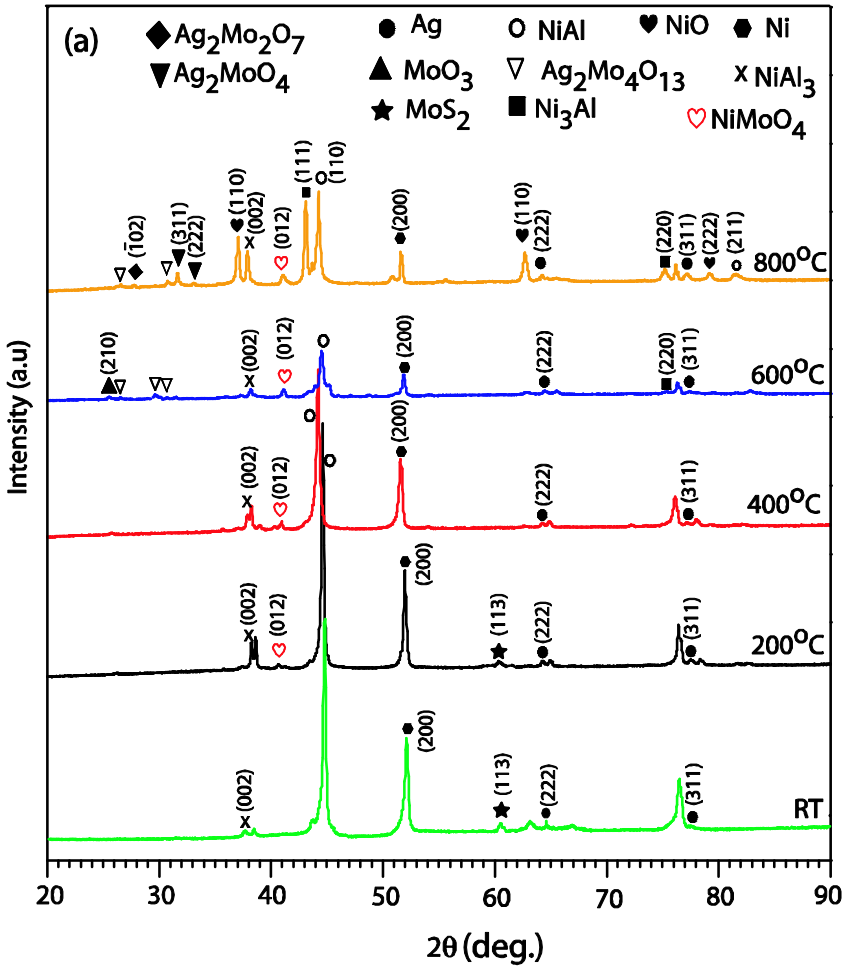

Fig. 4.26 (a) XRD patterns of wear track of NAMB0 composite coatings at different test temperatures under 0.3 m/s speed.

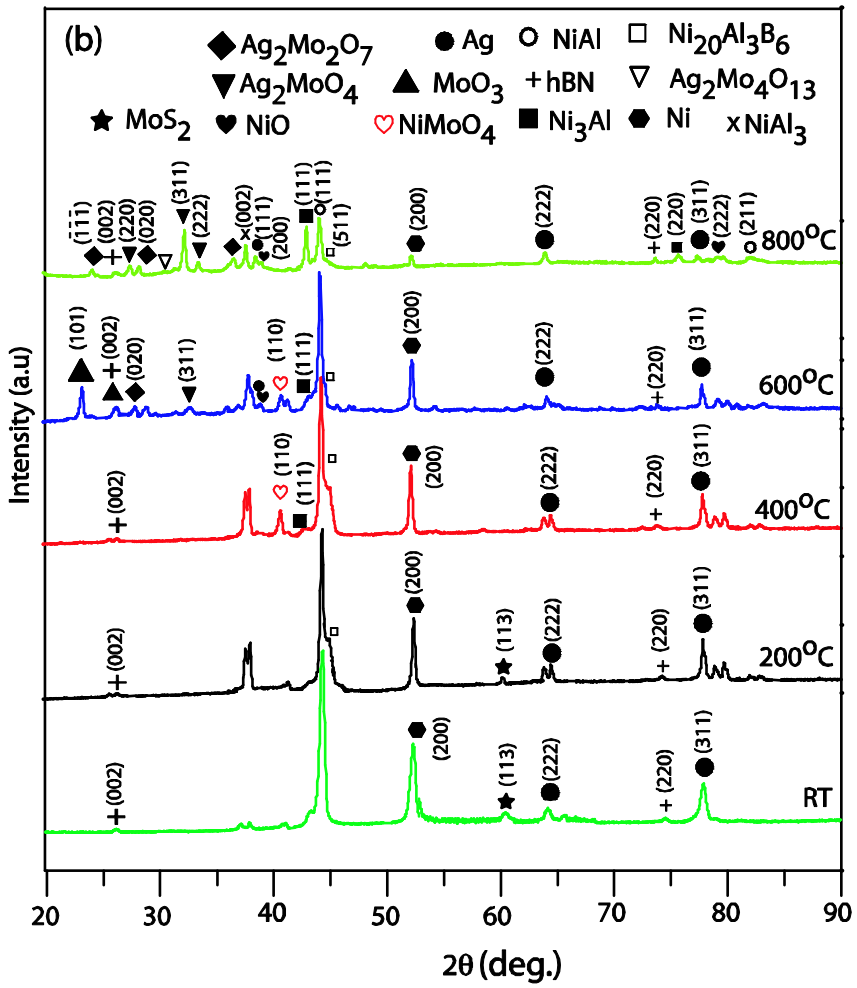

Fig. 4.26 (b) XRD patterns of wear track of NAMB5 composite coatings at different test temperatures under 0.3 m/s.

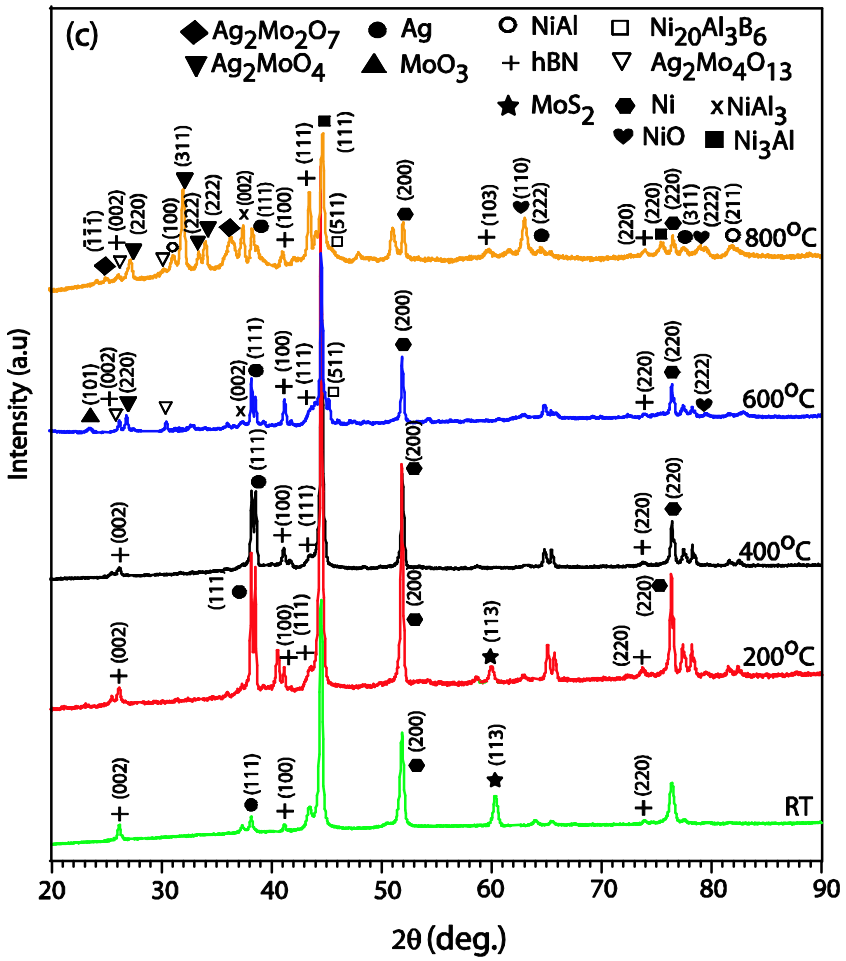

Fig. 4.26 (c) XRD patterns of wear track of NAMB10 composite coatings at different test temperatures under 0.3 m/s speed.

The worn surfaces of the coating have also examined under Raman spectroscopy to reveal the presence of new phases formed during sliding which might have not been detected through X-ray diffraction due to their low amount. Figure 4.27 presents the micro-Raman spectra of worn tracks of the composite coatings (a) NAMB0 (b) NAMB5 and (c) NAMB10 at different test temperatures i.e., RT, 200, 400, 600 and 800 °C at a sliding speed of 0.3 m/s. Only a broad peak of Ag_2MoO_4 is seen on the tracks worn at RT, 200 and 400 °C, whereas the peaks corresponding to MoO_3, Ag_2MoO_4, $NiMoO_4$ and NiO could be observed on the surface of NAMB0 coating worn at 600 °C. However, peaks of Ag_2MoO_4, $Ag_2Mo_4O_{13}$, $Ag_2Mo_2O_7$, NiO and $NiMoO_4$ have been

found to be present at 800 °C which reflects the occurrence of tribo-chemical reactions during the sliding process leading to the formation of lubricious compounds like silver and nickel molybdates.

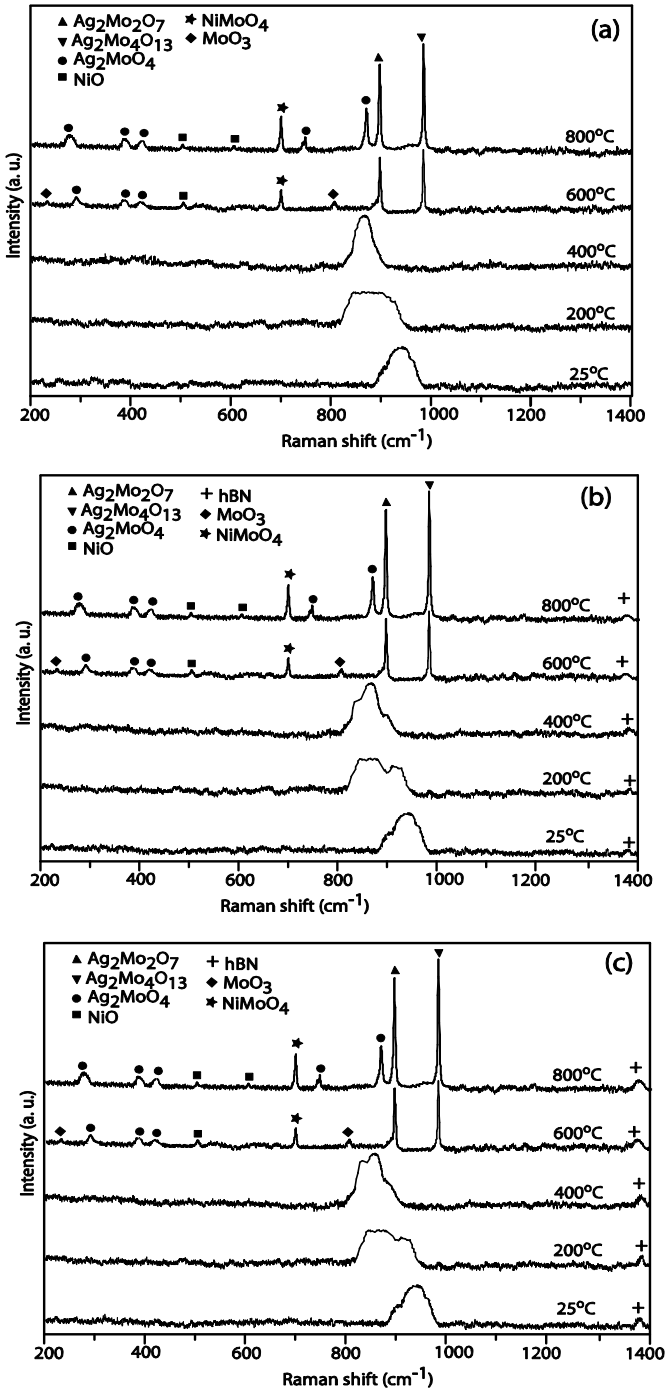

Fig. 4.27 Raman spectra of worn tracks of the composite coatings (a) NAMB0 (b) NAMB5 (c) NAMB10 after sliding at different test temperatures.

4.4 DISCUSSION

All the coatings show a fluctuating trend of variation of coefficient of friction with time but with varying amplitude of fluctuations depending on the testing temperature and the type of the coating. The amplitude of fluctuations is observed to be relatively high for all the coatings at RT and 400 °C than that observed for 200 °C as evident from a comparison of Figs. 4.17 (a, b and c). However, the amplitude of fluctuations is found to reduce at elevated temperatures 600 and 800 °C for all the coatings in comparison to RT, 200 and 400 °C which could be seen from a comparison of Figs. 4.17 (a through e). At 800 °C the variation of coefficient of friction is relatively smooth for coatings containing hBN in comparison to the one without hBN. The fluctuations in the variation of friction coefficient with time may be attributed to the initial roughness of the mating bodies which gets eventually smoothened as the sliding progresses and the surfaces attain better compatibility. A relatively larger amplitude of fluctuations at RT, 200 and 400 °C in comparison to 600 and 800 °C may be explained on the basis of the SEM micrographs of the worn surfaces of coatings shown in Figs.4.20 (a, b, c), 4.21 (a, b, c), 4.22 (a, b, c) and alumina ball given in Figs. 4.23 (a, b, c), 4.24 (a, b, c) and 4.25 (a, b, c) which present a relatively rough surface with abrasive marks in the direction of sliding and the presence of a discontinuous and loosely bound layer of transferred material. On the other hand the SEM micrographs of surfaces of coatings illustrated in Figs. 4.20 (d, e), 4.21 (d, e), 4.22 (d, e) and alumina ball depicted in Figs.4.23 (d, e), 4.24 (d, e), 4.25 (d, e) worn at 600 and 800 °C reveal the presence of a smooth and compacted transfer layer on the worn surface which might have diminished the amplitude of fluctuations at these temperatures. Also, the coefficient of friction shown by NAMB5 coating is consistently lower at each temperature in comparison to NAMB10 coating as evident from Figs. 4.17 (a through e). The coefficient of friction shown by NAMB0 coating is the highest among all the coatings

and it has shown the highest value of friction coefficient at 400 °C beyond which the friction is observed to decrease with increasing temperature till 800 °C as seen from Fig. 4.18. An increase in coefficient of friction in NAMB0 from 200 °C to 400 °C may be attributed to the loss of lubricating action of MoS_2 as indicated by Chen et al. (2013) also, giving rise to adhesion as evident from the worn surface of NAMB0 coating shown in Fig. 4.20 (c). However, beyond this temperature the silver and Mo react to form silver molybdates which are effective in reducing the friction. The presence of Ag_2MoO_4, Ag_2MoO_7 and NiO which are high temperature lubricants, on the worn surface as revealed by the XRD and Raman Spectrum of worn track as shown in Figs. 4.26 and 4.27 might have reduced the friction beyond 400 °C in NAMB0 coating. The presence of glaze and a compacted transfer layer at 600 °C and 800 °C on the worn surface of NAMB0 coating shown in Figs. 4.20 (d), (e) may also explain the decrease in friction at elevated temperature. One may also observe significant reduction in coefficient of friction with the addition of 5 wt. % hBN in the coating which is evident from the comparison of COF shown by NAMB0 and NAMB5 in Fig. 4.18. However, the friction coefficient is found to be more for NAMB10 (containing 10 wt. % hBN) in comparison to NAMB5 but it is still lower than that shown by NAMB0. A decreased COF for coatings containing hBN may be due to the synergetic action of hBN in conjunction with Ag and MoS_2 which might have provided the enhanced lubricity at all the temperatures right from RT to 800 °C in NAMB5 and NAMB10. A continuous decrease in coefficient of friction for coatings containing hBN i.e., NAMB5 and NAMB10 also reflects the effectiveness of hBN as a high temperature solid lubricant. The reduced coefficient of friction in NAMB5 and NAMB10 in comparison to NAMB0 may also be explained on the basis of the morphology of worn surface of these coatings given in Figs. 4.20 to 4.22 and the counterface alumina ball (Figs. 4.23 to 25) slid against these coatings at different

temperatures. The worn surfaces of coatings (Figs. 4.20 to 22) show the presence of loose wear debris particles, scoring marks along with the presence of a transfer layer which is either loosely bound or is well compacted. Also the extent of cover provided by the transfer layer to the underlying surface is different depending on the respective coating and temperature. The detachment or cracking of transfer layer could also be seen in some micrographs particularly for NAMB0 and NAMB10 coatings. Similar, features have also been observed on the worn surfaces of alumina ball as illustrated in Figs. 4.23 to 25 which also show the presence of a layer of transferred material from coated surface. A decreasing coefficient of friction in NAMB5 and NAMB10 may be explained on the basis of the formation of transfer layer, its degree of compaction, the extent of coverage over the surface and cracking of this layer depending on the test temperature and coating. At relatively low temperatures i.e., RT and 200 °C the layer is discontinuous and loosely bound (Figs. 4.21 a, b and 4.22 a, b) whereas at elevated temperatures the transfer layer (Figs. 4.21 d, e, f and 4.22 d, e, f) is relatively more compact and continuous and covers a larger area which effectively inhibits the direct contact between the mating surfaces and reduces the friction coefficient. However, a higher coefficient of friction shown by NAMB10 in comparison to NAMB5 may be attributed to the increased amount of hBN which deteriorates the performance because of the poor sintering characteristics and therefore, results in a relatively poor compaction of transfer layer which can be judged by a comparison of Figs. 4.21 and 4.22. This poorly compacted layer on NAMB10 is liable to get detached easily giving rise to lose wear debris and the direct contact between mating bodies, both of which help in raising the friction. Also, the formation of well compacted transfer layer and the glaze at 600 °C and 800 °C shown in Figs.4.21 (d, e) and Figs.4.22 (d, e) reduces the friction with increasing temperature by inhibiting the direct contact between the coating and the counterpart alumina ball while simultaneously providing a

layer of low shearing capability at the interface. Several researchers (Hou et al., 2015, Li et al., 2016, Li et al., 2017 and Chen et al., 2013) have reported that formation of glaze layers is beneficial in reducing friction and wear at elevated temperatures, hence the observations of the present study are in consonance with earlier findings. The other reason for a relatively lower coefficient of friction in NAMB5 and NAMB10 in comparison to that observed for NAMB0, may be ascribed to the transfer of hBN to the counterface alumina ball shown in Fig. 4.24 (a to e) and Fig. 4.25 (a to e) which results in contact between transferred hBN and coating surface containing hBN and provides easy shearing capability due to lamellar structure of hBN. This may also explain a continued low coefficient of friction shown by NAMB5 coating during the entire duration of test at 800 °C as seen in Fig.4.17 (e). It is well known that occurrence of tribo-chemical reactions during sliding process, particularly at higher temperatures, results in formation of some oxides like MoO_3, NiO etc. and other new phases like Ag_2MoO_4, $Ag_2Mo_2O_7$, $Ag_2Mo_4O_{13}$ which are lubricious in nature. These oxides and molybdates of silver have been shown to act as friction reducing species by several researchers (Liu et al. 2012, 2013; Chen et al. 2013; Du et al., 2011 and Li et al., 2009). It has been reported that $Ag_2Mo_4O_{13}$ melts once temperature is low and becomes soft when temperature increases, and it formulates a film across the space separating the contacting pair during the friction process (Liu et al., 2012, 2013). The structure of Ag_2MoO_4 can be preserved as a layered structure that have a combination of Ag_2O and MoO_3 layers which further has a silver layer in between them. Due to its layered structure Ag_2MoO_4 offers an excellent high temperature lubricating capability. The structure of $Ag_2Mo_2O_7$ is just similar to Ag_2MoO_4 and the weak O-Ag-O bond existing in $Ag_2Mo_2O_7$ helps in lowering the friction coefficient at elevated temperatures. Chen et al. (2013) have also indicated that molybdate phases having layered structure have the ability to diminish friction coefficient and wear at

elevated temperatures. In the present investigation, the presence of NiO, MoO_3, $NiMoO_4$, Ag_2MoO_4, $Ag_2Mo_2O_7$, $Ag_2Mo_4O_{13}$ has been observed on the worn surface of coatings slid under relatively higher temperatures of 600 and 800 °C as evident from Fig. 4.26 (a, b and c). This may explain a lower coefficient of friction at these temperatures for all the coatings, in the light of the discussion presented above. It has been indicated that hBN is a promising solid lubricant which is thermally stable up to 900°C (Du et al., 2011). Since, all the coatings have the same amount of Ag and MoS_2, and hence a similar probability of formation of the lubricious phases mentioned above. Therefore, a lower coefficient of friction shown by the coatings containing hBN reflects the ability of hBN to work in conjunction with Ag and MoS_2 in decreasing the friction at elevated temperatures.

The wear rate for NAMB0 coating has been observed to decrease from room temperature to 200 °C followed by an increase till 400 °C beyond which the wear rate is found to decrease with increasing temperature as evident from Fig. 4.19. However, the wear rate of coatings containing hBN i.e., NAMB5 and NAMB10 has been found to decrease continuously with increasing temperature from RT to 800 °C as seen from Fig. 4.19. A decrease in wear rate of NAMB0 coating till 200 °C may be attributed to the lubrication provided by MoS_2 and the presence of a transfer layer on the worn surface of NAMB0 (Fig. 4.20 b) slid under a temperature of 200 °C whereas an increase in wear rate from 200 to 400 °C may be explained on the basis of the micrograph of the worn surface of this coating given in Fig. 4.20 (c) which shows the presence of wide grooves and the absence of a continuous tribo-layer on the surface which might have resulted in direct contact between alumina ball and coating and therefore, a higher volume loss. However, a decrease in wear rate beyond 400 °C may be attributed to the formation of silver molybdates and other high temperature lubricants and the glazed layer on the worn surface of NAMB0 (Fig. 4.20 d, e) which might have inhibited the direct contact between

ball and coating. The decreasing rate of wear for NAMB5 and NAMB10 coatings could be attributed to (i) the formation of Ni and Mo oxides, silver molybdates, (ii) the transfer of hBN to the counterface and (iii) the synergetic action of hBN in conjunction with Ag, MoS_2 at temperatures from RT to 400 °C. However, the formation of lubricious molybdates at 600 and 800 °C and their presence at the surface might have provided the effective lubrication leading to a reduction in wear rate, as explained earlier for friction coefficient. The other factor contributing to a continuous decrease in wear rate with increasing temperature may be the presence of the transfer layer, its degree of compaction and extent of coverage over the worn surface. The presence of transfer layer has been observed on the worn surface of coatings and the ball as well but it appears to be more compact in case of NAMB5 coating in comparison to NAMB10 which could be clearly seen from a comparison of Figs. 4.21 and 4.22. A loosely bound layer visible on the surface of NAMB10 (Fig. 4.22) is not as effective as a well compacted one (Fig. 4.21) in improving the friction and wear performance. Also, the extent of cover provided by the transfer layer is more in case of NAMB5 than in NAMB10 and this might have caused more hindrance to the direct contact between the mating bodies resulting in a reduced rate of wear. The worn surfaces of alumina ball shown in Figs. 4.24 and 4.25 reveal the presence of a transfer layer but this layer appears to have detached in case of ball slid against NAMB10 (Fig. 4.25) and this might have given rise to a direct contact of ball and coated surface. This may explain a relatively higher wear rate in coating NAMB10 (containing 10 wt. % hBN) in comparison to NAMB5 (containing 5 wt. % hBN) as evident from Figs. 4.18 and 4.19.

The mechanism of wear in NAMB0 coating has been found to be a mixture of ploughing and abrasion at room temperature (RT), whereas at 200 °C the combination of abrasion and adhesion. At 400 °C the tribo-oxidation and abrasion are dominated

mechanisms, while at 600 and 800 °C dominating wear mechanism is adhesive for this coating. For NAMB5 coating the operative mechanisms are adhesion from RT to 400 °C and glaze layer (tribo-layers) formation at elevated temperatures. The mechanism of wear for NAMB10 coating is abrasive at RT whereas a mix of adhesion and glaze layer (tribo-layers) formation at 600 and 800 °C in the current study.

Both the friction and the wear rate have been observed to decrease significantly at all the temperatures in NAMB5 coating as evident from Figs. 4.18 and 4.19. At the same time the presence of hBN has also been observed at all the temperatures on the counterface alumina ball. Under low temperature regime from RT to 400 °C, due to rubbing action even if the temperature at the interface might have gone beyond the effective lubricating regime of Ag and MoS_2, the more thermally stable hBN might have been acted as an effective lubricant in reducing the friction and wear consistently. Since, all the coatings contain same amounts of Ag and MoS_2 and have the lubricious silver and nickel molybdates present at the worn track as shown by XRD patterns and Raman spectrum given in Fig. 4.26 and Fig. 4.27 so a lower friction and wear shown by coatings containing hBN may be attributed to the presence of hBN which might have reduced the friction and wear over and above the reducing capability of molybdates. This clearly reflects the synergistic action of hBN in aiding the other lubricants like MoS_2 and Ag in improving the friction and wear performance of coating, not only at elevated temperatures but also at room temperature.

4.5 HIGH TEMPERATURE TRIBOLOGICAL BEHAVIOR OF COATINGS UNDER DIFFERENT SLIDING SPEEDS

The ensuing section highlights the results on the tribological behavior of NAMB0, NAMB5 and NAMB10 coatings under various sliding speeds (0.3, 0.5, 0.7 and 0.9 m/s) and temperatures (RT, 200, 400, 600, 800 °C). The observed friction and wear behavior has been discussed comprehensively with the help of the features present on the worn surfaces of coatings as well as counterface ball along with their X-ray diffraction patterns and Raman spectra.

4.5.1 DRY SLIDING FRICTION AND WEAR

(a) Dry Sliding Friction

(i) Variation of coefficient of friction with time

Figures 4.28 to 4.30 illustrate the typical variation of friction coefficient with time for NAMB0, NAMB5 and NAMB10 coatings at RT, 200, 400, 600 and 800 °C slid under sliding speeds of 0.3, 0.7 and 0.9 m/s, respectively. A similar behavior has also been observed for 0.5 m/s, hence, not included here. All the coatings are observed to show a fluctuating trend of variation at all the speeds and temperatures. However, the amplitude of fluctuation is found to decrease with increasing speed from 0.3 to 0.9 m/s which may be confirmed from a comparison of Figs. 4.28, 4.29 and 4.30. Also, NAMB5 coating has a relatively smoother variation in comparison to NAMB0 and NAMB10. The amplitude of fluctuations is relatively small for all the coatings at 200 °C in comparison to RT and 400 °C. At 400 °C, the NAMB5 coating has less fluctuations in COF in comparison to other coatings at the same temperature. However, the fluctuations in COF for all coatings

are found to decrease significantly as the temperature is increased to 800 °C. At 800 °C, the NAMB5 coating has very smooth variation of COF compared to NAMB0 coating. One may also observe that COF shown by NAMB5 coating is the lowest in comparison to other coatings at all the temperatures and speeds used in the present study.

(ii) Variation of average coefficient of friction with temperature

The variation of average COF with temperature at different speeds for NAMB0, NAMB5 and NAMB10 coatings is illustrated in Fig. 4.31 (a through d). The trend of variation of COF is observed to be same for NAMB0 at different speeds namely, 0.3, 0.5, 0.7 and 0.9 m/s. The average COF for NAMB0 coating is observed to first decrease from RT to 200 °C followed by an increase till 400 °C, beyond which a significant decrease is found to occur till 800 °C and COF reaches a value of 0.28 at 800 °C for 0.3 m/s speed. The coefficient of friction has been observed to decrease consistently with increasing temperature for both NAMB5 and NAMB10 at all the speeds. However, NAMB5 has the lowest COF at all the temperatures and all the speeds in comparison to other coatings. The COF shown by NAMB0 is the highest whereas that shown by NAMB5 coating is the lowest at all the temperatures (RT, 200, 400, 600 and 800 °C) and speeds (0.3, 0.5, 0.7 and 0.9 m/s). The COF for NAMB10 is observed to lie in-between the values shown by NAMB0 and NAMB5. The lowest value of coefficient of friction shown by NAMB5 is 0.1 at 0.7 m/s and 800 °C.

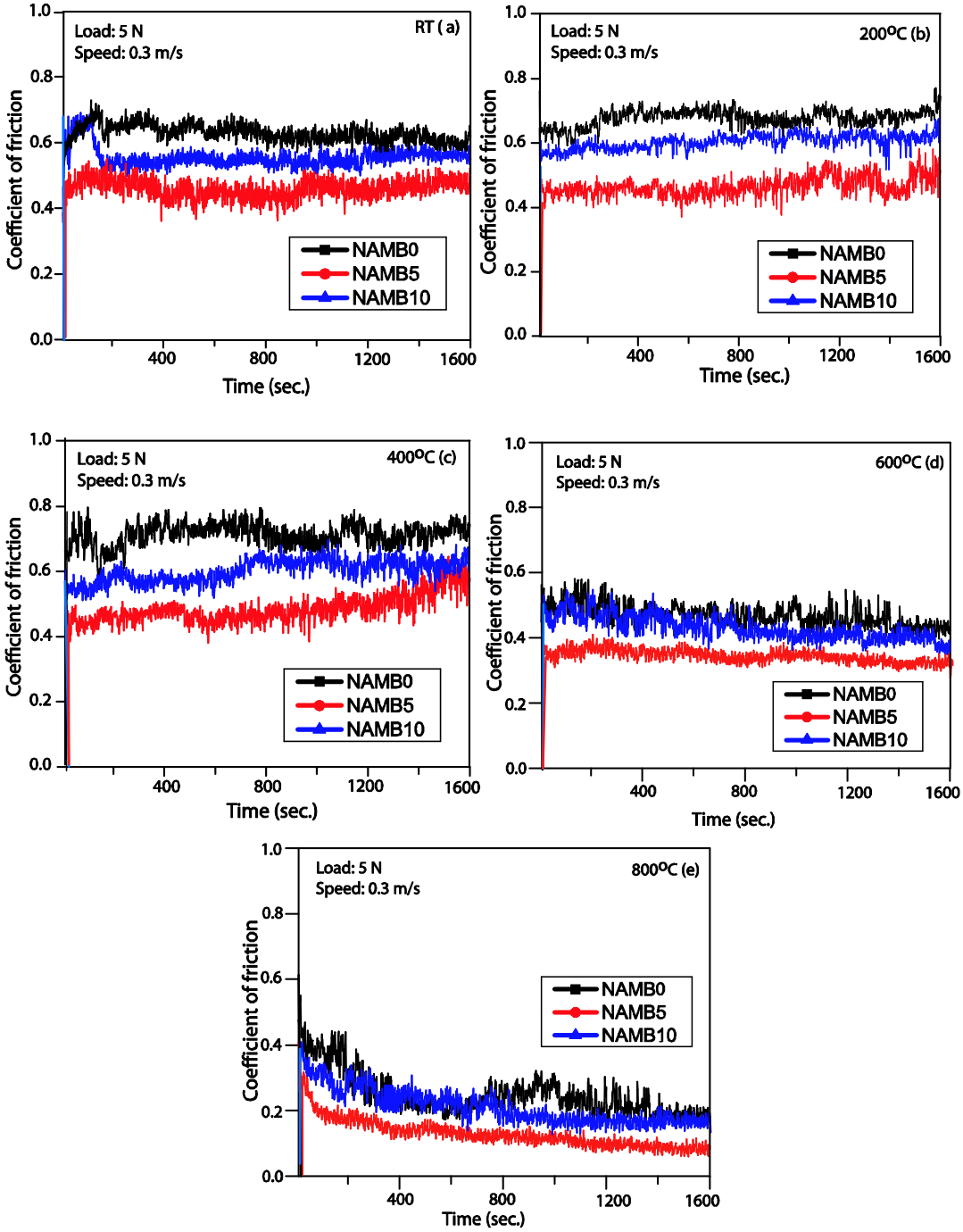

Fig. 4.28 Variation of coefficient of friction with time at (a) RT, (b) 200 °C; (c) 400 °C; (d) 600 °C; and (e) 800 °C for coatings under 0.3 m/s speed.

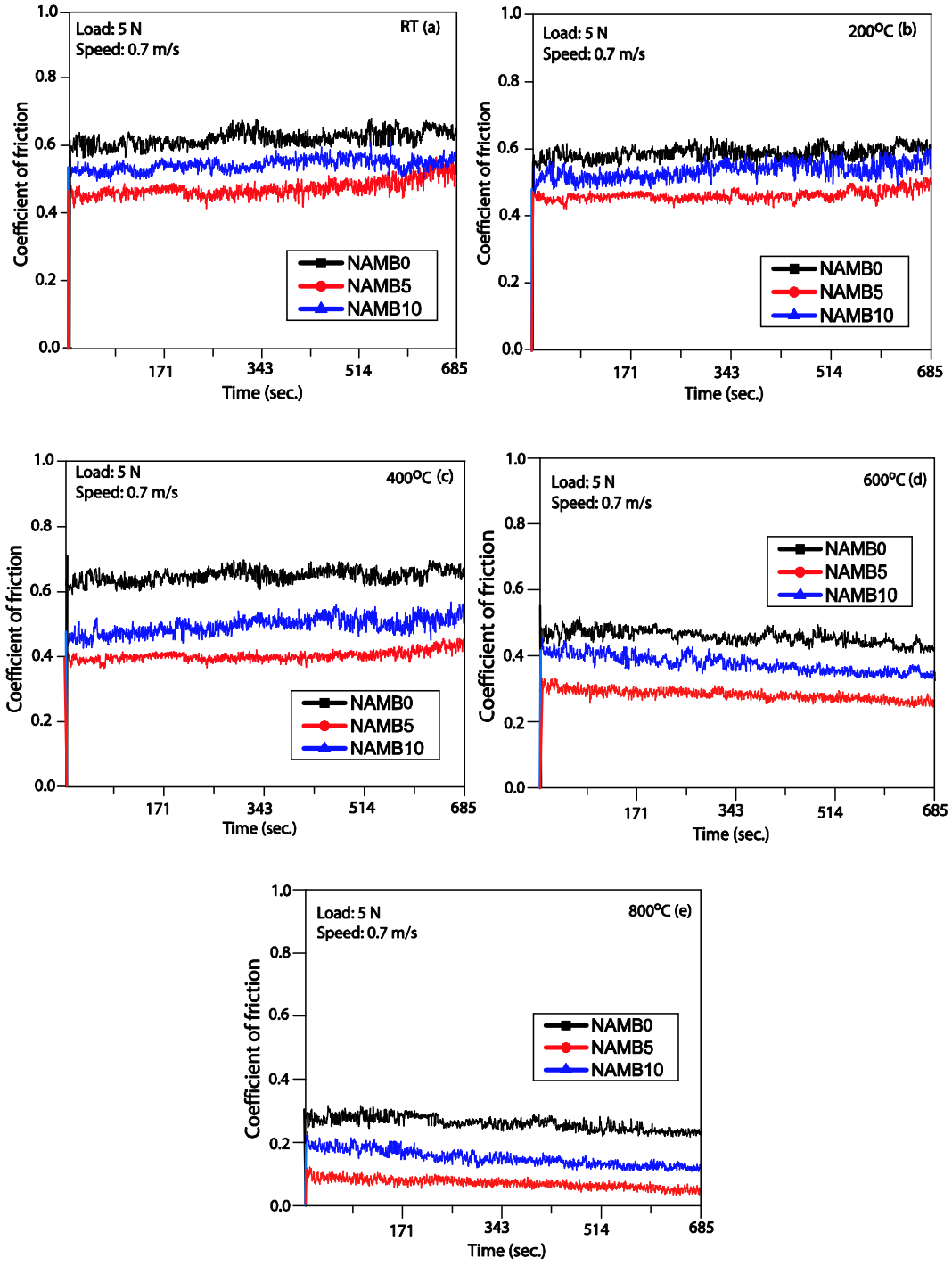

Fig. 4.29 Variation of coefficient of friction with time at (a) RT, (b) 200 °C (c) 400 °C (d) 600 °C and (e) 800 °C for coatings under 0.7 m/s speed.

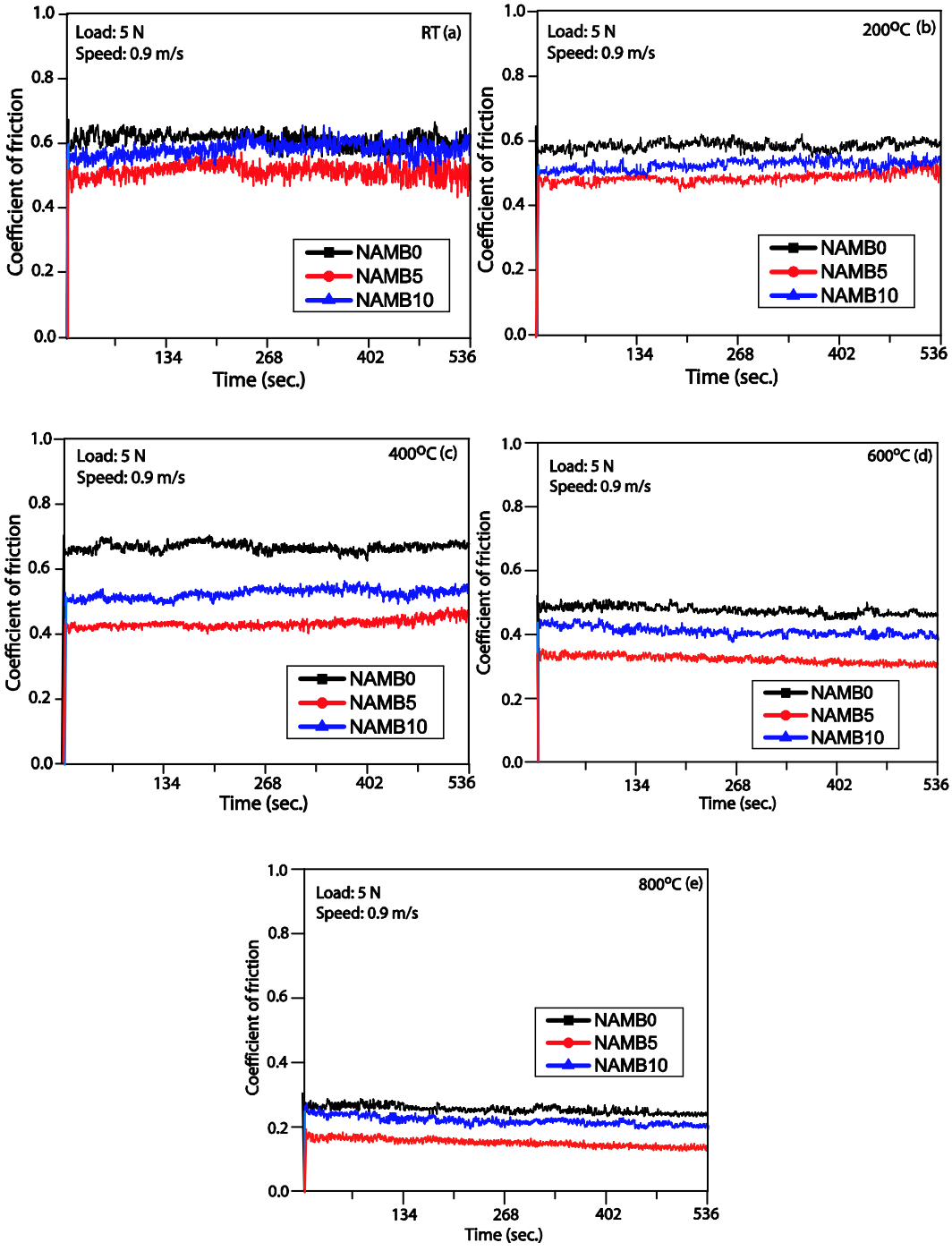

Fig. 4.30 Variation of coefficient of friction with time at (a) RT, (b) 200 °C, (c) 400 °C, (d) 600 °C and (e) 800 °C for coatings under 0.9 m/s speed.

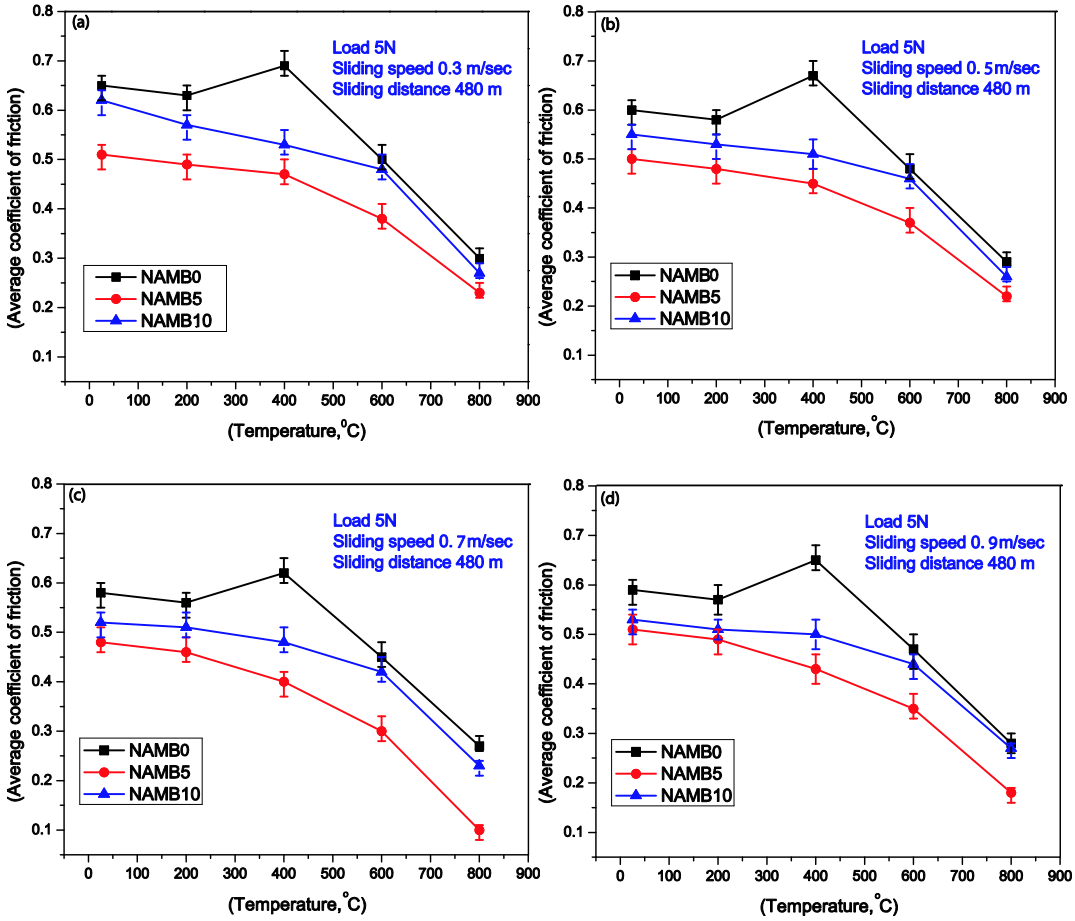

Fig. 4.31 Variation of average coefficient of friction with temperature for NAMB0, NAMB5 and NAMB10 coatings (a) 0.3 m/s, (b) 0.5 m/s, (c) 0.7 m/s and (d) 0.9 m/s.

(iii) Variation of average coefficient of friction with sliding speed

Figures 4.32 (a through e) represent the variation of average COF with sliding speed at different temperatures. In general, the COF in all the coatings is observed to decrease with increasing speed from 0.3 to 0.7 m/s followed by a slight increase as the speed is raised to 0.9 m/s. It could further be observed that all the coatings have the minimum COF at a speed of 0.7 m/s. Also, NAMB5 coating has the lowest coefficient of friction at all the speeds and temperatures as evident from Figs. 4.32 (a through e).

However, one may observe that speed does not have a prominent effect on friction for all the coatings like temperature.

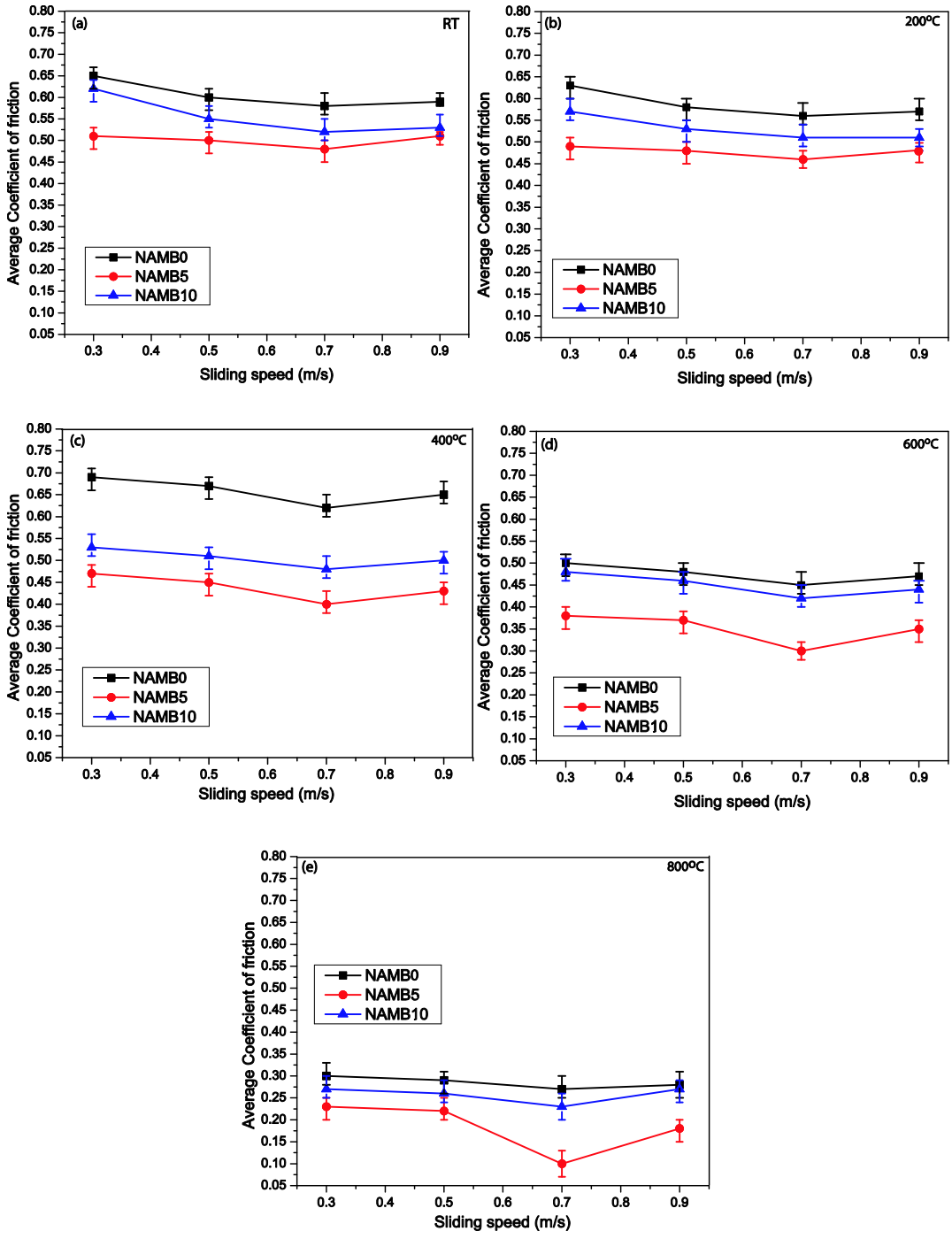

Fig. 4.32 Variation of average coefficient of friction with speed at (a) RT, (b) 200 °C; (c) 400 °C; (d) 600 °C and (e) 800 °C for all the coatings.

(b) Dry Sliding Wear

(i) Variation of wear rate with temperature

The variation of wear rate with temperature at different speeds for all the coatings slid against Al_2O_3 ball is illustrated in Fig.4.33 (a through d). The wear rate of NAMB0 composite coating is found to decrease in low temperature regime (RT to 200 °C), followed by an increase up to 400 °C as observed from Fig.4.33. However, the wear rate decreases again as the temperature is raised beyond 400 °C and reaches a value of 7.5 x 10^{-5} mm^3/Nm at 800 °C at 0.3 m/s. Similar trend of variation has been observed at all the speeds for NAMB0 coating as evident from Figs. 4.33 (a through d). The wear rate of NAMB5 and NAMB10 is observed to decrease continuously with increasing temperature from RT to 800 °C. However, NAMB5 coating has shown the lowest wear rate at all the temperatures and speeds in comparison to other coatings as evident from Fig.4.33. Hence, one may infer that the NAMB5 coating has a better wear resistance at all the temperatures and speeds with a minimum value of wear rate (2 x 10^{-5} mm^3/Nm) at 800 °C at 0.7 m/s.

(ii) Variation of wear rate with sliding speed

The variation of wear rate with sliding speed of all the coatings at RT, 200, 400, 600 and 800 °C is presented in Fig. 4.34. In general, the wear rate for all the coatings is observed to decrease with increasing speed from 0.3 to 0.7 m/s followed by a marginal increase till 0.9 m/s. A relatively sharp decrease in wear rate could be seen for NAMB5 coating as the speed is increased to 0.7 m/s at 800 °C which is followed by a steeper increase beyond 0.7 m/s in comparison to NAMB0 and NAMB10 as evident from Fig.

4.34. However, it could be seen that NAMB5 has a consistently lower wear rate at all the speeds and temperatures.

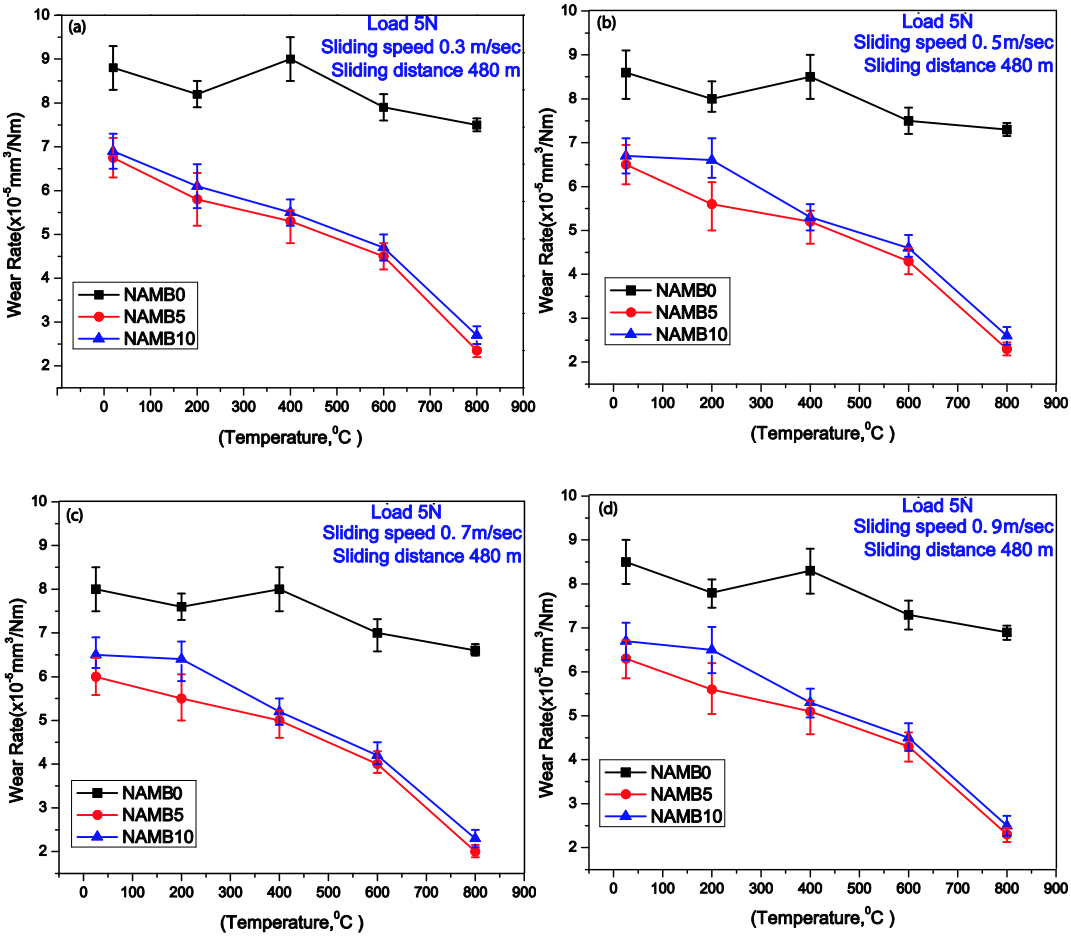

Fig. 4.33 Variation of wear rate with temperature at different speeds for NAMB0, NAMB5 and NAMB10 coatings (a) 0.3 m/s; (b) 0.5 m/s; (c) 0.7 m/s and (d) 0.9 m/s.

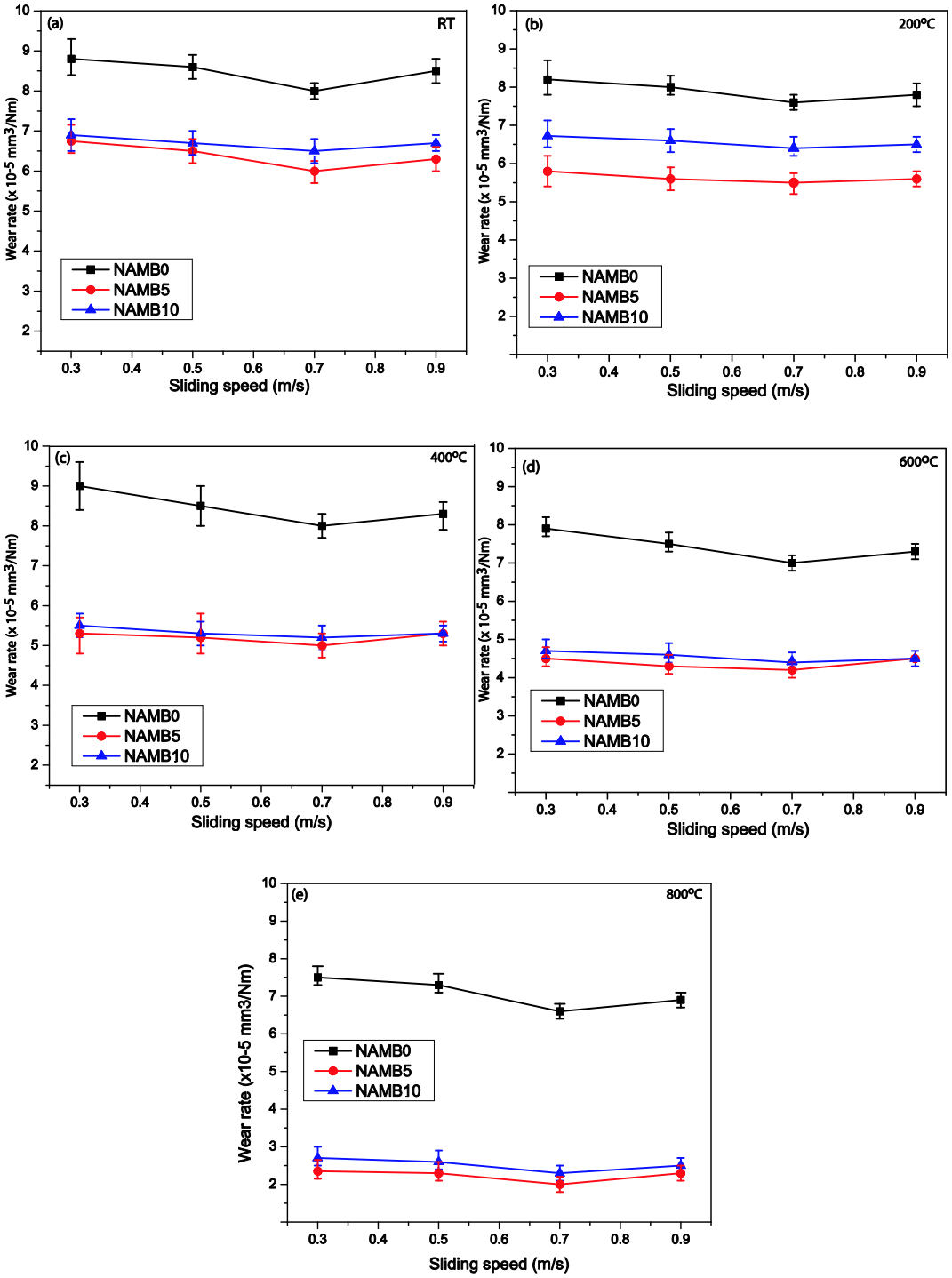

Fig. 4.34 Variation of wear rate with speed at (a) RT, (b) 200 °C, (c) 400 °C, (d) 600 °C and (e) 800 °C for all the coatings.

4.5.2 EXAMINATION OF SLIDING SURFACES

Figures 4.35, 4.36 and 4.37 show SEM micrographs of worn surfaces of NAMB0, NAMB5 and NAMB10 coatings after sliding at RT, 200, 400, 600 and 800 °C, respectively, under 0.3 m/s sliding speed. Some shallow grooves and pits in the direction of sliding along with some loose wear debris could be observed on the surface of NAMB0 coating at RT (Fig. 4.35 (a)). The surface worn at 400 °C (Fig. 4.35 b) reveals relatively deeper grooves along with the presence of a transfer layer and signs of detachment of this layer at few places. Whereas, the surface worn at 800 °C (Fig. 4.35 c) is covered with a glaze layer at several locations and there are no visible grooves along sliding direction on the worn surface of NAMB0.

Figures 4.36 (a through c) illustrate the worn surface morphology of NAMB5 at RT, 400, and 800 °C, respectively. The worn surface of NAMB5 at RT (Fig. 4.36 a) appears to be covered by a relatively smooth transfer layer with some loose wear particles scattered over the surface and shows no visible sign of wear tracks, whereas at 400 °C, the worn surface (Fig. 4.36 b) is covered by a compacted tribo-layer covering a relatively large area in comparison to that at RT**.** However, one can observe the presence of a very well compacted and smooth glazed layer on the worn surface of NAMB5 coating given in Fig. 4.36 (c) which covers almost entire area of surface.

Figures 4.37 (a through c) show the worn surface of NAMB10 coating at RT, 400 and 800 °C, respectively. The wear tracks show the presence of a discontinuous transfer layer along with wear debris particles at some locations as observed in Fig. 4.37 (a), whereas at 400 °C (Fig. 4.37 b) it shows the presence of a relatively compact transfer layer composed of reaction products probably oxides. The surface worn at 800 °C (Fig. 4.37 (c)) shows the presence of a discontinuous glazed tribo-layer and some white

particles possibly of hBN.

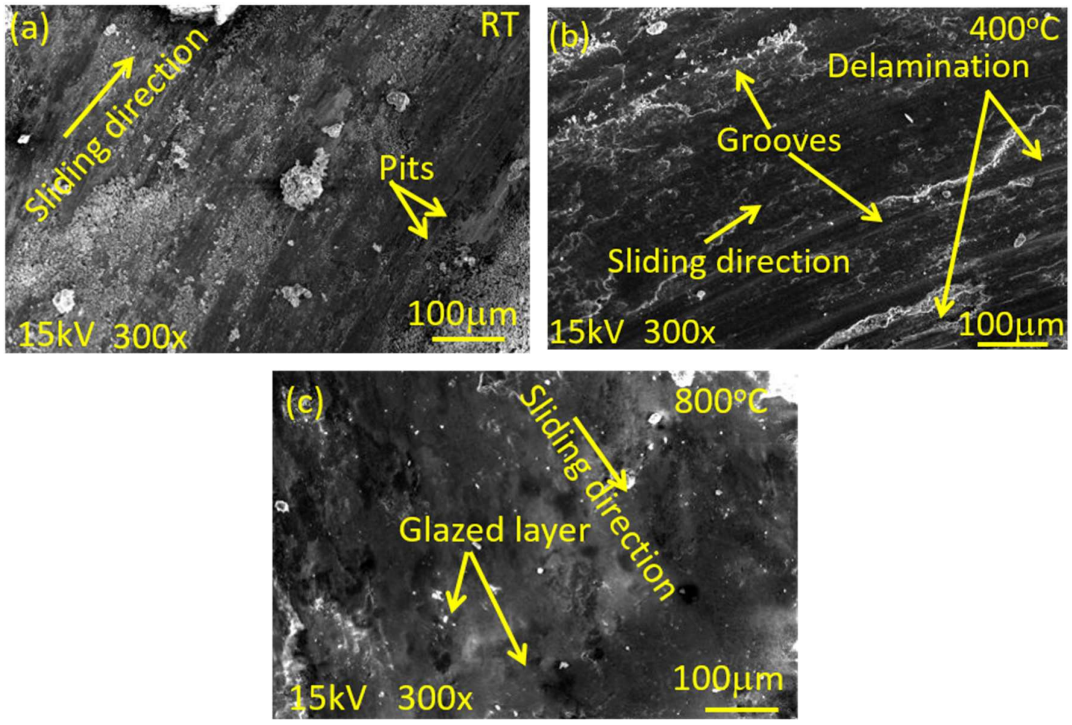

Fig. 4.35 SEM micrographs of the worn surfaces: (a) RT, (b) 400 °C and (c) 800 °C of NAMB0 coating at 0.3 m/sec sliding speed.

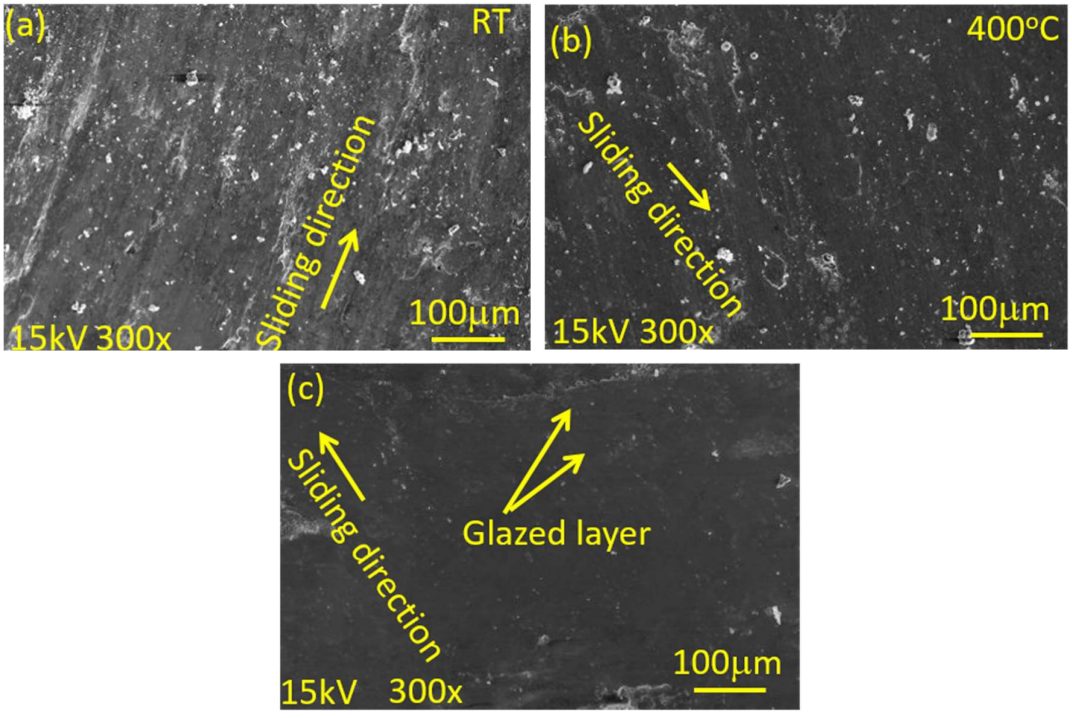

Fig. 4.36 SEM micrographs of the worn surfaces: (a) RT, (b) 400 °C and (c) 800 °C of NAMB5 coating at 0.3 m/sec sliding speed.

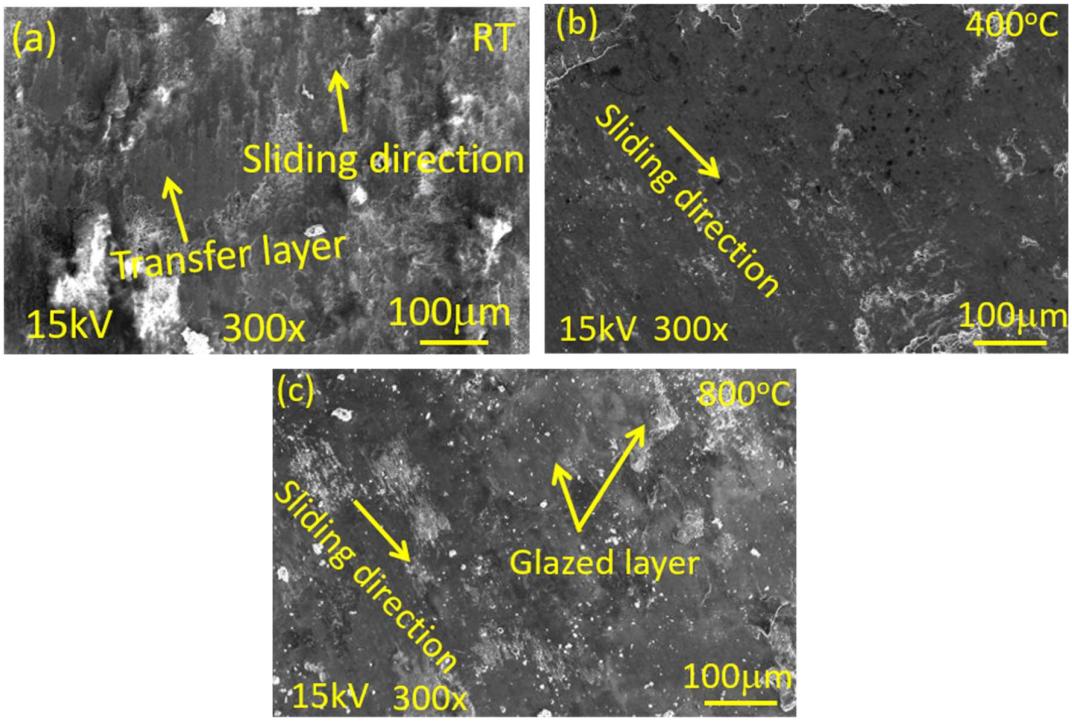

Fig. 4.37 SEM micrographs of the worn surfaces: (a) RT, (b) 400 °C and (c) 800 °C of NAMB10 coating at 0.3 m/sec sliding speed.

Figures 4.38, 4.39, and 4.40 show SEM micrographs of worn surfaces of NAMB0, NAMB5 and NAMB10 coatings at RT, 400, and 800 °C under 0.7 m/s sliding speed, respectively. Fig. 4.38 (a) shows the presence of a loosely bound transfer layer of wear debris on the surface of NAMB0 at RT along with fine abrasive grooves and some loose wear particles distributed over the surface. The worn surface (Fig. 4.38 b) having some wider grooves running parallel to sliding direction could be seen at 400 °C with the presence of relatively compact transfer layer and some loose wear debris particles. However, at 800 °C, the surface appears to be covered by glazed layer and loose wear particles probably of oxides as evident from Fig. 4.38 (c).

Figures 4.39 (a through c) present the morphology of wear track of NAMB5 coating. At RT, Fig. 4.39 (a), the wear tracks are observed to be covered with well compacted transfer layer of wear debris along with some loose wear particles and some

discernible abrasive marks in the direction of sliding. At a temperature of 400 °C, the wear tracks appear to be covered by a smooth and compact tribo-layer all over the surface (Fig. 4.39 b) covering a larger area in comparison to that observed for RT. However, one can observe the presence of a very smooth, compacted tribo-layer, and glaze/oxide layer on the surface of NAMB5 coating worn at 800 °C as seen in Fig. 4.39 (c).

Figures 4.40 (a through c) illustrate the worn surface morphology of NAMB10 coating at RT, 400 and 800 °C, respectively at a sliding speed of 0.7 m/s. The surface worn at RT, reveals the presence of a discontinuous transfer layer which appears to be smooth at some places along with loose wear debris particles at some locations as observed in Fig. 4.40 (a). However, at 400 °C (Fig. 4.40 c) one may observe the presence of a relatively compact transfer layer covering a relatively large area, but appears to have detached at few locations. The surface worn at 800 °C (Fig. 4.40 (c)) shows the presence of a glazed tribo-layer along with a layer of loosely bound oxide particles.

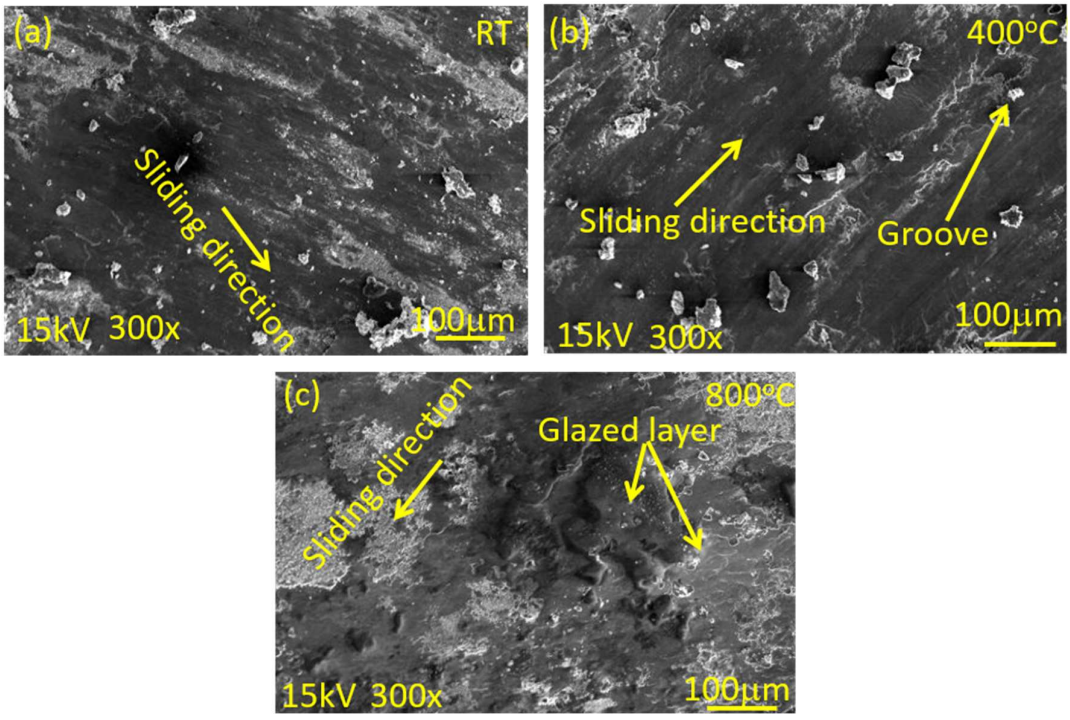

Fig. 4.38 SEM micrographs of the worn surfaces: (a) RT, (b) 400 °C and (c) 800 °C of NAMB0 coating at 0.7 m/sec sliding speed.

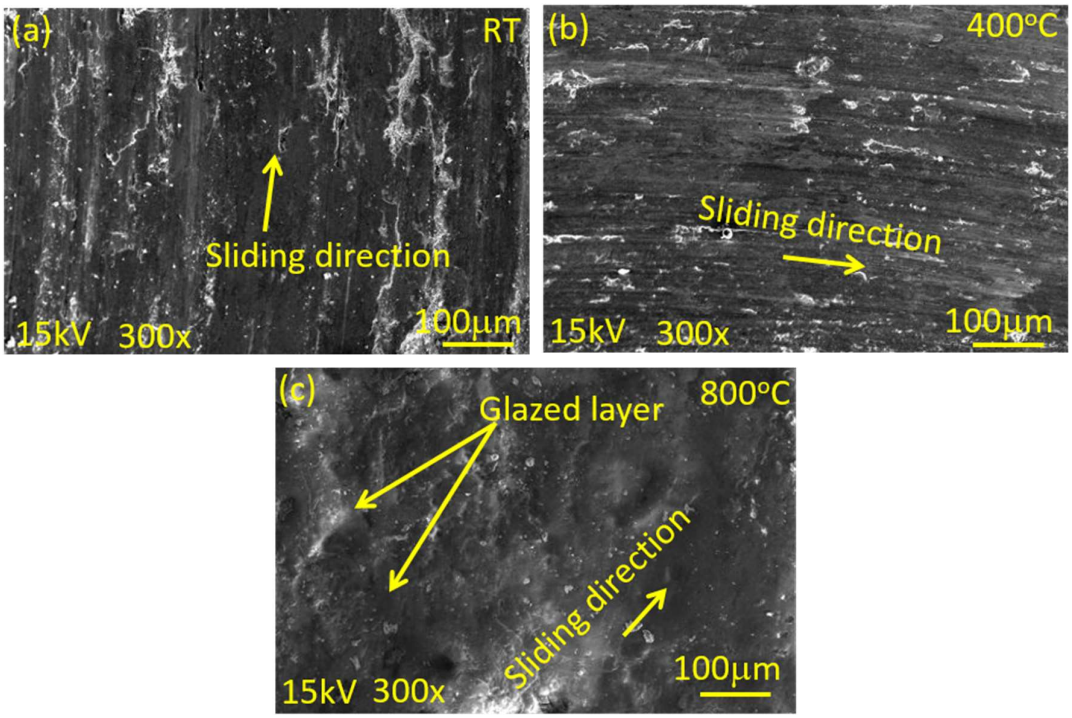

Fig. 4.39 SEM micrographs of the worn surfaces: (a) RT, (b) 400 °C and (c) 800 °C of NAMB5 coating at 0.7 m/sec sliding speed.

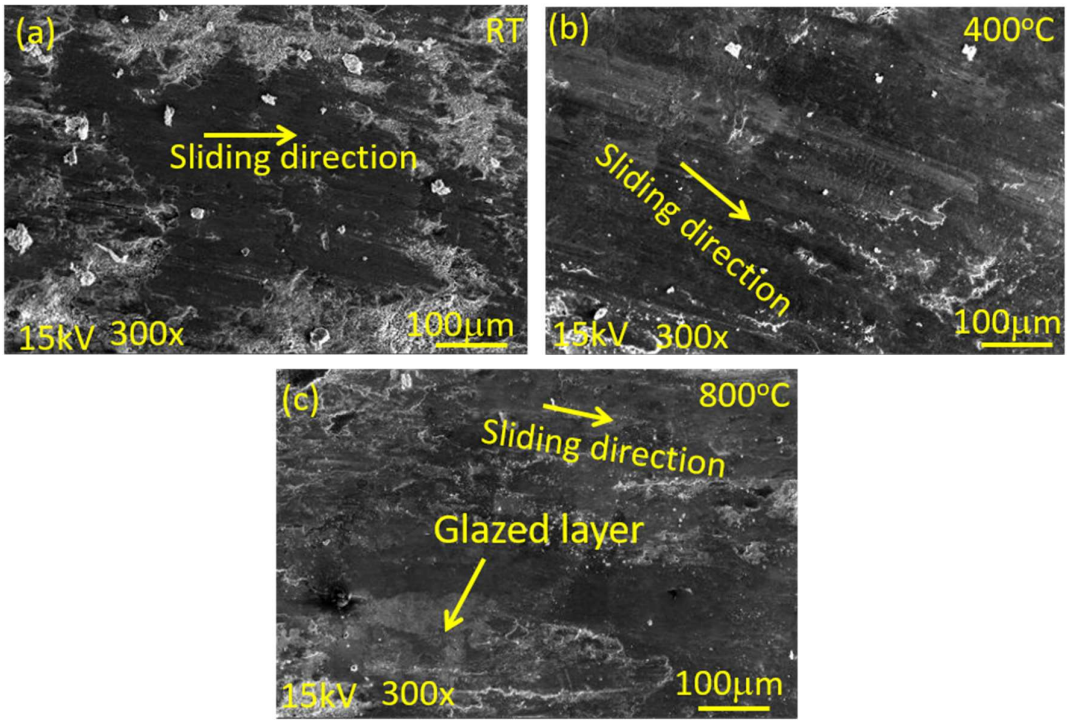

Fig. 4.40 SEM micrographs of the worn surfaces: (a) RT, (b) 400 °C and (c) 800 °C of NAMB10 coating at 0.7 m/sec sliding speed.

Figures 4.41, 4.42, and 4.43 show SEM micrographs of the worn surfaces of NAMB0, NAMB5 and NAMB10 coatings at RT, 400 and 800 °C under 0.9 m/s sliding speed, respectively. The worn surface at RT illustrated in Fig. 4.41 (a) shows the presence of a transfer layer of wear debris with lumps of debris particles at few places and grooves running along the sliding direction. At 400 °C (Fig. 4.41 b) the worn surface reveals the presence of a smooth, compact but discontinuous transfer layer which appears to have been detached at several locations. However, at 800 °C, the surface is covered by a glazed layer as evident from Fig. 4.41 (c).

Figures 4.42 (a through c) show the morphology of the worn surface of NAMB5 at RT, 400 and 800 °C, respectively, at 0.9 m/s sliding speed. At room temperature, (Fig. 4.42 a) the wear track have patchy but smooth transfer layer along with loose wear debris particles and some scoring marks. Whereas at 400 °C, the surface reveals the presence of compacted transfer layer (Fig. 4.42 b) covering a relatively larger area of worn surface**.** However, one can observe the presence of a very smooth, well compacted tribo-layer, and glaze/oxide layer on the worn surface of NAMB5 coating shown in Fig. 4.42 (c).

Figures 4.43 (a through c) illustrate the worn surface of NAMB10 coating at RT, 400 and 800 °C at 0.9 m/s sliding speed. The worn surface at RT (Fig. 4.43 (a)) shows the presence of a loosely bound transfer layer of debris covering a small area of worn surface and some loose wear particles along with lumps of wear debris, whereas at 400 °C (Fig. 4.43 (b)), one may observe the presence of a well compacted transfer layer which appears to have detached at some locations along with some visible scoring tracks. The surface worn at 800 °C (Fig. 4.43 (c)) shows the presence of a smooth compacted layer i.e. (oxide/glaze) layer along with some loose debris particles.

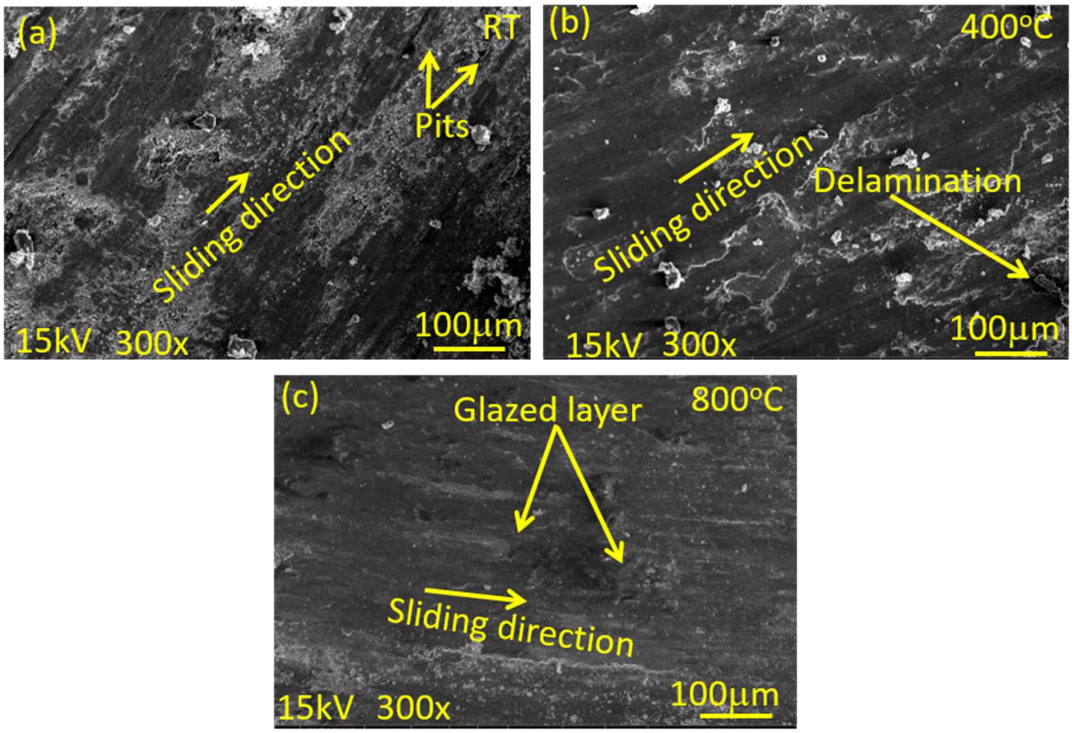

Fig. 4.41 SEM micrographs of the worn surfaces: (a) RT, (b) 400 °C and (c) 800 °C of NAMB0 coating at 0.9 m/sec sliding speed.

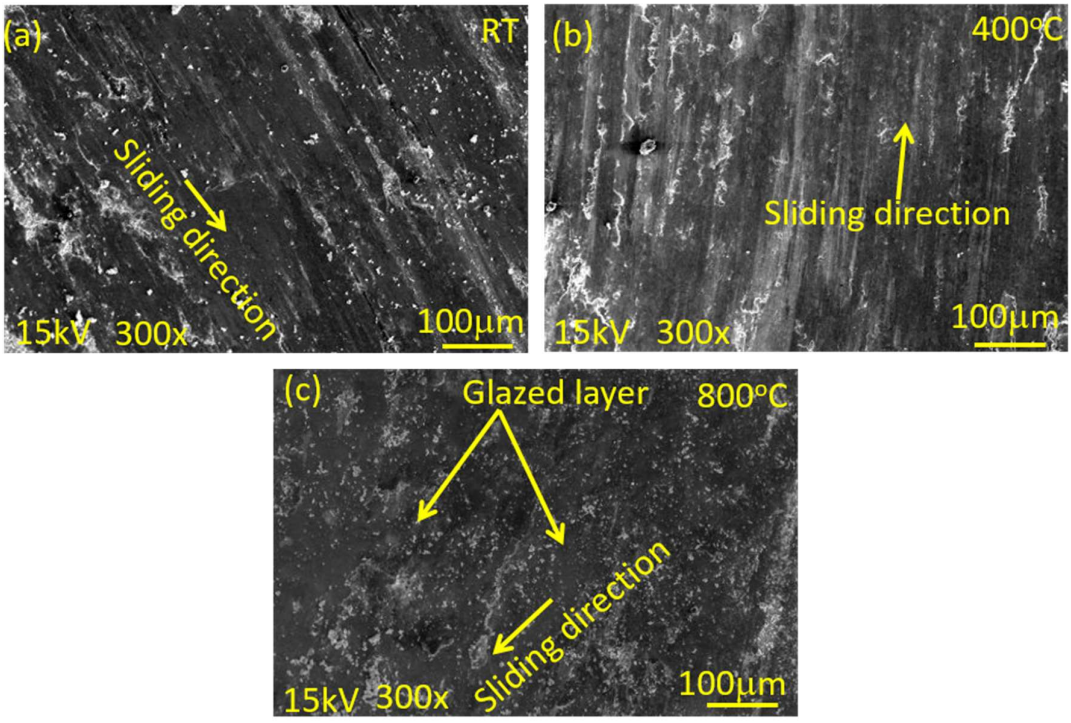

Fig. 4.42 SEM micrographs of the worn surfaces: (a) RT, (b) 400 °C and (c) 800 °C of NAMB5 coating at 0.9 m/sec sliding speed.

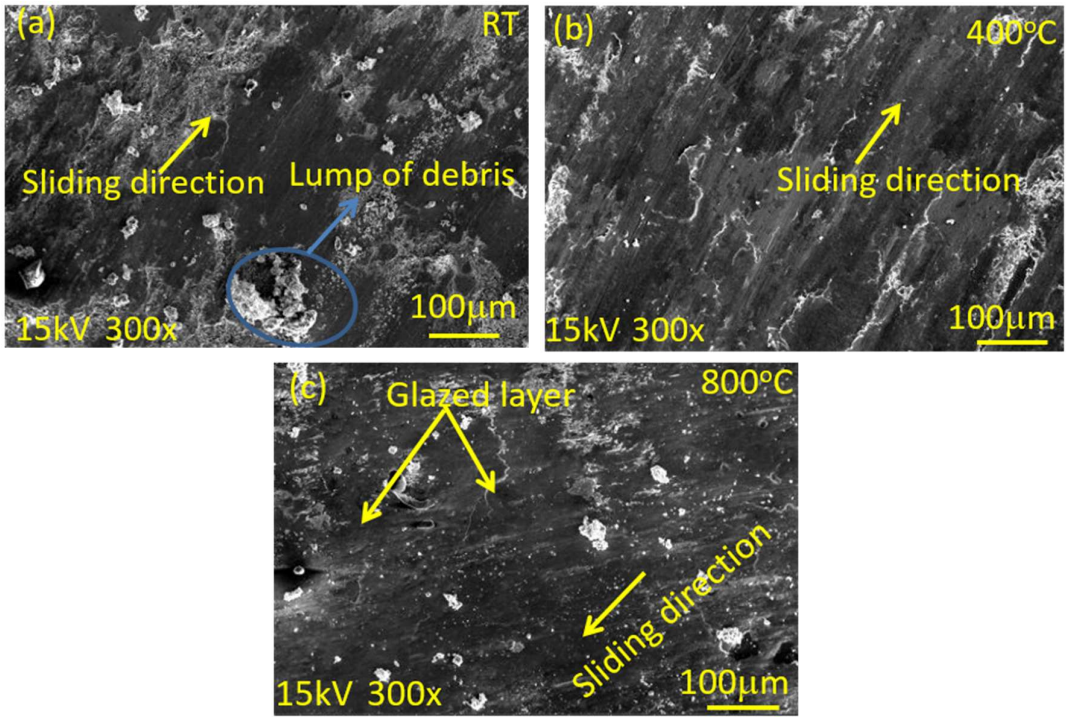

Fig. 4.43 SEM micrographs of the worn surfaces: (a) RT, (b) 400 °C and (c) 800 °C of NAMB10 coating at 0.9 m/sec sliding speed.

The morphologies of worn surfaces of alumina ball slid against NAMB0 composite coating at a sliding speed of 0.3 m/s under RT, 400 and 800 °C are illustrated in Fig. 4.44 (a through c). The transfer of material from coated specimen can be observed on the counterface alumina ball which has been confirmed by EDS analysis. However, the EDS spectrums are not included here. Fig. 4.44 (a) corresponding to room temperature shows some loose wear debris and abrasive marks in the direction of sliding, whereas Fig. 4.44 (b) at 400 °C, presents a rough and broken transfer layer with detachment of transferred coating material. The worn surface of alumina ball slid against NAMB0 composite coating at 800 °C shown in Fig. 4.44 (c) is relatively smooth and covered with a well compacted layer of material transferred from the coating.

The worn surface morphologies of alumina ball slid against NAMB5 composite coating under a speed of 0.3 m/s at RT, 400 and 800 °C, respectively, are

presented in Fig. 4.45 (a to c). The transfer of material from coated specimen to the counterface alumina was confirmed by the EDS analysis. Fig. 4.45 (a) presents some loosely adhered and patchy transfer layer with signs of detachment of transferred material at a few places. However, Fig. 4.45 (b) and (c) reveal some well compacted and smooth plateaus of transfer layer covering relatively larger area and containing materials transferred from coating.

SEM images of worn surfaces of alumina ball slid against NAMB10 at different temperatures of RT, 400, 800 °C are shown in Figs. 4.46 (a to c) corresponding to a sliding speed of 0.3 m/s. Fig. 4.46 (a) corresponding to RT presents a discontinuous transfer layer and abrasive marks along with some smooth areas, whereas, Fig. 4.46 (b) and (c) at 400 and 800 °C, respectively, show a relatively rough morphology containing loosely bound transferred materials without any evidence of compaction.

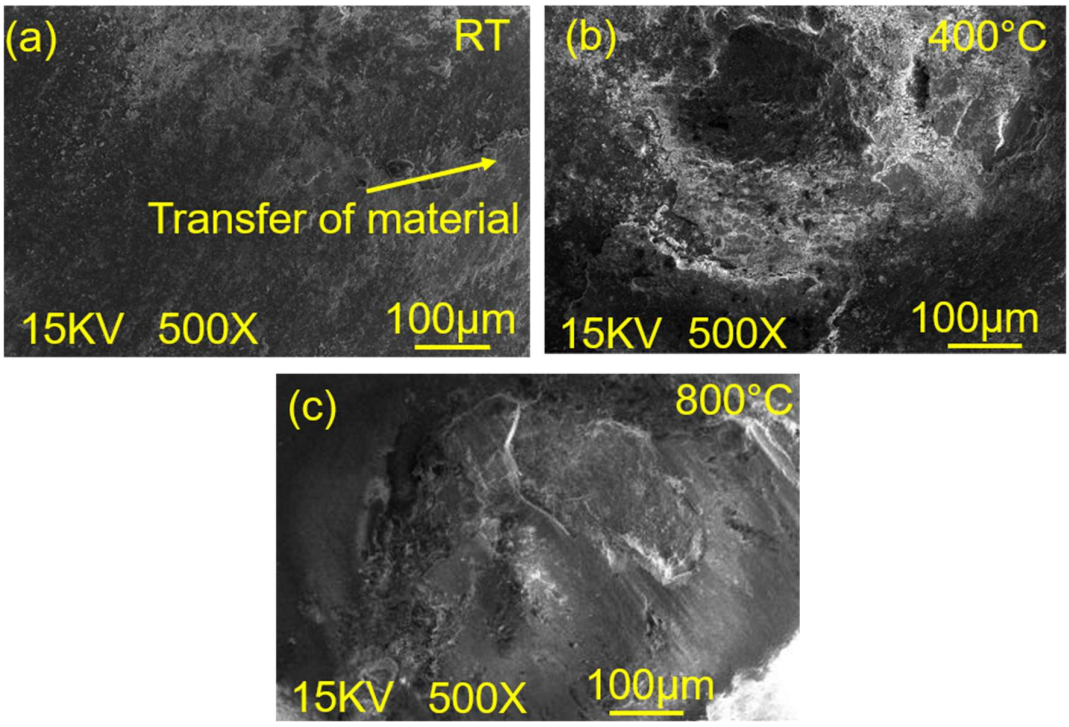

Fig. 4.44 SEM images of worn surface alumina ball slid against NAMB0 coating :(a) RT (b) 400 °C and (c) 800 °C under 0.3 m/s speed.

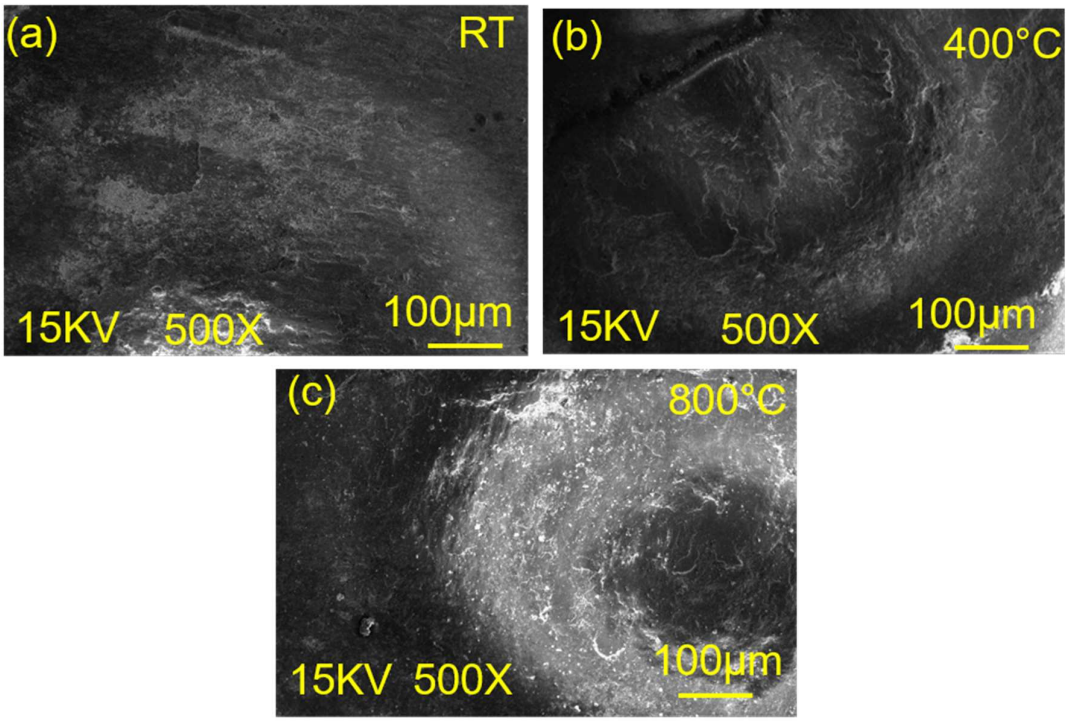

Fig. 4.45 SEM images of worn surface alumina ball slid against NAMB5 composite coating :(a) RT, (b) 400 °C and (c) 800 °C at 0.3 m/s speed.

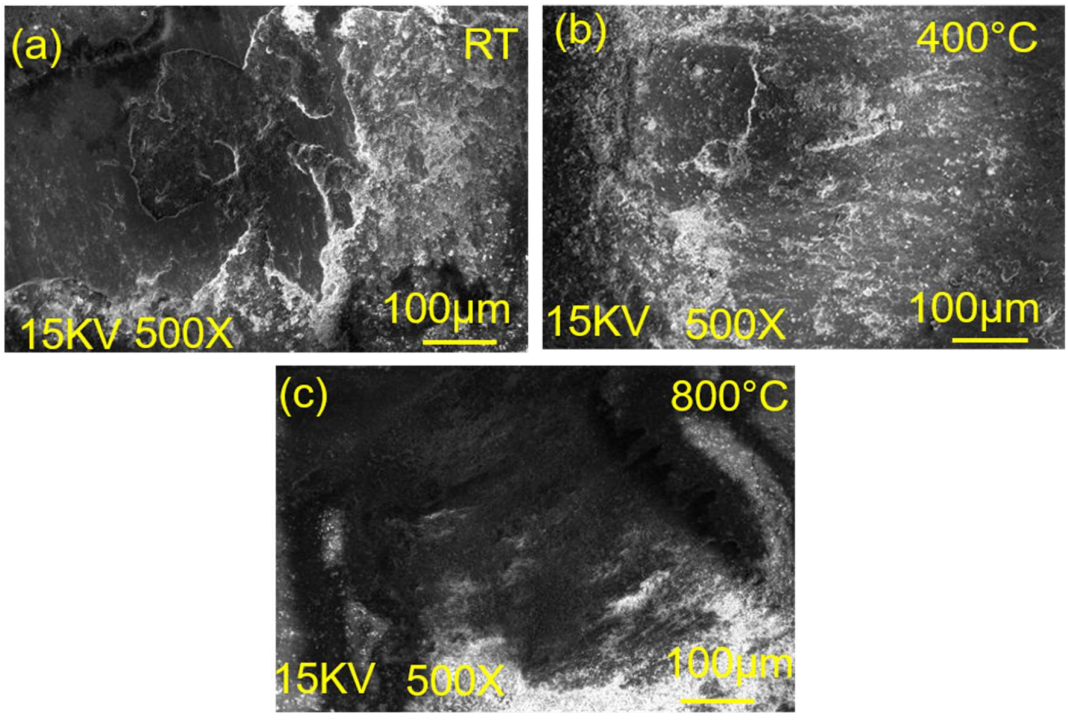

Fig. 4.46 SEM images of worn surface alumina ball slid against NAMB10 composite coating :(a) RT, (b) 400 °C and (c) 800 °C at 0.3 m/s speed.

The morphologies of worn surfaces of alumina ball slid against NAMB0 composite coating under RT, 400 and 800 °C at a sliding speed of 0.7 m/s are illustrated in Fig. 4.47 (a through c). The surfaces show the presence of transferred material from coating to counterface alumina ball during the sliding action as confirmed by the EDS analysis at all the temperatures. Fig. 4.47 (a) presents some loosely adhered, patchy, and broken transfer layer with signs of detachment of transferred material at a few places. However, at 400 °C, (Fig. 4.47 (b)), the layer of transferred material appears to have broken at some places, which may lead to a direct contact between coating to ball. The worn surface of alumina ball illustrated in Fig.4.47 (c) at 800 °C reveals the presence of a smooth and compacted tribo-layer along with the transferred material from coated specimen covering relatively larger area.

The worn surface morphologies of alumina ball slid against NAMB5 coatings are illustrated in Fig. 4.48 (a to c) at RT, 400 and 800 °C, respectively, under a sliding speed of 0.7 m/s. The transfer of coating material including solid lubricants has been observed from the coated specimen to the counterpart alumina ball and the same has been confirmed by the EDS analysis. The worn surface shown in Fig. 4.48 (a) reveals the presence of a compacted transfer layer and some fine wear debris particles at few places. Figs. 4.48 (b and c) also show the presence of a compacted layer of transferred material but the degree of compaction appears to be more in Fig. 4.48 (c) than in Fig. 4.48 (b). Also, this layer is observed to have a larger coverage of area in case of 800 °C than for RT and 400 °C.

SEM micrographs of worn surface of alumina ball slid against NAMB10 coating at 0.7 m/s speed and under RT, 400, 800 °C are shown in Figs. 4.49 (a to c). The material transfer from the coating to the counterface alumina ball is found to occur for

all the coatings at all the temperatures, which has been confirmed by EDS analysis. At RT, Fig. 4.49 (a), shows some abrasive marks and grooves along with a fragmented transfer layer. In Fig. 4.49 (b) and (c), one can observe a rough morphology and loosely bound transferred material.

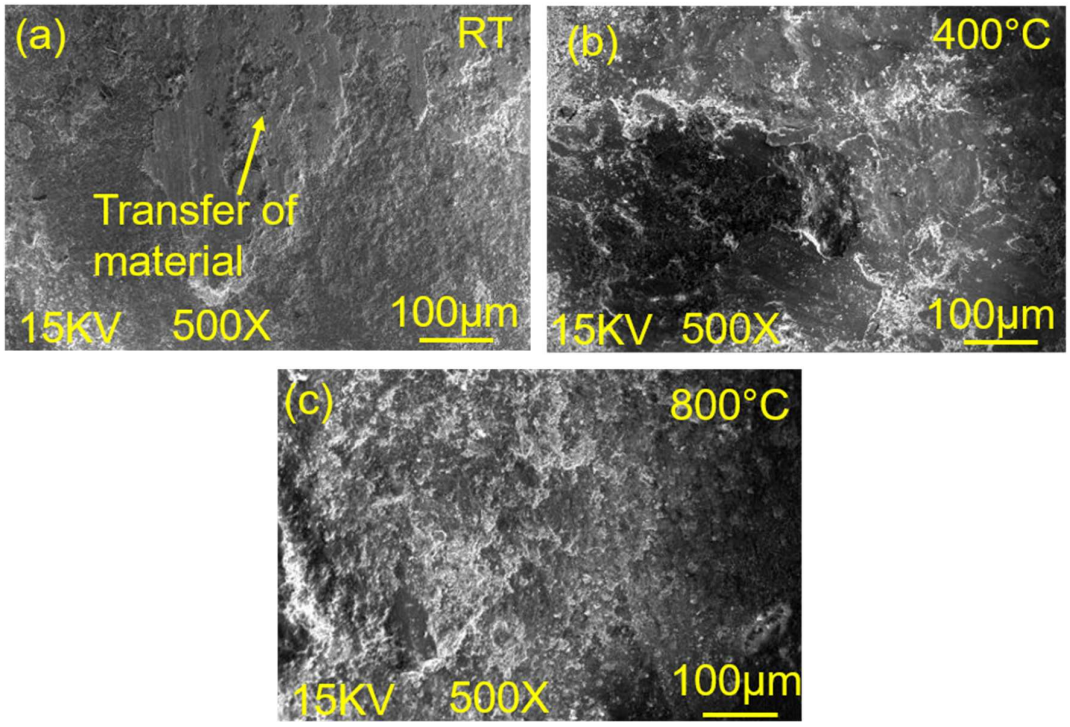

Fig. 4.47 SEM images of worn surface alumina ball slid against NAMB0 coating :(a) RT, (b) 400 °C and (c) 800 °C under 0.7 m/s speed.

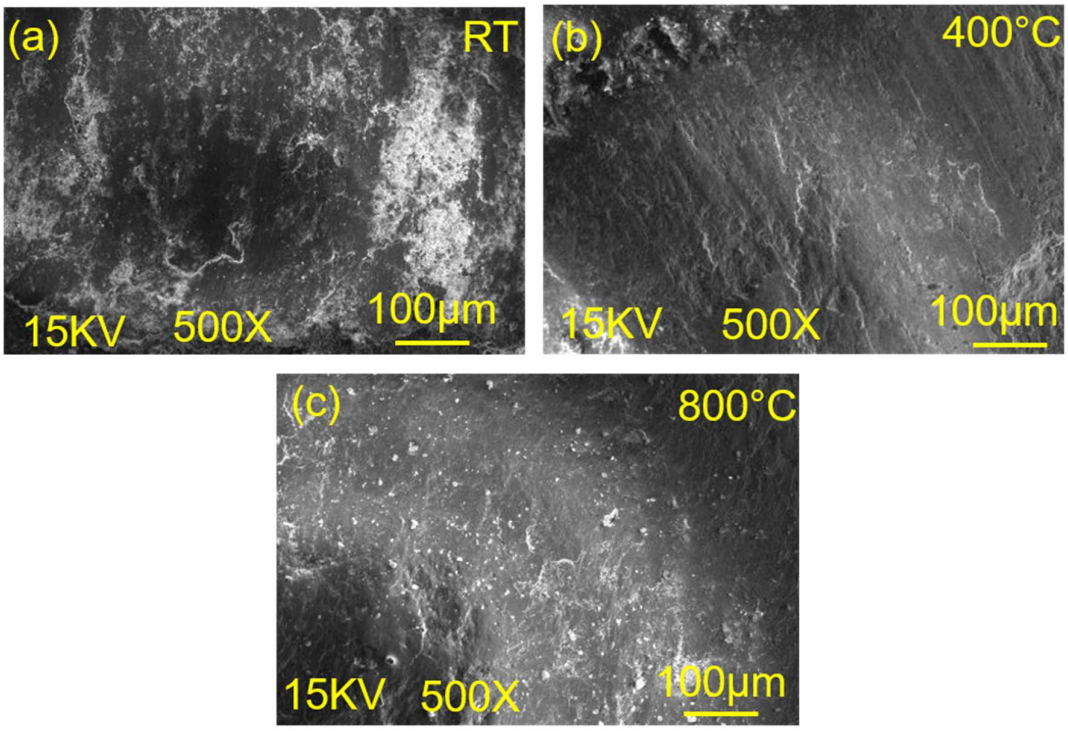

Fig. 4.48 SEM images of worn surface alumina ball slid against NAMB5 composite coating :(a) RT, (b) 400 °C and (c) 800 °C at 0.7 m/s speed.

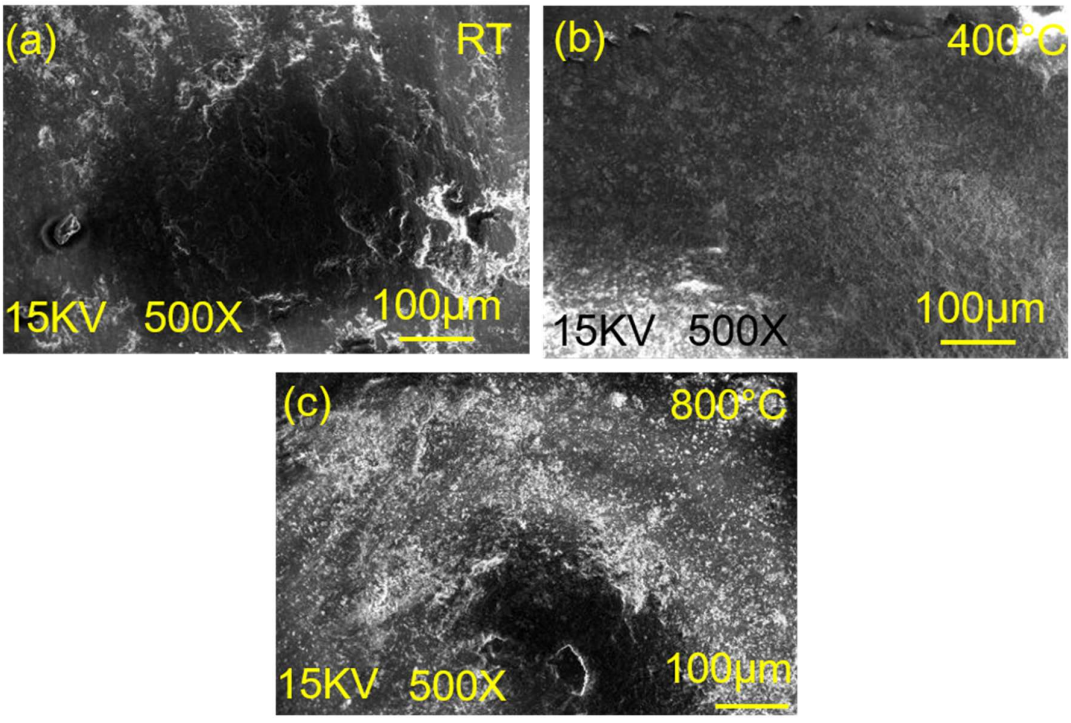

Fig. 4.49 SEM images of worn surface alumina ball slid against NAMB10 composite coating :(a) RT, (b) 400 °C and (c) 800 °C at 0.7 m/s speed.

The morphologies of worn surfaces of alumina ball slid against NAMB0 coating under RT, 400 and 800 °C at a sliding speed of 0.9 m/s are illustrated in Figs. 4.50 (a through c). The surfaces show the presence of transferred material from coating to counterface alumina ball as confirmed by EDS analysis (not included) at all the temperatures. At RT, (Fig. 4.50 (a)), a patchy transfer layer along with some smooth regions has been observed on the worn surface of alumina ball. However, at 400 °C the layer of transferred material appears to have detached giving rise to contact between ceramic and coating (Fig. 4.50 (b)). The alumina ball SEM morphology illustrated in Fig. 4.50 (c) at 800 °C reveals the presence of a compacted tribo-layer containing the transferred material from coated specimen which is expected to reduce the friction and wear at 800 °C by forming a lubricating layer of low shear strength.

The worn surface morphologies of alumina ball slid against NAMB5 coatings are illustrated in Fig.4.51 (a to c) at RT, 400 and 800 °C, respectively, under a sliding speed of 0.9 m/s. The transfer of coating material including solid lubricants from the coated specimen to the counterpart alumina ball has been confirmed by the EDS analysis. Fig. 4.51 (a) presents a broken transfer layer with very fine wear debris at a few places. Figs. 4.51 (b) and (c) reveal the presence of a layer of transferred material but the area of coverage provided by this layer is more at 800 °C than at 400 °C as evident from a comparison of Fig. 4.51 (b and c).

Figures 4.52 (a to c) present the SEM images of worn surface of alumina ball slid against NAMB10 coating at 0.9 m/s speed at RT, 400 and 800 °C, respectively**.** All of the surfaces reveal the presence of the material transfer from the coating to the alumina ball due to the sliding action as confirmed by EDS analysis. At RT, Fig. 4.52 (a), shows loosely adhered transfer layer without any evidence of proper compaction. In Fig. 4.52

(b), one can observe a rough morphology and loose transferred material which does not appear to have compacted properly. The surface worn at 800 °C shows the presence of loosely bound transferred material scattered all over the surface as seen from Fig 4.52 (c).

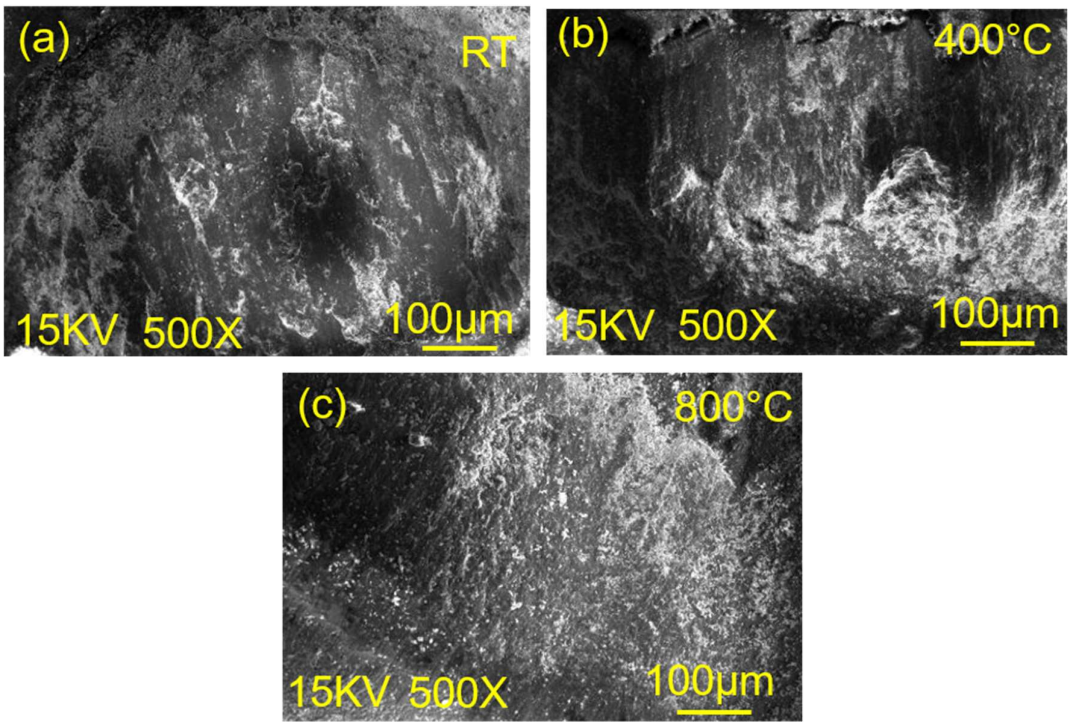

Fig. 4.50 SEM images of worn surface alumina ball slid against NAMB0 composite coating :(a) RT, (b) 400 °C and (c) 800 °C at 0.9 m/s speed.

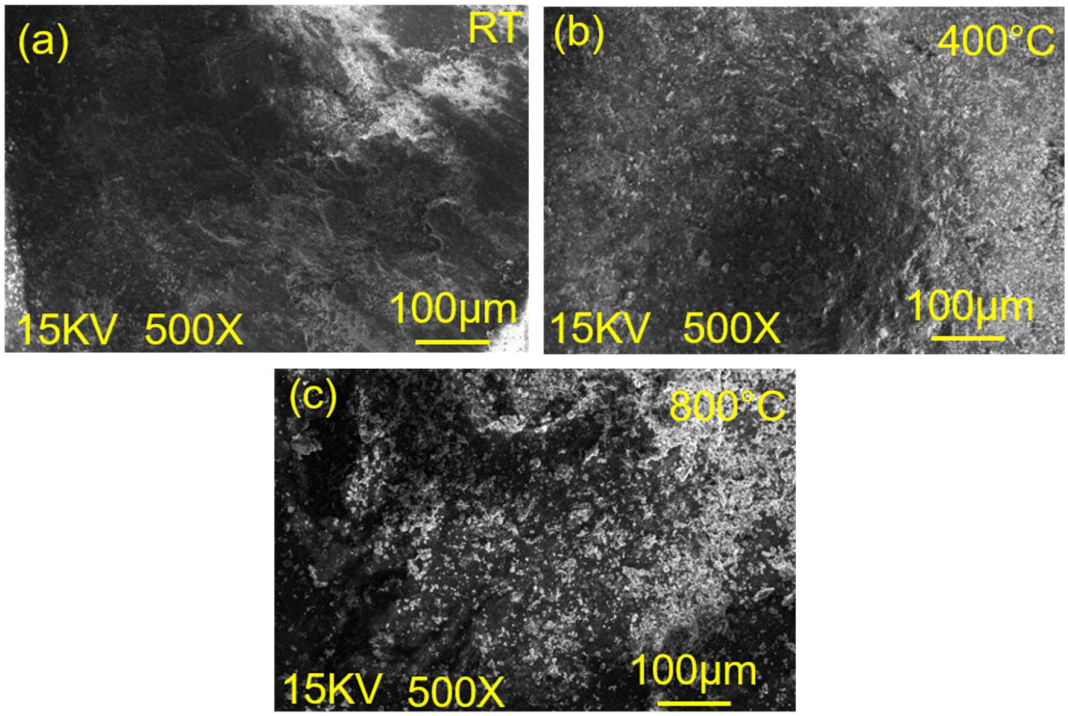

Fig. 4.51 SEM images of worn surface alumina ball slid against NAMB5 composite coating :(a) RT (b) 400 °C and (c) 800 °C at 0.9 m/s speed.

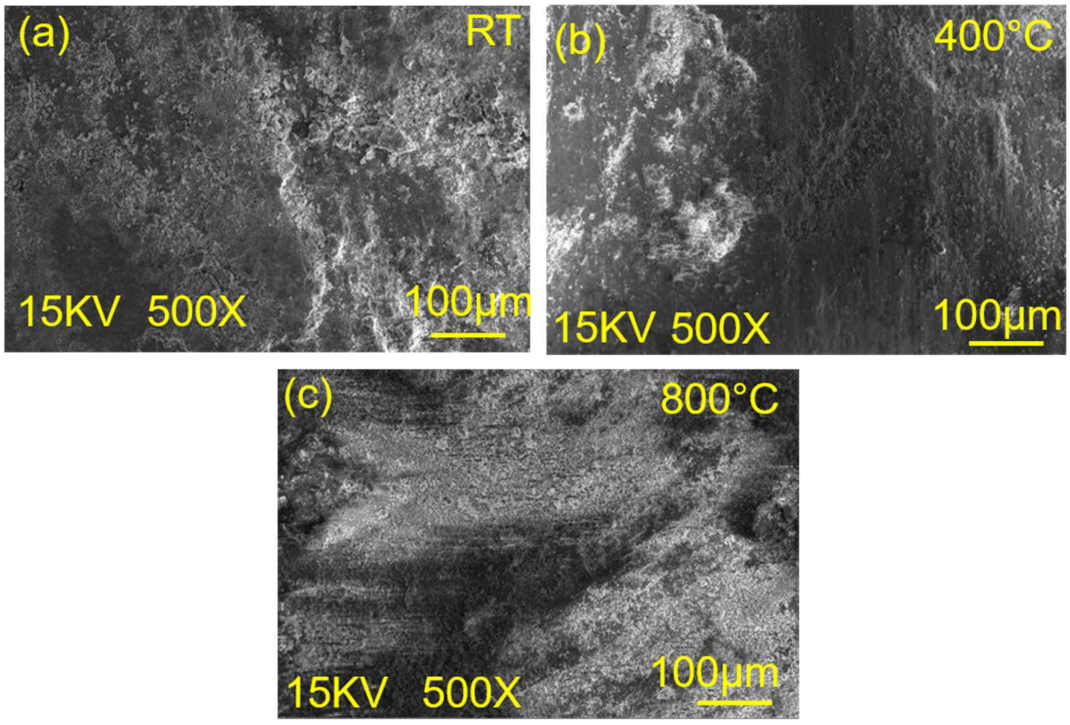

Fig. 4.52 SEM images of worn surface of alumina ball slid against NAMB10 composite coating at (a) RT, (b) 400 °C and (c) 800 °C at 0.9 m/s speed.

Figures 4.53, 4.54 and 4.55 show the X-ray diffraction patterns of coatings worn at different temperatures under 0.3, 0.7 and 0.9 m/s sliding speed, respectively. It could be seen from XRD patterns that the diffraction peaks of all the composite coatings after friction test at 400 °C, are similar to as-sprayed coatings. The worn surface mainly contains Ni_3Al (JCPDF file no.65-3245), Ag (JCPDF file no.89-3722), NiAl (JCPDF file no.65-0431), $NiMoO_4$ (JCPDF file no.86-0362), Ni (JCPDF file no.03-1051), hBN (JCPDF file no. 85-1068). Furthermore, the new diffraction peaks of MoO_3 and $Ag_2Mo_4O_{13}$ are found at 600 °C. After the 800 °C tribological testing, the diffraction peaks corresponding to the presence of $Ag_2Mo_2O_7$ (JCPDS file no. 75-1505), Ag_2MoO_4 (JCPDS file no. 76-1747) and NiO (JCPDS file no. 89-7390) which form through the tribo-reaction during the friction process at this temperature could also be seen in the patterns. The molybdates of silver and NiO have been shown to be lubricious at elevated temperatures (Liu et al., 2012, 2013).

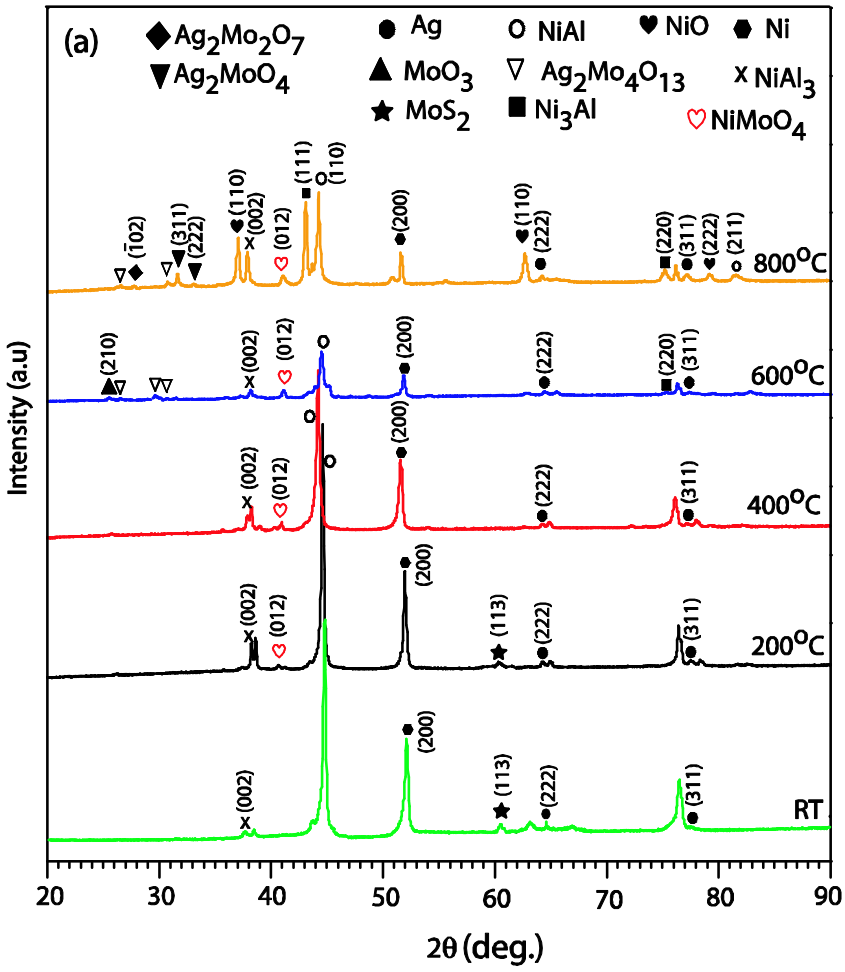

Fig. 4.53 (a) XRD patterns of wear track of NAMB0 composite coatings at different test temperatures under 0.3 m/s speed.

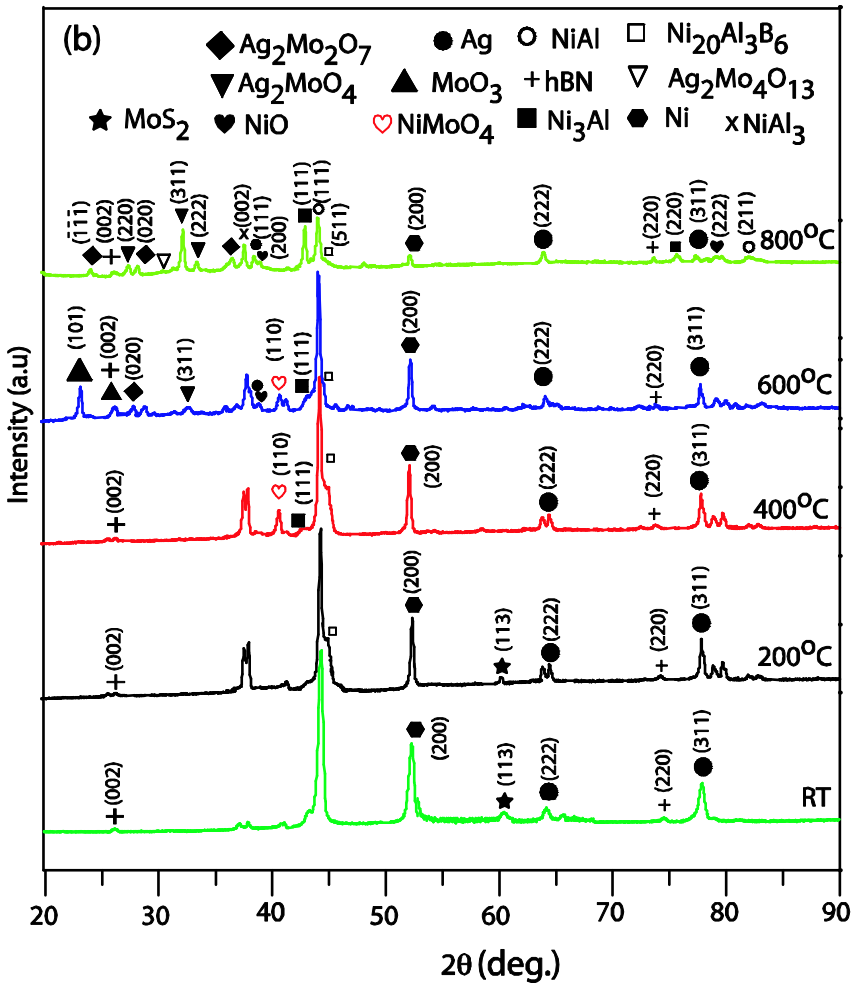

Fig. 4.53 (b) XRD patterns of wear track of NAMB5 composite coatings at different test temperatures under 0.3 m/s speed.

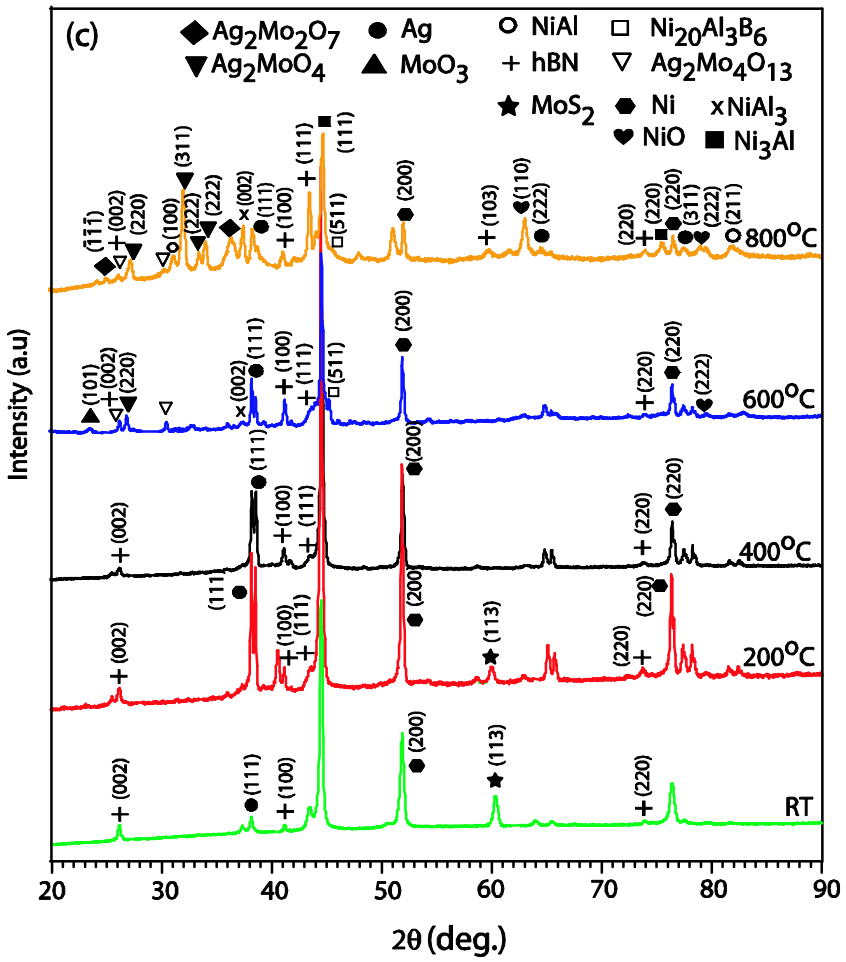

Fig. 4.53 (c) XRD patterns of wear track of NAMB10 composite coatings at different test temperatures under 0.3 m/s speed.

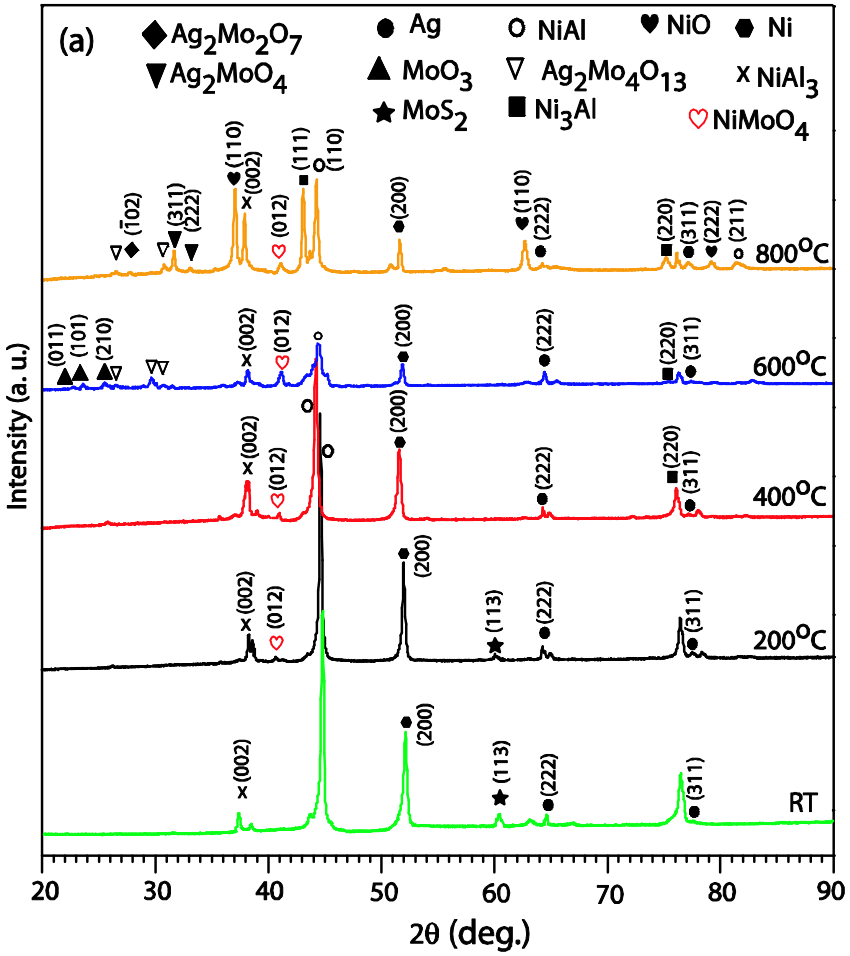

Fig. 4.54 (a) XRD patterns of wear track of NAMB0 composite coatings at different test temperatures under 0.7 m/s speed.

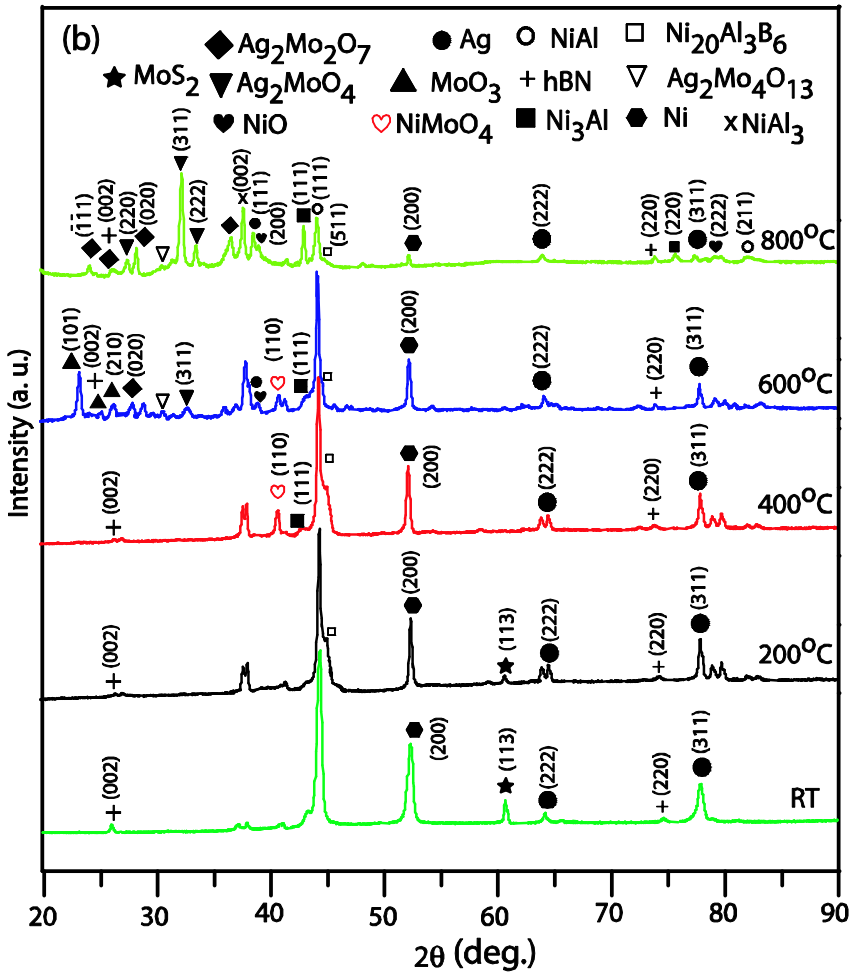

Fig. 4.54 (b) XRD patterns of wear track of NAMB5 composite coatings at different test temperatures under 0.7 m/s speed.

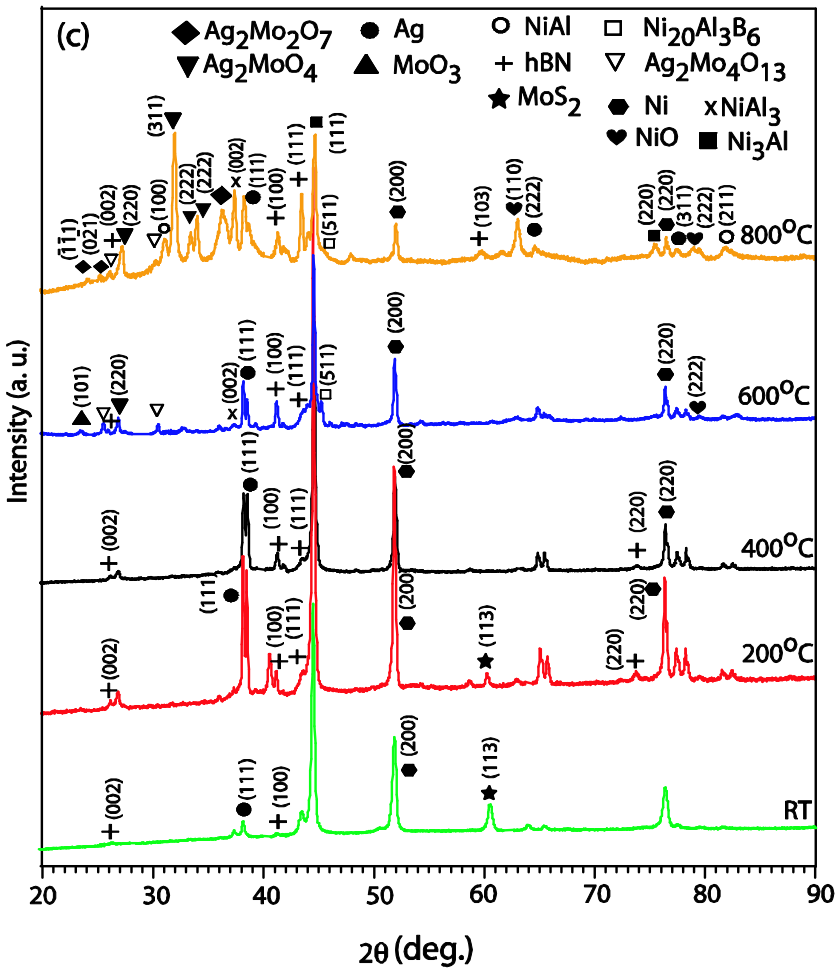

Fig. 4.54 (c) XRD patterns of wear track of NAMB10 composite coatings at different test temperatures under 0.7 m/s speed.

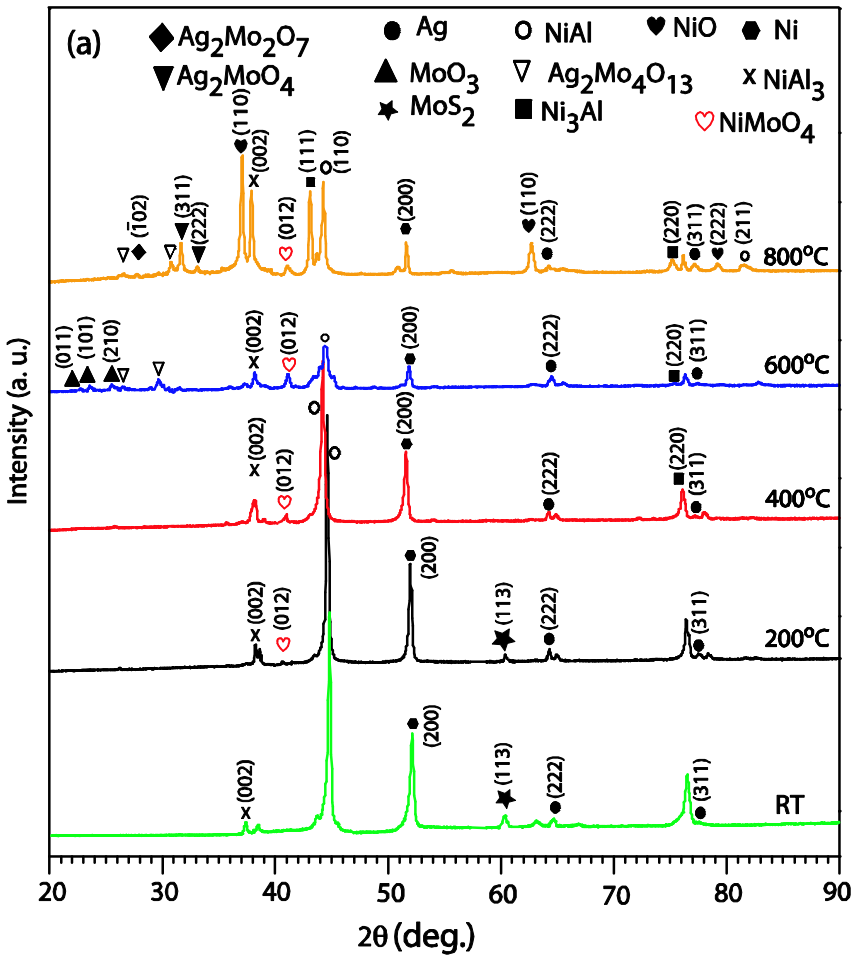

Fig. 4.55 (a) XRD patterns of wear track of NAMB0 composite coatings at different test temperatures under 0.9 m/s speed.

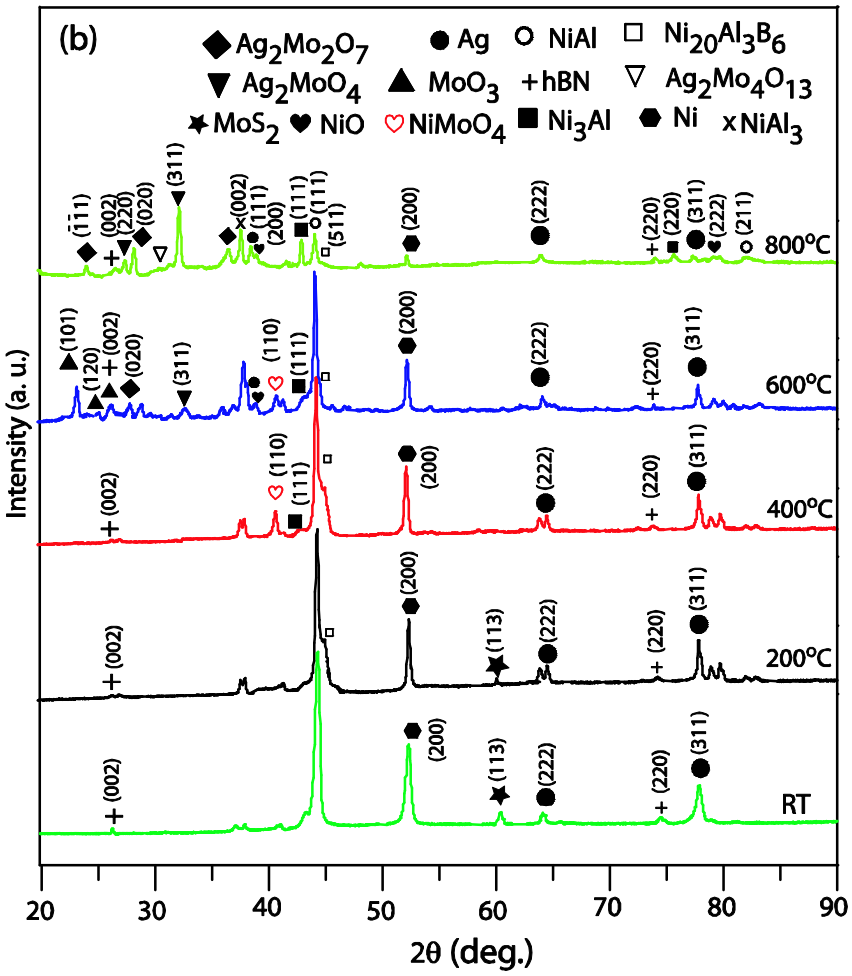

Fig. 4.55 (b) XRD patterns of wear track of NAMB5 composite coatings at different test temperatures under 0.9 m/s speed.

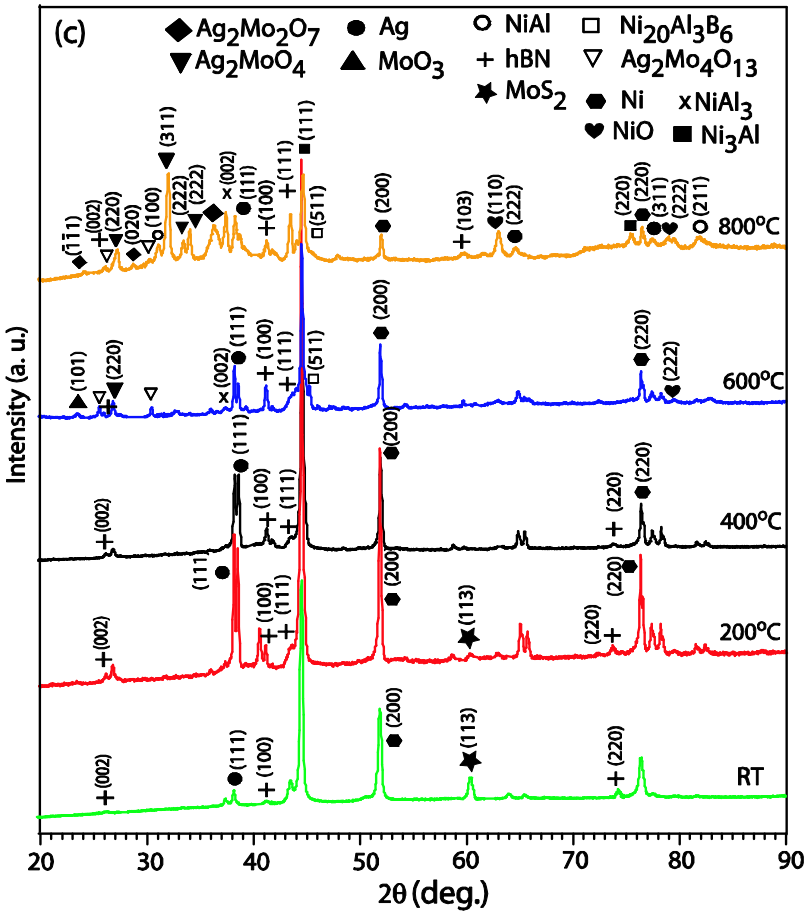

Fig. 4.55 (c) XRD patterns of wear track of NAMB10 composite coatings at different test temperature under 0.9 m/s speed.

Figures 4.56, 4.57 and 4.58 illustrate the Raman spectra of the worn tracks of (a) NAMB0 (b) NAMB5 (c) NAMB10 coatings from (RT-800 °C) at 0.3, 0.7 and 0.9 m/s speeds. At RT, 200 and 400 °C, no peak except a broad peak of Ag_2MoO_4 could be seen on worn surface for all the coatings as evident from Figs 4.56. 4.57 and 4.58. At 600 °C, the peaks corresponding to MoO_3, Ag_2MoO_4, $NiMoO_4$ and NiO phases could be seen on the wear tracks of NAMB0 coating at all the sliding speed. At 800 °C, the worn tracks show the presence of Ag_2MoO_4, $Ag_2Mo_4O_{13}$, $Ag_2Mo_2O_7$, NiO and $NiMoO_4$ peaks which might have formed due to tribo-chemical reactions during sliding. The Ag_2MoO_4 has been shown to possess the ability to provide effective lubrication from medium-to high-temperatures (Liu et al., 2013).

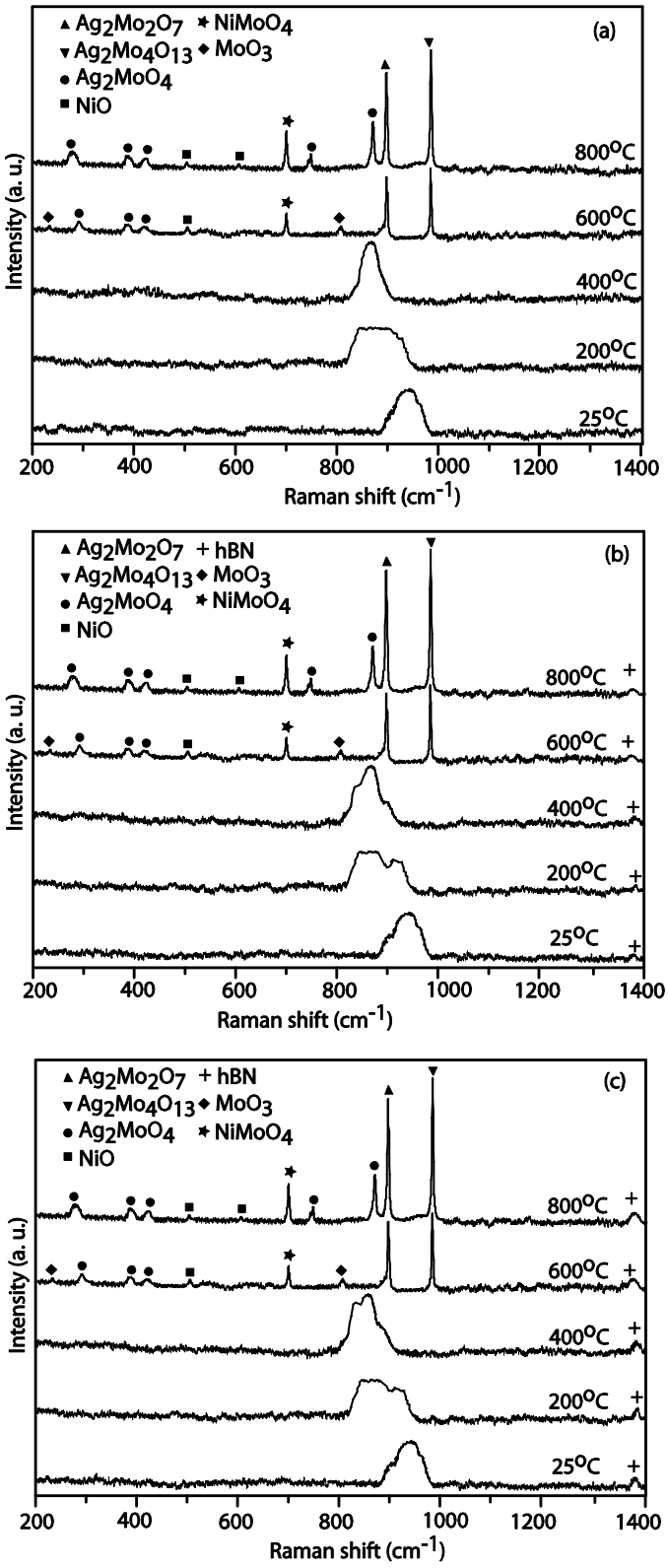

Fig. 4.56 Raman spectra with in wear track of the coatings (a) NAMB0 (b) NAMB5 (c) NAMB10 at different test temperatures under 0.3 m/sec speed.

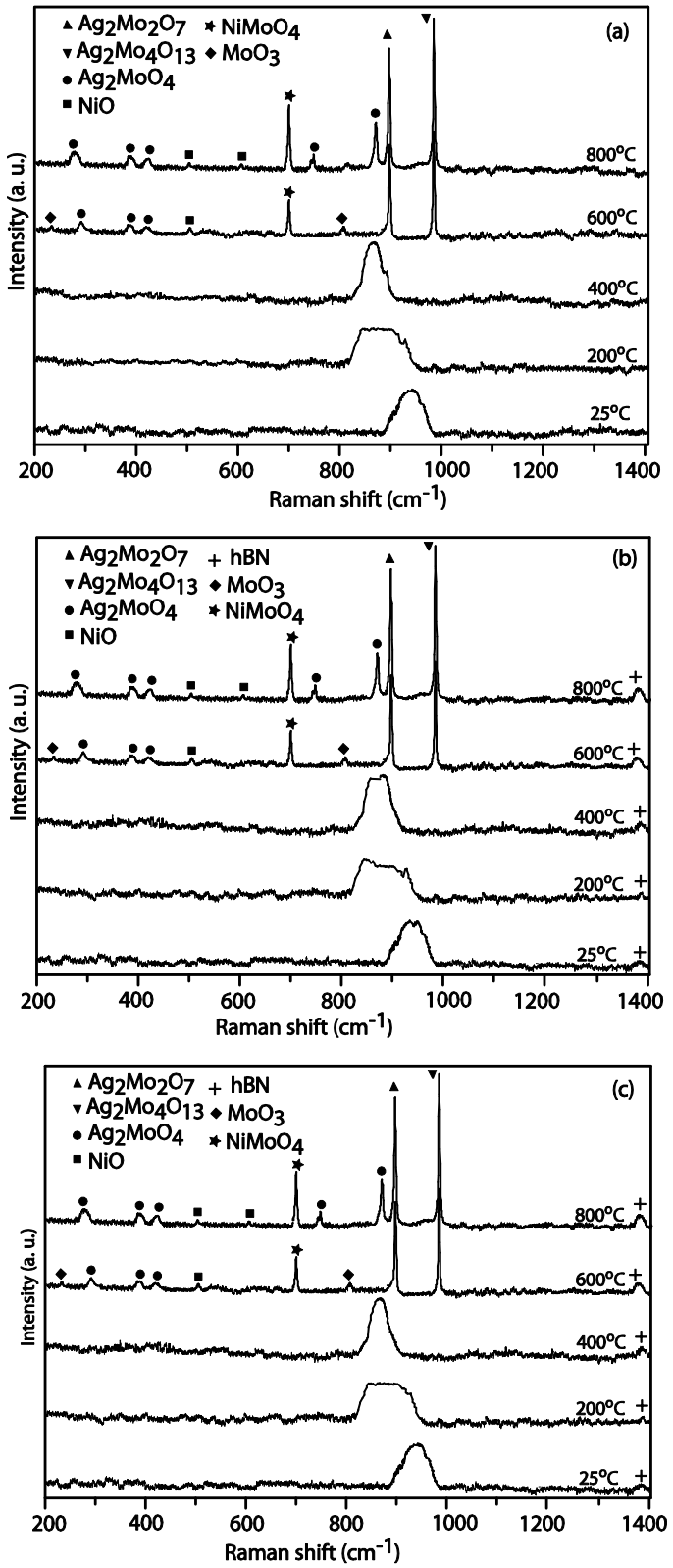

Fig. 4.57 Raman spectra within wear track of the coatings (a) NAMB0 (b) NAMB5 (c) NAMB10 at different test temperatures under 0.7 m/sec speed.

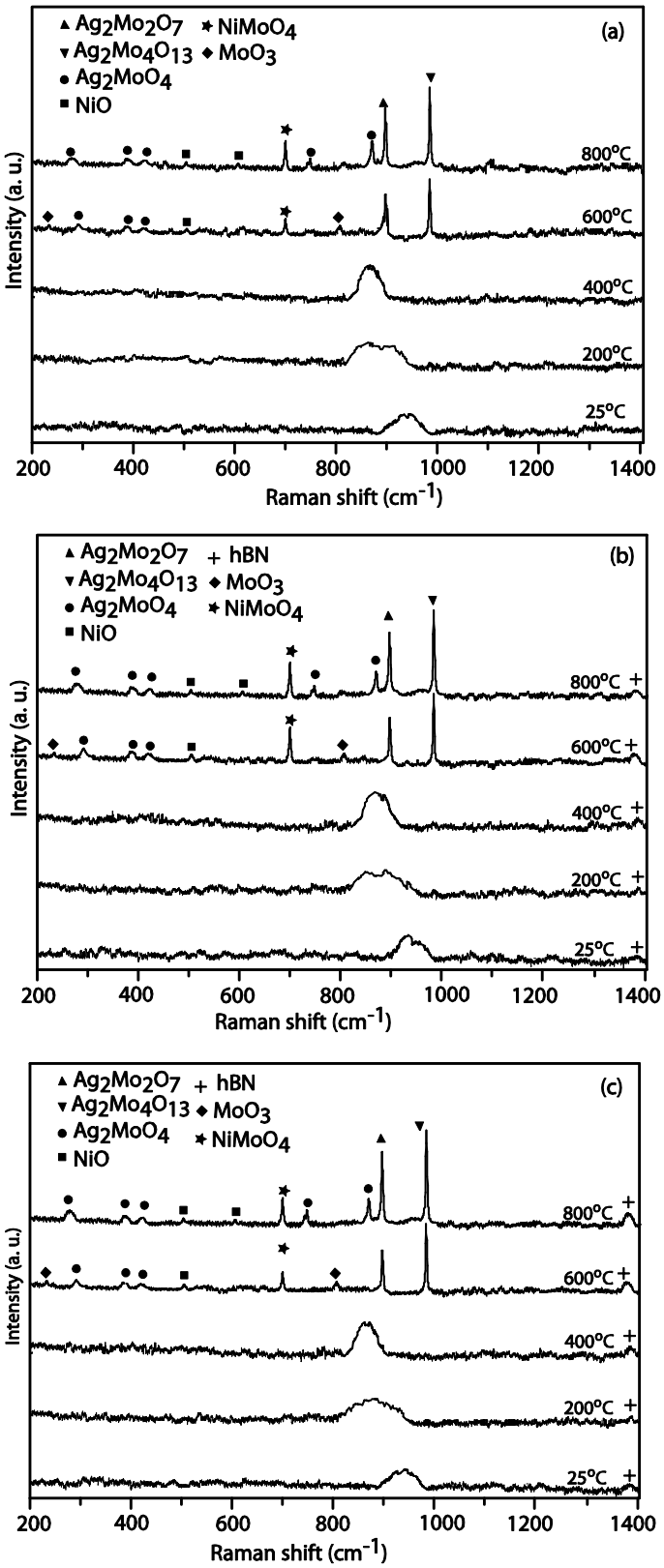

Fig. 4.58 Raman spectra within wear track of the coatings (a) NAMB0 (b) NAMB5 (c) NAMB10 at different test temperatures under 0.9 m/sec speed.

4.6 DISCUSSION

All the coatings show a fluctuating trend of variation of coefficient of friction with time at all the sliding speeds but with varying amplitude of fluctuations depending on the test temperature and the type of coating. However, the amplitude of fluctuation is found to decrease with increasing speed from 0.3 to 0.9 m/s which may be confirmed from a comparison of Figs. 4.28 (a, b and c), Figs. 4.29 (a, b and c), and Figs.4.30 (a, b and c). The amplitude of fluctuations is observed to be relatively small for all the coatings at 200 °C in comparison to RT and 400 °C as evident from a comparison of Figs. 4.28 (a, b and c), Figs. 4.29 (a, b and c), and Figs.4.30 (a, b and c). At 400 °C, the NAMB5 coating has less fluctuations in COF in comparison to other coatings at the same temperature. However, the fluctuations in COF for all coatings are observed to decrease significantly as the temperature is increased to 800 °C in comparison to RT and 400 °C as evident from a comparison of Figs. 4.28 (a, c and e), Figs. 4.29 (a, c and e) and Figs.4.30 (a, c and e). At 800 °C, the NAMB5 coating displays a very smooth variation of COF in comparison to NAMB0 and NAMB10 coating as evident from a comparison of Figs. 4.28 (e), Figs. 4.29 (e), and Figs. 4.30 (e). The NAMB5 coating is found to maintain a lower coefficient of friction of value 0.1 under 0.7 m/s speed. One may also observe that COF shown by NAMB5 coating is the lowest in comparison to other coatings at from RT to 800 °C at all the sliding speeds as evident from a comparison of Figs. 4.28 (a through e), Figs. 4.29 (a through e) and Figs. 4.30 (a through e). The fluctuations in the variation of friction coefficient with time may be attributed to the initial roughness of the mating bodies which eventually get smoothened as the sliding progresses. A relatively larger amplitude of fluctuations at RT and 400 °C in comparison to 800 °C may be explained on the basis of the SEM micrographs of the worn surfaces of coatings shown in Figs.4.35 (a, b, c) to 4.43 (a, b, c) and alumina ball given in Figs. 4.44 (a, b, c) to 4.52

(a, b, c) at 0.3 m/s, 0.7 m/s and 0.9 m/s**,** respectively**,** which present a relatively rough surface having scoring marks in the direction of sliding and the presence of a discontinuous and loosely bound layer of transferred material. This might have given rise to relatively large fluctuations at relatively low temperatures of RT and 400 °C. On the other hand the SEM micrographs of surfaces of coatings illustrated in Figs. 4.35 (c) to 4.43 (c) and alumina balls presented in Figs. 4.44 (c) to 4.52 (c) at 0.3 m/s, 0.7 m/s and 0.9 m/s, respectively**,** worn at 800 °C reveal the presence of a smooth, glaze/oxide layer and compacted transfer layer on the worn surface which might have diminished the amplitude of fluctuations at these temperatures. A decrease in coefficient of friction from RT to 200 °C for NAMB0, NAMB5 and NAMB10 coatings at all the sliding speeds as seen from (Fig. 4.31) may be attributed to the presence of lubricating effect MoS_2 and silver. An increase in coefficient of friction in NAMB0 coating from 200 to 400 °C (Fig.4.31) at a particular speed may be attributed to the loss of effectiveness of MoS_2 to act as a lubricant and excessive softening of silver around 400 °C which has also been reported earlier by Chen et al. (2013). The relatively higher COF shown by NAMB0 coating may be explained by comparing the morphologies of worn surfaces given in Figs. 4.35, 4.36, 4.37, 4.38, 4.39, 4.40, 4.41, 4.42, and 4.43. The worn surface of NAMB0 coating has relatively deep grooves, signs of delamination, and either absence of transfer layer or a relatively lesser area coverage provided by the transfer layer which can be judged by a comparison of Figs. 4.35 (b) at 0.3 m/s, 4.38 (b) at 0.7 m/s, and 4.41 (b) at 0.9 m/s. This might have given rise to direct contact between alumina and coated specimen resulting in a relatively higher friction in NAMB0 in comparison to other coatings. A reduction in friction coefficient at 800 °C could be attributed to the formation of glaze Figs. 4.35 (c) at 0.3 m/s, 4.38 (c) at 0.7 m/s and 4.41 (c) at 0.9 m/s for NAMB0 coating which is expected reduce friction at high temperatures by inhibiting the direct

contact of alumina ball with coating. A reduction in both friction and wear due to formation of glaze layers has been reported earlier also by Li et al. (2013), Zhen et al. (2014, 2016). The formation of silver molybdates and other lubricious oxides at elevated temperatures due to tribo-chemical reactions as evidenced by XRD patterns given in Figs. 4.53, 4.54 and 4.55 at 0.3, 0.7 and 0.9 m/s sliding speed might have also contributed in lowering the fiction at elevated temperatures. One may also observe significant reduction in coefficient of friction with the addition of 5 wt. % hBN in the coating which is evident from the comparison of COF shown by NAMB0 and NAMB5 in Fig. 4.31. However, the friction coefficient is found to be more for NAMB10 (containing 10 wt. % hBN) in comparison to NAMB5 but it is still lower than that shown by NAMB0. A decreased COF for coatings containing hBN may be due to the synergetic action of hBN in conjunction with Ag and MoS_2 which might have provided the enhanced lubricity at all the temperatures right from RT to 800 °C in NAMB5 and NAMB10. The COF of NAMB5 and NAMB10 coatings has been observed to decrease continuously with increasing speed 0.3 to 0.7 m/s at all the temperatures followed by a slight increase till 0.9 m/s as seen from Fig.4.31 as opposed to NAMB0 which has shown an increase in COF from 200 to 400 °C. Also, both NAMB5 and NAMB10 coatings have a lower friction coefficient in comparison to NAMB0 at all the temperatures and speeds as evident from Figs. 4.31 and 4.32. The reduced coefficient of friction in NAMB5 and NAMB10 in comparison to NAMB0 may also be explained on the basis of the morphologies of worn surface of these coatings given in Figs. 4.35 to 4.43 and the counterface alumina ball Figs. 4.44 to 4.52 slid against these coatings at different temperatures and speeds. The worn surfaces of coatings (Fig. 4.35 to 43) show the presence of loose wear debris particles, scoring marks along with the presence of a transfer layer which is either loosely bound or is well compacted. Also the extent of cover provided by the transfer layer to the underlying

surface is different depending on the respective coating, temperature and speed. The detachment or cracking of transfer layer could also be seen in some micrographs particularly for NAMB0 and NAMB10 coatings. Similar, features have also been observed on the worn surfaces of alumina ball as illustrated in Figs. 4.44 to 52 which also show the presence of a layer of transferred material from coated surface. A decreasing coefficient of friction with temperature in NAMB5 and NAMB10 coatings may be explained on the basis of the formation of transfer layer, its degree of compaction, the extent of coverage over the surface and cracking of this layer depending on the test temperature, coating and speed. At relatively low temperatures i.e., RT and 400 °C the layer is discontinuous and loosely bound ((Figs. 4.35 (a, b), 4.36 (a, b), 4.37(a, b)) whereas at elevated temperatures the transfer layer (Figs. 4.35 (c), 4.36 (c) and 4.37 (c) is relatively more compact, continuous and covers a larger area which is helpful in effectively inhibiting the direct contact between the mating surfaces and results in reduced friction coefficient at 0.3 m/s. Similar effect is also seen at other sliding speeds. However, a higher coefficient of friction shown by NAMB10 in comparison to NAMB5 may be attributed to the increased amount of hBN which deteriorates the performance because of its poor sintering characteristics and therefore, results in a relatively poor compaction of transfer layer which can be judged by a comparison of Figs. 4.36, 4.37 at 0.3m/s, Figs. 4.39, 4.40 at 0.7 m/s, and Figs. 4.42, 4.43 at 0.9 m/s. This poorly compacted layer on NAMB10 is liable to get detached easily giving rise to loose wear debris and the direct contact between mating bodies, both of which help in raising the friction. A reduction in friction coefficient at 800 °C could be attributed to the formation of glaze ((Figs. 4.36 (c), 4.37 (c) at 0.3 m/s, Figs. 4.39 (c), 4.40 (c) at 0.7 m/s and Figs. 4.42 (c), 4.43 (c)) at 0.9 m/s for NAMB5 and NAMB10 which helps in reducing the friction coefficient as explained earlier. It is well acknowledged fact that silver seizes to work as effective

lubricant above 400 °C and its lubricating function starts getting reduced as indicated by Hu et al. (2007), so it is the transfer of hBN and its presence at counterface which might have played a vital role in reducing the friction till 800 °C for NAMB5 and NAMB10 in comparison to that observed for NAMB0, as shown in Figs. 4.45 (a to c), 4.46 (a to c), at 0.3 m/s, Figs. 4.48 (a to c), 4.49 at 0.7 m/s, Figs. 4.51 (a to c), 4.52 (a to e) at 0.9 m/s. The transfer of material from coating to the ball results in contact between transferred hBN and coating surface containing hBN and provides easy shearing capability due to lamellar structure of hBN. This may also explain a continued low coefficient of friction shown by NAMB5 coating during the entire duration of test at 800 °C as seen in Figs. 4.28 (e), 4.29 (e) and 4.30 (e) at all the sliding speeds. XRD patterns and Raman spectra given in Figs. 4.53, 4.54, 4.55 and Figs. 4.56, 4.57 and 4.58 show the presence of silver molybdates, NiO and hBN besides other oxides and compounds which basically act as high temperature lubricating phases and form a lubricating film at the interface of mating bodies. No discernible change could be observed in X-ray diffraction patterns and Raman spectra of coatings from RT to 400 °C (Figs. 4.53 to 55 and Figs. 4.56 to 58) with all the patterns showing peaks corresponding to Ni_3Al, Ag, NiAl, $NiMoO_4$, and Ni. However, at high temperature of 600 °C and 800 °C the peaks corresponding to NiO, MoO_3, $Ag_2Mo_2O_7$ and Ag_2MoO_4 could be seen in Figs. 4.53, 4.54, 4.55 and Figs. 4.56, 4.57 and 4.58. The oxides like MoO_3, NiO and silver molybdates have been reported to provide effective lubrication at elevated temperatures by several researcher (Liu et al., 2012 and 2013, Chen et al., 2013, Du et al., 2011 and Li et al., 2009) this may explain a decreasing trend of COF beyond 400 °C. The presence of peaks corresponding to hBN may also explain a relatively lower COF in NAMB5 and NAMB10 coatings in comparison to NAMB0, which also reflects the effectiveness of hBN as a high temperature solid lubricant. Du et al. (2011) have indicated that hBN is a promising solid lubricant which

works satisfactorily without disintegration up to 900 °C.

A relatively lower wear rate in NAMB5 and NAMB10 in comparison to NAMB0 (Fig. 4.33 and 4.34) may also be explained on the similar lines. The wear rate for NAMB0, NAMB5 and NAMB10 coatings decreases from RT to 200 °C (Fig. 4.33) due to presence of Ag and MoS_2 which provide effective lubrication in this temperature regime. The increase in wear rate in NAMB0 coating from 200 to 400 °C can be explained on the basis of the SEM micrographs of the surfaces worn at 400 °C and presented in Figs. 4.35 (b), 4.38 (b), and 4.41 (b) at 0.3, 0.7 and 0.9 m/s speed. The wear track surfaces have wear marks, grooves, delamination, lump of wear debris, discontinuous tribo-layer which might have led to the direct contact between counterpart alumina ball and coated samples giving rise to a relatively higher loss of material from the coated surface. Beyond 400 °C, the presence of molybdates and oxide/glaze layer might have reduced the wear of the coating by inhibiting direct contact between tribo-pair which can be seen from (Figs. 4.35 (c) at 0.3m/s, 4.38 (c) at 0.7 m/s, and 4.41 (c) at 0.9 m/s). In NAMB5 and NAMB10 coatings a consistent decrease in wear rate with increasing temperature may be attributed to (i) the presence of hBN in coated samples and its transfer to counterface as indicated by EDS of alumina ball, (ii) synergistic action of hBN in conjunction with Ag and MoS_2 lubricants in providing effective lubrication from RT to 800 °C, (iii) development of molybdates and oxide/glaze layer at the interface of the two mating surfaces.

Both the friction coefficient and the wear rate are observed to decrease with increasing speed from 0.3 to 0.7 m/s with a slight increase till 0.9 m/s for all the coatings as shown in Figs. 4.32 and 4.34 which may again be explained on the basis of the formation of transfer layer of wear debris containing solid lubricants, its degree of

compaction and the protection provided by this layer to the underlying material which is evident from Figs. 4.35 (a to c), 4.36 (a to c) and 4.37 (a to e) at 0.3 m/s, Figs. 4.38 (a to c), 4.39 (a to c) and 4.40 (a to c) at 0.7 m/s, Figs. 4.41 (a to c), 4.42 (a to c), and 4.43 (a to c) at 0.9 m/s. Since, all the test have been conducted at a fixed load, the extent of compaction is expected to be more at a relatively higher speed of sliding due to enhanced frictional heating. The layer is observed to be present in Figs. 4.35, 4.36, 4.37, 4.38, 4.39, 4.40, 4.41, 4.42, and 4.43 but with a different degree of compaction and coverage of the sliding surface. The presence of transfer layer has been observed on the worn surface of coatings and the ball as well but it appears to be more compact in case of NAMB5 coating in comparison to NAMB10 which could be clearly seen from a comparison of Figs. 4.36, 4.37 at 0.3 m/s, Figs. 4.39, 4.40 at 0.7 m/s and Figs. 4.42, 4.43 at 0.9 m/s. A loosely bound layer visible on the surface of NAMB10 (Figs. 4.37, 4.40, 4.43) is not as effective as a well compacted one (Fig. 4.36, 39, 42) in improving the friction and wear performance. Also, the extent of cover provided by the transfer layer is more in case of NAMB5 than in NAMB10 and this might have caused more hindrance to the direct contact between the mating bodies resulting in a reduced wear loss. The worn surfaces of alumina ball shown in Figs. 4.45, 4.46, 4.48, 4.49, 4.51, 4.52 reveal the presence of a transfer layer but this layer appears to have detached in case of ball slid against NAMB10 (Figs. 46 ,49,52) and this might have given rise to relatively more direct contact of ball and coated surface. This may explain a relatively higher wear rate in coating NAMB10 (containing 10 wt. % hBN) in comparison to NAMB5 (containing 5 wt. % hBN) as evident from Figs. 4.31 and 4.33.

A marginal increase in both friction coefficient and wear rate of all the coatings beyond 0.7 m/s may be because of the higher chances of expulsion of wear debris from the sliding surface due to larger centrifugal force caused by relatively higher speed

(0.9 m/s). Hence, lesser amount of wear debris is available at the interface to form a transfer layer with relatively smaller area of coverage of the sliding surface as evident from Figs. 4.41 (a to c), 4.42 (a to c) and 4.43 (a to c) at 0.9 m/s leading to higher possibility of contact between coating and counterface and this might have given rise to higher friction and wear at this speed.

In low temperature regime (RT to 400 °C), the mechanism of wear in NAMB0 coating appears to be a mixture of ploughing, abrasion, adhesion, delamination whereas at elevated temperatures glaze layer formation depending upon the combination of speed and temperature is the dominant. For NAMB5 coating, tribological mechanisms are a mix of adhesion and abrasion depending on the temperature (RT to 400 °C) and glaze layer (tribo-layers) formation and adhesion at elevated temperatures (600 and 800 °C) at all the sliding speeds. The dominating mechanisms of wear for NAMB10 coating are tribo-oxidation and adhesion right from RT to 800 °C.

On the basis of the observed behavior and its discussion presented above, one may conclude that coating NAMB5 has the best performance at all the temperatures in regard to both the friction and the wear under the range of loads and speeds used in the present study indicating that there has to be an optimum amount of hBN and other optimized parameters like (speed and load) for attaining optimum tribological performance of such coatings. Since, all coatings have same amounts of MoS_2 and Ag but the coatings having hBN i.e. NAMB5 and NAMB10 have shown consistently lower friction and wear in comparison to NAMB0 with no hBN. This reveals an obvious synergistic action of hBN in combination with Ag and MoS_2 in providing lower friction and wear rate at all temperatures and speeds highlighting thus, the potential of hBN as an effective lubricant in stabilizing the friction over a wide range of temperatures and speeds.